Technical Report GL-94-1
January 1994

US Army Corps
of Engineers
Waterways Experiment
Station

In Situ Geophysical Investigation of the Pile Test Section, Sardis Dam, Mississippi

by José L. Llopis
Geotechnical Laboratory

Prepared for U.S. Army Engineer District, Vicksburg

Technical Report GL-94-1
January 1994

In Situ Geophysical Investigation of the Pile Test Section, Sardis Dam, Mississippi

by José L. Llopis
Geotechnical Laboratory

U.S. Army Corps of Engineers
Waterways Experiment Station
3909 Halls Ferry Road
Vicksburg, MS 39180-6199

Final report

Approved for public release; distribution is unlimited

Prepared for U.S. Army Engineer District, Vicksburg
Vicksburg, MS 39180-6190

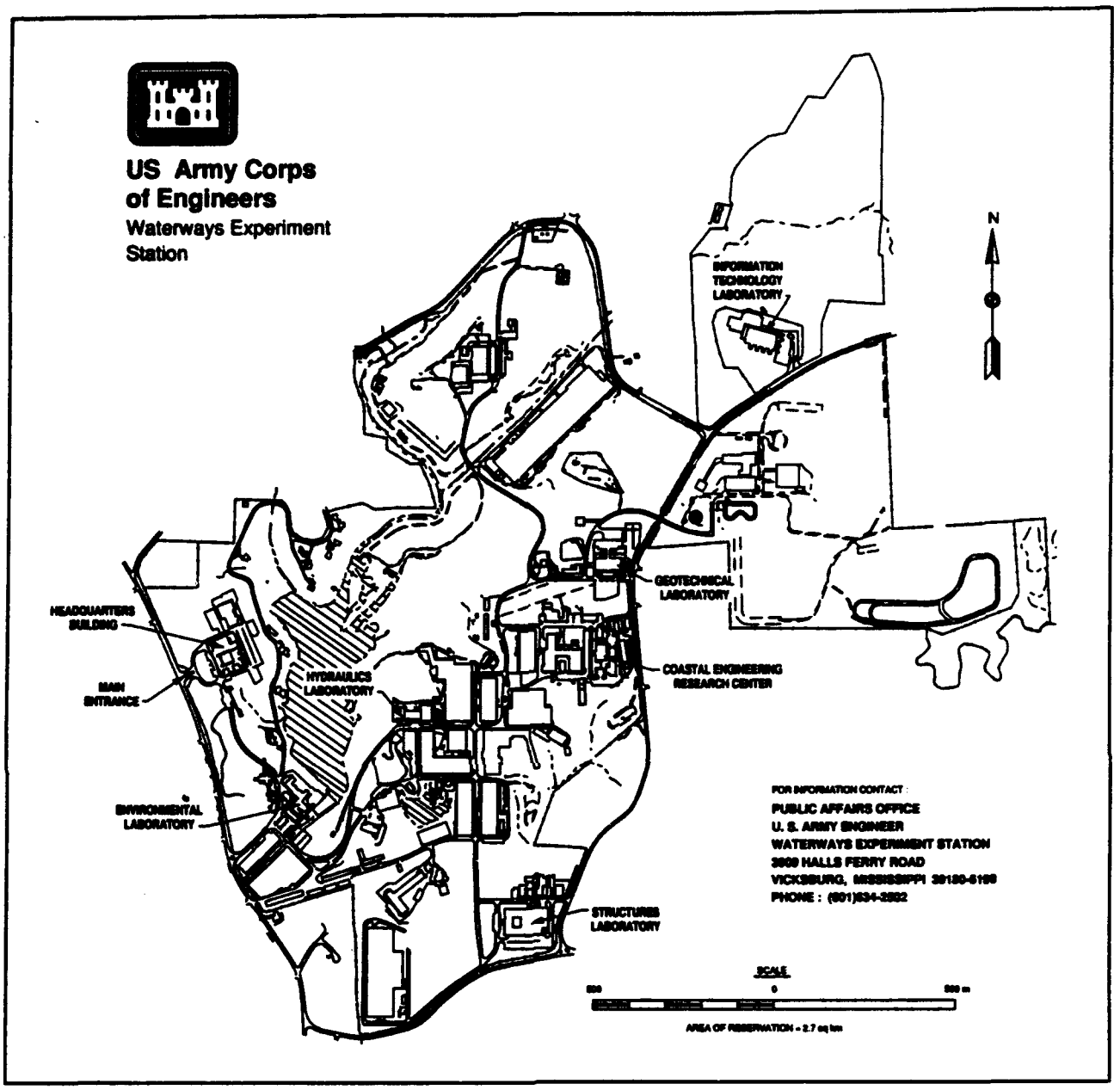

Waterways Experiment Station Cataloging-in-Publication Data

Llopis, José L.
In situ geophysical investigation of the pile test section, Sardis Dam, Mississippi / by José L. Llopis ; prepared for U.S. Army Engineer District, Vicksburg.
68 p. : ill. ; 28 cm. — (Technical report ; GL-94-1)
Includes bibliographic references.
1. Dams — Earthquake effects — Testing. 2. Dams — Mississippi — Sardis. 3. Earthquake hazard analysis. 4. Soil surveys — Geophysical methods. I. United States. Army. Corps of Engineers. Vicksburg District. II. U.S. Army Engineer Waterways Experiment Station. III. Title. IV. Series: Technical report (U.S. Army Engineer Waterways Experiment Station) ; GL-94-1.
TA7 W34 no.GL-94-1

Contents

Preface

A geophysical investigation was conducted at Sardis Dam, Sardis, Mississippi, by personnel of the U.S. Army Engineer Waterways Experiment Station (WES), during the periods 14-19 August, 23-26 September and 16-20 December 1991. The work was funded under the Repair, Evaluation, Maintenance and Rehabilitation (REMR) work unit entitled "Assessment of Requirements for Seismic Stability Remediation" and under the U.S. Army Engineer District, Vicksburg (LMK) Sardis Dam remediation study. Mr. Wayne Forrest, LMK, was overall project coordinator.

Mr. José L. Llopis of the Engineering Geophysics Branch (EGB), Earthquake Engineering and Geosciences Division (EEGD), Geotechnical Laboratory (GL), WES, was the Project Engineer for this phase of the study. The overall Project Engineer was Mr. Richard H. Ledbetter, Earthquake Engineering and Seismology Branch (EESB), EEGD. The field work was performed by Messrs. José L. Llopis, Thomas B. Kean II, and Thomas Harmon, EGB. Dr. Janet E. Simms, EGB, assisted in the data reduction and analysis of the study. Messrs. Selymn W. Guy and Leo V. Koestler III of the Data Acquisition Section,Instrumentation Services Division, provided instrumentation support. Messrs. Dennis Beausoliel and Frank James of the Operations Branch, Engineering and Construction Services provided technical and logistical support. Mr. Sam Stacy, LMK, provided invaluable technical support during site preparation phase of this study.

The work was performed under the direct supervision of Mr. Joseph R. Curro, Jr., Chief, EGB, and under the general supervision of Drs. A. G. Franklin, Chief, EEGD, and William F. Marcuson III, Chief, GL.

At the time of publication of this report, Director of WES was Dr. Robert W. Whalin. Commander was COL Bruce K. Howard, EN.

Conversion Factors, Non-SI to SI Units of Measurement

Non-Si units of measurement used in this report can be converted to SI units as follows:

Multiply	By	To Obtain
degrees (angle)	0.01745329	radians
feet	0.3048	meters
feet per second	0.3048	meters per second
gallons	3.785412	cubic decimeters
inches	2.54	centimeters
kips (force)	4.448222	kilonewtons
miles (US statute)	1.609347	kilometers
pounds (force)	4.448222	newtons
pounds (mass)	0.4535924	kilograms
square miles	2.589998	square kilometers

1 Introduction

Background

The U.S. Army Engineer District, Vicksburg (LMK) has undertaken several studies to evaluate the probable behavior of Sardis Dam, Sardis, MS during and after an earthquake. The studies were conducted because of concerns about the stability of the dam under seismic conditions and the possibility of liquefaction of portions of the dam and its foundation. Results of the investigation have concluded that some modifications should be made to the dam to improve its stability relative to seismic loading. One remedial measure that is being considered to increase soil stability is to drive prestressed concrete piles through weak layers of the dam and into stronger layers below. The piles are designed to restrain large flow deformations and have the additional benefit of densifying the surrounding soil. A pile test section was constructed on the downstream toe of the dam to evaluate this method of remediation.

As part of the ongoing LMK Sardis Dam remediation study and as a part of the Repair, Evaluation, Maintenance and Rehabilitation (REMR) work unit entitled "Assessment of Requirements for Seismic Stability Remediation" personnel of the US Army Waterways Experiment Station (WES) conducted a geophysical investigation at the pile test section at Sardis Dam. The objective of the geophysical investigation was to assess soil strength changes due to remediation efforts at the test section.

The remediation technique testing consisted of driving 16- to 24-in. square prestressed concrete piles into the test section. To determine the possible densification effects of this remediation measure, crosshole shear-wave (S-wave), downhole S-wave and surface vibratory tests were conducted prior to, immediately after, and 3 months after pile driving activities. The S-wave velocity is used in determining the shear modulus of the soil. The equation relating S-wave velocity to shear modulus and density is:

$$V_s = \sqrt{\frac{G}{\rho}}$$

where

V_s = S-wave velocity
G = shear modulus
ρ = density

While the S-wave velocity is directly related to shear modulus seems natural enough, the inverse relationship to density seems to be contrary to intuition. The S-wave velocity usually increases in spite if an increase in density not because of it. The same factors which increase density also decrease porosity and thus increase the shear modulus.

Site description

General site description

Sardis Dam is located in northwestern MS approximately 60 mi. south of Memphis, TN and 10 mi. southwest of the town of Sardis, MS as shown in Figure 1. The dam was constructed on the Little Tallahatchie River, and controls flow from 1545 mi^2 of drainage area. The reservoir has a surface area of about 14 mi^2 at minimum pool (conservation pool). Conservation pool is maintained at El. 236.0 ft. National Geodetic Vertical Datum (NGVD) (U.S. Army 1985).

The dam is composed of a main embankment, abutment dikes, spillway, and outlet works. The main dam has an approximate length of 8500 ft. The crown width is approximately 40 ft. wide at the dam crest. The maximum height of the dam above the streambed is 117 ft. (U.S. Army 1985). Figure 2 shows a typical cross section of the dam.

Sardis dam is a hydraulically placed embankment consisting of a fine grained central core and two flanking sand shells. The construction method that was used is demonstrated in Figure 3. Material from a nearby borrow area was pumped into the zone between the downstream and upstream shells. The finer grained material (mostly silt) flowed toward the center and formed the central core whereas, the coarser material was deposited near the fill pipe and formed the shells. The colloidal fraction of the effluent was drained off to a disposal area (U.S. Army 1985).

The dam's foundation consists of Recent and Tertiary aged deposits. A generalized geologic profile is shown in Figure 4. The foundation has a 10 to 20-ft thick zone of natural silty clay, designated as the topstratum clay in Figure 4 and extends 1200 ft upstream of the dam centerline. In areas of the original streambed the topstratum clay was nonexistent and a 10-ft thick silty

clay rolled fill was placed in this area. The topstratum clay is underlain by pervious alluvial sands (substratum sands) which are approximately 40 ft thick and underlain by Tertiary silts and clays. During the dam construction, the topstratum clay was removed from beneath the downstream portion of the dam to help control under seepage (U.S. Army 1988). Loess deposits of Recent age cap the higher elevation abutments.

Pile test section

The pile test section, located on the downstream toe of the dam, was level with surface elevations ranging between approximately 223 and 224 ft (Figure 5). Boring information from the test site indicated that the upper 5 ft of each boring consisted of silty sand, silt or clay fill materials. Underlying the fill material and extending to depths of approximately 45 to 50 ft are fine to medium grained sands with occasional clay strata and lenses. Tertiary age materials underlie the sand strata. These materials are best characterized as stiff lean clay with silty sand strata.

The main pile test section, located between Sta. 44+30 and 45+78, was divided into 3 test sections referred to as Pile Groups A, B and C (Figure 6). Square, 24-, 20-, and 16-in prestressed concrete piles were driven into Pile Groups A, B, and C, respectively. Spacings between piles for each pile group and the pile driving pattern are shown in Figure 6. The piles were 55 ft in length and were driven such that the tops of the piles were slightly below the ground surface. The pile tips were driven slightly into the Tertiary materials (tip elevation approximately 168 ft).

2 Geophysical Test Principles and Field Procedures

As mentioned earlier crosshole S-wave, downhole S-wave, and surface vibratory tests were run to ascertain S-wave velocity changes in the pile test section. The tests were run to determine velocity changes as a function of depth and time. The general location and layout of the geophysical tests are shown in Figure 7. The geophysical survey procedures, including a brief description of each survey as it pertains to this investigation are given below. Further information regarding geophysical testing and interpretation procedures used in this study is given in Engineer Manual EM 110-1-1802 (Department of the Army 1979).

Crosshole tests

Crosshole tests were run to determine horizontal S-wave velocities as a function of depth. The location of the four borings used for crosshole testing are shown in Figure 7. An advantage of the crosshole test as opposed to surface seismic refraction test is its ability to detect low velocity layers underlying or sandwiched between layers of higher velocity. One shortcoming of the crosshole method is that boreholes are required for testing. Thus, crosshole tests seismic tests are more costly than a surface seismic refraction test. However, the crosshole technique is considered to be more definitive and accurate than the surface seismic refraction test for measuring S-wave velocities. Basically, the testing consists of measuring the arrival time of an S-wave that has traveled from a source in one borehole to a detector in another borehole at the same elevation. This procedure is then repeated for the next test elevation. Knowing the distance between borings and the time the S-waves take to travel across this distance the velocity can be computed (distance divided by time).

The borings used for the crosshole testing were drilled to a depth of 55 ft with a diameter of approximately 6.5 to 7 in. The borings were then cased with 4-in inside diameter (ID) Schedule 40 polyvinyl chloride (PVC) casing and capped at the bottom. The annular space between the casing and the walls of the boring were grouted with a material that approximated the density of the surrounding in situ material. In this case, a mixture obtained by mixing 1 lb. of bentonite and 1 lb. of portland cement to approximately 6.25 lb.

(0.75 gal.) of water. The grouting was carried out in one continuous operation, filling the annular space between the drilled hole and the casing with a tremie pipe, from the bottom of the borehole to the surface.

Borehole deviation (drift) surveys were conducted to determine the precise vertical alignment of each boring. Figure 8 shows the deviation probe and instrumentation used to conduct the borehole deviation surveys. The incremental borehole deviation for each elevation along with the total deviation for the boring are indicated on the control panel. A borehole deviation survey was performed for each site visit. Accurate reduction of data from the crosshole tests requires knowledge of the drift of each boring so that a straight-line distance between borings at each test depth can be established. An analysis of the crosshole data obtained at each test elevation was made with the aid of the computer program CROSSHOLE developed at WES (Butler, Skoglund and Landers 1978).

S-wave velocities were obtained by placing an S-wave source in a source hole and detectors, at the same elevation, in two other boreholes (receiver holes). The detectors consisted of a triaxial array of geophones (two mounted horizontally at 90 deg. to each other, and one vertically oriented) in one container. The container housing the geophones was clamped firmly to the casing wall by means of an expanding pneumatic piston. A downhole vibrator was used as a source of S-waves. The S-wave testing procedure consisted of lowering the vibrator in the borehole to a selected test elevation and clamping the vibrator firmly to the sidewalls of casing by means of an inflatable rubber bladder. When the vibrator was in position, the operator tested a range of frequencies (50 to 250 Hz) and selected one that propagated well (one with a high amplitude) through the transmitting medium. The time required for the S-wave to travel from source to receiver hole was recorded using a portable, 24 channel seismograph with data-enhancement capability. Figure 9 illustrates the crosshole S-wave technique.

The data was collected by selecting one boring as the source boring and transmitting the signal to two receiver borings. When the data collection was completed for these hole sets, the source was placed into the next hole and the next two borings used as receiver holes. This process was repeated until each boring was used as a source hole. The source-receiver configuration used for this project is presented in Table 1. This testing configuration allowed a reciprocity check between hole set 1 and 3 and hole set 2 and 4. This testing pattern was repeated on each successive site visit. It is noted that neither the vibrator nor the geophones could be lowered past a depth of 45 ft. in hole 4 for either the second or third trips; apparently the casing was disturbed in some manner during the pile driving operations.

Table 1
Source and receiver boring pattern for S-wave crosshole tests

Source boring	Receiver boring	Receiver boring
1	2	3
2	3	4
3	4	1
4	1	2

Downhole tests

Downhole tests were conducted by placing an S-wave energy source on the ground surface close to the mouth of a borehole, and a triaxial array of geophones placed in the borehole. In this type of survey the travel path of seismic signal is forced to traverse all of the strata between the source and detector. The downhole test also has the ability to detect inversion layers and therefore, complements the crosshole test. An illustration of the downhole S-wave technique is shown in Figure 10.

The survey is conducted by impacting one end of a large wooden plank located on the ground surface near the mouth of a borehole with a sledgehammer and measuring the time the seismic disturbance takes to travel from the source to the triaxial array of geophones in the borehole. Before moving the geophone to the next elevation the test is repeated however, the plank is struck on the opposite end thus, reversing the polarity of the S-wave. By striking the board on opposite ends and reversing the polarity of the generated S-waves, the arrival time can be determined by identifying on the record where the two successive wave forms separate or change polarity as depicted in Figure 11. This procedure was repeated at 5 ft depth increments for each borehole shown in Figure 7.

Surface vibratory tests

The location and layout of the two surface vibratory tests run at the site are shown in Figure 7. These tests were conducted to determine the Rayleigh-wave (R-wave) velocity of the materials comprising the three pile groups and a region outside the test area (baseline). The R-wave velocity is slightly lower than the S-wave velocity, in fact for homogeneous media and for Poisson's ratios commonly found in soil materials, the difference in velocities is less than 9 percent (Ballard 1964 and Vrettos and Prange 1990).

The test is conducted by generating a discrete frequency waveform on the ground surface and measuring the phase velocity with a line of geophones placed on the ground surface. The R-waves for this investigation were generated by a truck mounted vibrator as shown in Figure 12. The vibrator truck

uses an electro-hydraulic vibrator with a maximum force output of 20 kips. The test procedure consisted of laying out a straight array of geophones and positioning the truck at an offset location which was in line with the geophone array. The offset distance was determined by the frequency and the force level of the vibrator. The vibrator was then operated at discrete selected frequencies (5-90 Hz) with the R-waves being monitored by the geophones (the geophone nearest the vibrator served as zero time). At lower frequencies a relatively large offset was used to allow sufficient distance for the waveform to develop whereas, at higher frequencies, where the vibrator output force is lower, a smaller offset distance was employed. Offset adjustments were sometimes necessary to reduce the effects of signals arriving along unwanted paths (e.g. reflected and refracted paths). The geophone array incorporated 24 geophones with spacings of 5 and 10 ft.

The time of arrival (referenced to the zero geophone) of a particular event at each geophone in the array was measured and plotted versus the respective distances of the geophones from the reference geophone. The R-wave velocity for each frequency was determined from the slope of the best-fit line obtained for the plot. Knowing the frequency and the R-wave velocity, a corresponding wave length was computed by dividing the velocity by the frequency. Wave velocities thus derived are assumed to be average values for an effective depth of one-half the wavelength. The R-wave data collection and reduction techniques are illustrated in Figure 13.

3 Test Results

Crosshole tests

The CROSSHOLE program results for the crosshole tests conducted during trips 1, 2 and 3 are presented as plots of velocity versus depth as shown in Figures 14 through 16, respectively. The velocities obtained for each boring set during trip 1 (Figure 14) agree very well with the exception of the upper 15 ft. The velocity discrepancy between boring sets in the upper 15 ft is probably due to the inability to accurately pick the time of arrival of the S-wave because of signal attenuation through the loose soil (fill) in this depth interval. Velocity agreement between boring sets for trips 2 and 3 (Figures 15 and 16) are also very good. It is noted that the velocities measured between borings 4 and 1, indicated in Figures 15 and 16 by the filled circles, are significantly higher than the velocities for the other borehole sets. The pile, located between borings 1 and 4 (Figure 17), has a marked effect on the surrounding soil as illustrated by the high S-wave velocity between these two borings. The increased S-wave velocity between these borings was presumably chiefly caused by the densified soil surrounding the pile rather than the pile itself. Based on an S-wave velocity for concrete of 8000 fps (Rix 1988) the time for an S-wave to travel trough a 24-in concrete pile would be approximately 0.25 msec, a very small fraction of the average travel time of 13.5 msec.

Average velocity profiles were determined for the three trips and are shown in Figure 18. The Figure 18 shows that the post-treatment velocities are considerably higher than the pre-treatment velocities. It is noted that the velocities obtained from crosshole tests conducted between borings 4 and 1 were not used to determine the average velocity profiles for trips 2 and 3 (post-treatment).

Downhole tests

The results of the downhole tests obtained during the three site visits are presented in Figures 19 through 30. The plots are presented as time versus slant distance. The slant distance is the distance from the source to the receiver and for depths greater than 20 ft, depth and slant distance are approximately equal. A summary of the downhole test results for trips 1, 2, and 3 are presented in Figures 31 through 33, respectively. Figures 31 through 33

show that for a given trip the downhole S-wave velocities agree very well between borings. Figure 34 presents the average downhole velocities for the each of the three trips. The results indicate basically two velocity layers with the layer interface occurring at an approximate depth of 30 ft. Referring to Figure 34 it can be seen that the average velocities for trip 1 are lower than those for trips 2 and 3 however, they are not considered significantly lower. Thus, it can be concluded that no significant S-wave velocities differences were noted between pre- and post-treatments using the downhole testing method.

Surface vibratory tests

The vibratory tests were analyzed basically in two ways in an attempt to determine differences in soil velocity caused by the pile driving operations. The first method consisted of determining the R-wave velocity for each pile group as a function of time (for each trip). This was accomplished by analyzing the vibratory signal over a particular pile group to determine that group's phase velocities. Plots of velocity versus depth for the pile groups and background area were generated. The plots of velocity versus depth over each pile group as a function of time for Line 1 are presented in Figures 35 through 38 whereas, the plots for Line 2 are shown in Figures 39 through 42.

To assess the effects of the treatment on a particular pile group velocity, an analysis of variance (ANOVA) was performed. Duncan's new multiple range test (Dowdy and Wearden 1983) at the 95 percent confidence level was used to determine if there was a significant difference between the pre- and post-treatments average velocities for each pile group and background area. The results of the analysis are presented in Table 2.

Table 2 indicates that the Line 1 velocities in Pile Groups A, B, and C experienced a significant increase between the pre- and post-treatment. Pile Groups A and C showed no significant difference in velocity between trips 2 and 3. However, there was an unexplained significant increase in velocity between trips 2 and 3 in Pile Group B. There were no significant velocity differences for the background area, as would be expected.

Line 2 showed a velocity increase over Pile Group A between the pre- and post-treatment. No significant velocity change was noted in Pile Group B. The placement of Line 2 was planned such that it would run along the top of a line of piles on the downstream edge of Pile Group B. It is possible that the line totally missed the pile group thus, possibly explaining the lack of a difference in velocities between trips. Line 2 did not actually pass over Pile Group C so no difference in velocity should be expected and the data confirm this assumption. As was the case for Line 1, Line 2 showed no velocity differences for the background materials.

Table 1
Summary of ANOVA determinations for R-wave velocities, fps

Velocities with common underlining are not different at 95% confidence as determined by Duncan's new multiple range test

Line 1				Line 2			
Pile Group	Trip Number			Pile Group	Trip Number		
A (24 in.)	1 450	3 578	2 597	A (24 in.)	1 518	2 639	3 667
B (20 in.)	1 499	2 586	3 663	B[1] (20 in.)	1 582	2 586	3 646
C (16 in.)	1 501	3 617	2 621	C[2] (16 in.)	2 551	1 557	3 558
Background	1 513	2 542	3 542	Background	2 534	3 541	1 572

[1] Vibratory line 2 passed over the edge of Pile Group B (refer to Figure 7)
[2] Vibratory line 2 did not pass over Pile Group C (refer to Figure 7)

Using the same ANOVA method employed above, vibratory Lines 1 and 2 were analyzed to determine how the R-wave velocity differed as it traveled across the different test sections and background materials for a given trip. The velocity versus depth plots for Lines 1 and 2 are presented in Figures 43 through 49. The results of the analysis are presented in Table 3.

The ANOVA results for Lines 1 and 2 indicate no velocity differences between the pile groups and the background area prior to pile driving activities (Trip 1). The data for Line 1 - Trip 2, indicates that the background velocity was significantly less than the velocity for Pile Group C but not different than the velocities of Pile Groups A and B. The data also demonstrate that the velocities between pile groups are not different for Line 1 - Trip 2. The analysis of Line 1 - Trip 3 shows that there is no difference between the background and Pile Groups A and C and no difference between Pile Groups C and B. Pile Group B showed a significantly higher velocity than those measured at Pile Group A or in the background area.

The analysis of Line 2 - Trips 2 and 3 indicate the same general trend that is Pile Groups C and B and the background materials had no significant differences in velocity. Also, Pile Group A and B had similar velocities. Again, it is noted that Line 2 passed near Pile Group C but not over it as shown in Figure 7. The order of velocities, from high to low, for Line 2 - Trips 2 and 3 was Pile Group A > B > C > background. It is noted again that Line 2 did not pass directly over Pile Groups B and C. The order of the velocities corresponds with the proximity of the Line 2 to the Pile Groups. In general, the closer the line is to a pile group the higher the velocity.

From a statistical analysis, the vibratory method was able to distinguish a change in soil velocity due to the installation of the piles. One of the objectives of the vibratory test was to determine if the pile group velocity was affected by the pile size and spacing. Based on the ANOVA, it appears that the vibratory tests do not correlate velocity with pile group.

Table 3
Summary of ANOVA determinations for average R-wave velocities, fps

Velocities with common underlining are not different at 95% confidence as determined by Duncan's new multiple range test

Line 1		Line 2	
Trip Number	Pile Group	Trip number	Pile Group
1	A B C BG 450 499 501 513	1	A C BG B 518 557 572 582
2	BG B A C 542 586 597 621	2	BG C B A 534 551 586 639
3	BG A C B 542 578 617 663	3	BG C B A 541 558 646 667

Note: BG denotes background

Summary

This report documents the results of an in situ geophysical investigation conducted at the pile test section located on the downstream toe of Sardis Dam. The purpose of the investigation was to determine which, if any, of the geophysical tests used could detect any soil property changes as a result of driving piles in the test section. The three geophysical tests conducted used at the site were the crosshole and downhole S-wave tests and surface vibratory test. Tests were conducted prior to, immediately after and 3 months after piles were driven.

Of the three geophysical techniques tested at the site, the crosshole S-wave test showed the greatest velocity difference between the pre- and post-treatment. No significant velocity differences were noted using the crosshole test between Trips 2 and 3. The interpretation of the downhole S-wave tests failed to exhibit any significant velocity differences between borings for a given trip or any velocity differences between trips. An ANOVA technique was used to analyze the surface vibratory data. The analysis showed that, in general, there was a significant velocity increase between the pre- and post treatments for those sections of the vibratory lines passing directly over a pile test section. No conclusions could be made regarding the effects of pile group spacing on velocity.

References

Ballard, R. F., Jr. (1964). "Determination of soil shear moduli at depths by in situ vibratory techniques," Miscellaneous Paper 4-691, U.S. Army Engineer Waterways Experiment Station, Vicksburg, MS.

Butler, D. K., Skoglund, G. R., and Landers, G. B. (1978). "CROSSHOLE: An interpretive computer code for crosshole seismic test results, documentation, and examples," Miscellaneous Paper S-78-8, U.S. Army Engineer Waterways Experiment Station, Vicksburg, MS.

Department of the Army (1979). "Geophysical exploration," Engineer Manual EM 1110-1-1802, Office of the Chief of Engineers, Washington, D.C.

Dowdy, S. and Wearden, S. (1983). *Statistics for research*. John Wiley & Sons, New York.

Rix, G. J. (1988). "Experimental study of factors affecting the Spectral-Analysis-of-Surface-Waves method," Ph.D. diss., University of Texas, Austin.

U.S. Army (1985). "Sardis Dam earthquake study, Design Memorandum No. 5, earthquake resistant remedial measures design for Sardis Dam, Sardis, Mississippi," U.S. Army Engineer District, Vicksburg, MS.

_____. (1988). "Sardis Dam earthquake study, Supplement No. 1 to Design Memorandum No. 5, earthquake resistant remedial measures design for Sardis Dam, Sardis, Mississippi," U.S. Army Engineer District, Vicksburg, MS.

Vrettos, C. and Prange, B. (1990). "Evaluation of in situ effective shear modulus from dispersion measurements," *Journal of Geotechnical Engineering* 116(10), 1581-85.

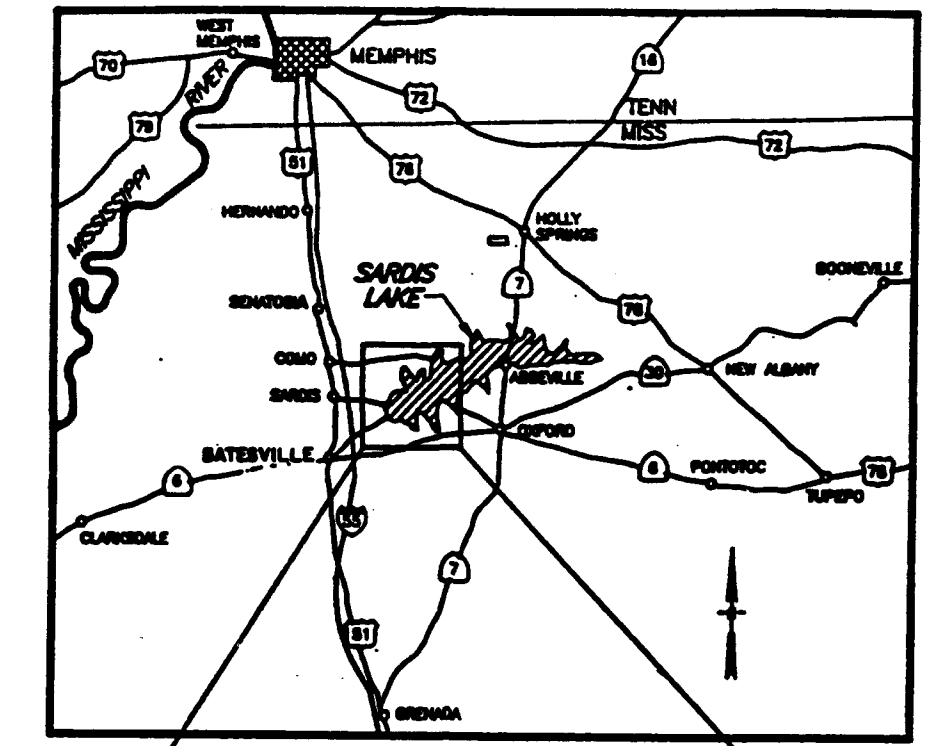

VICINITY MAP
NOT TO SCALE

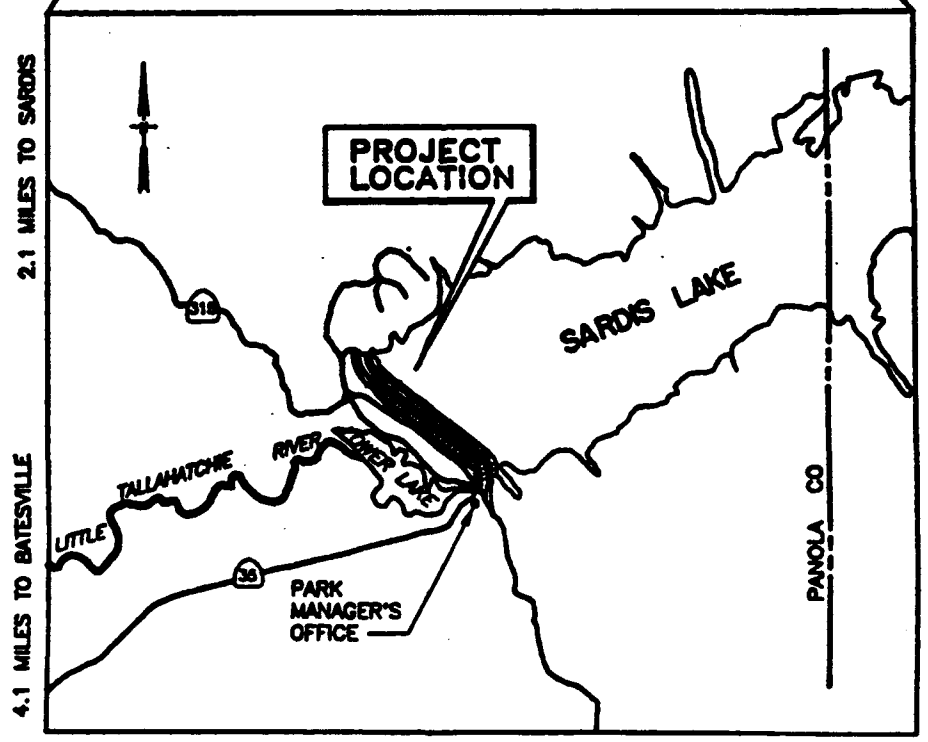

LOCATION MAP
NOT TO SCALE

Figure 1. Vicinity and location maps

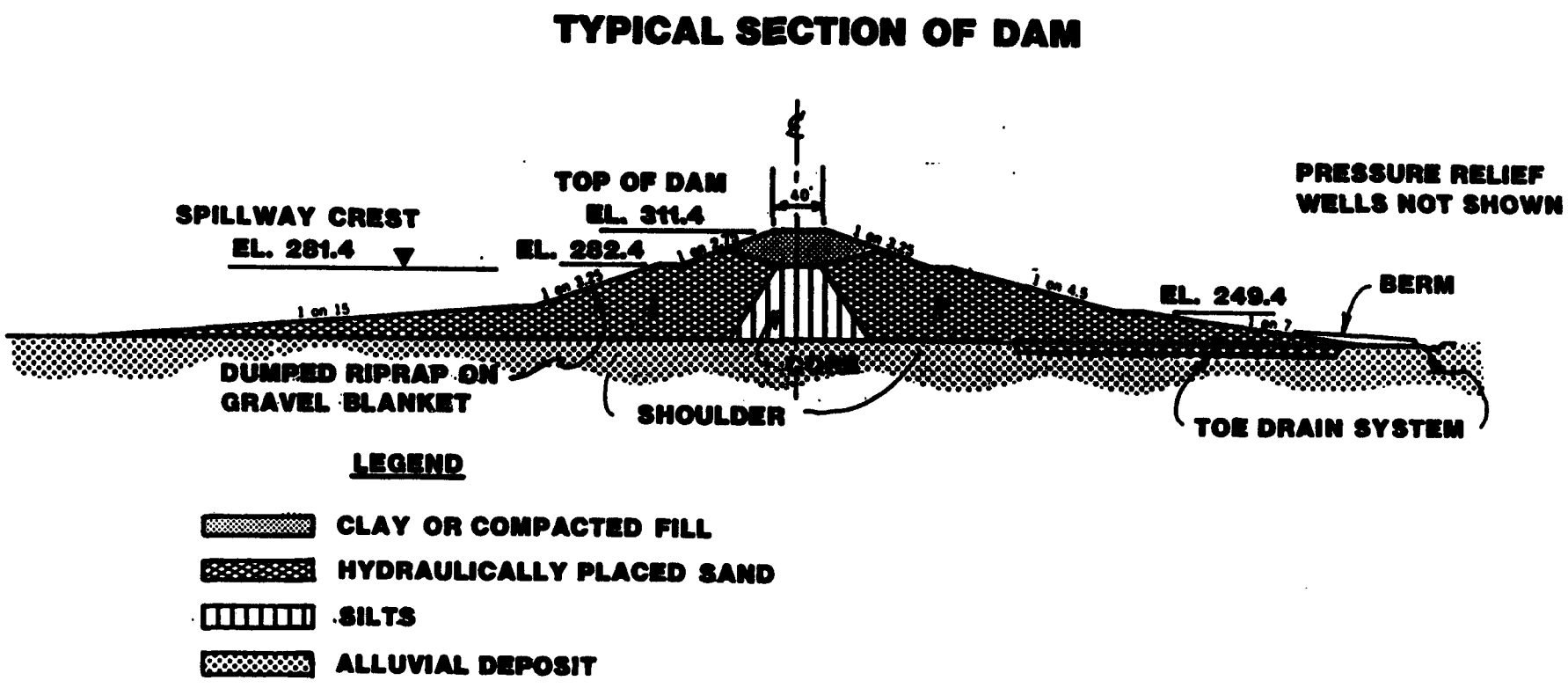

Figure 2. Typical section of Sardis Dam

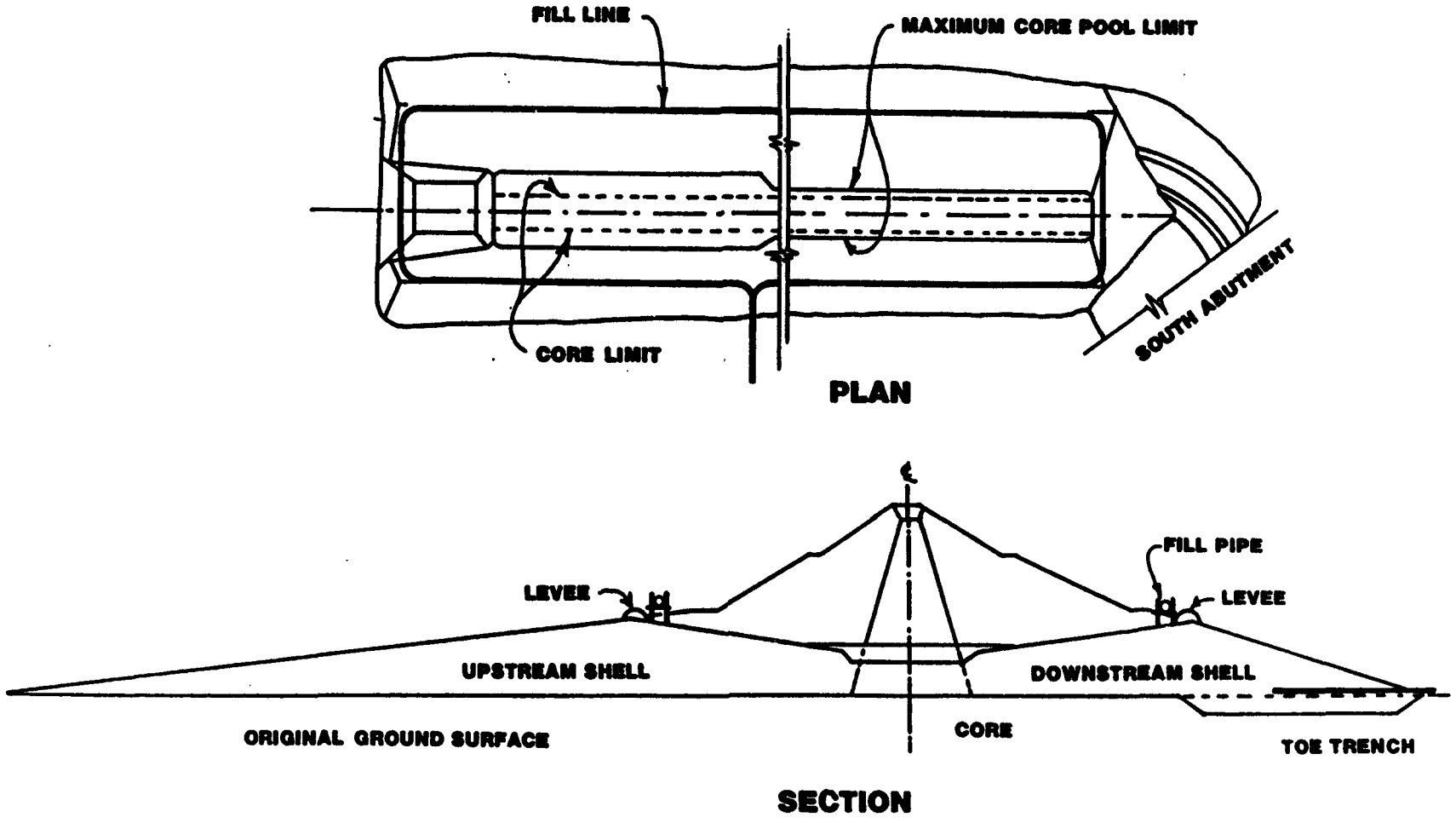

Figure 3. Hydraulic fill placement

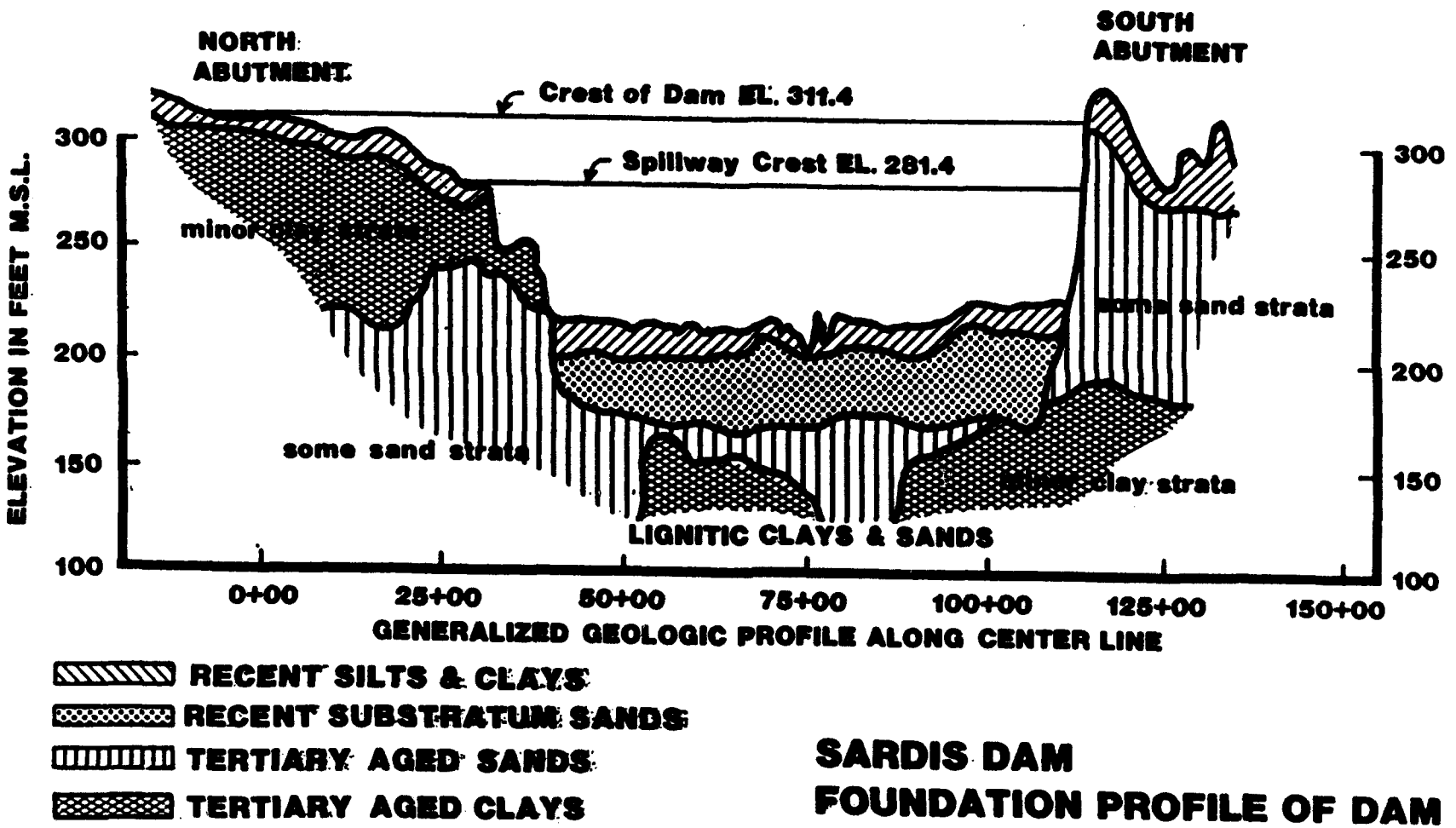

Figure 4. Foundation profile of Sardis Dam

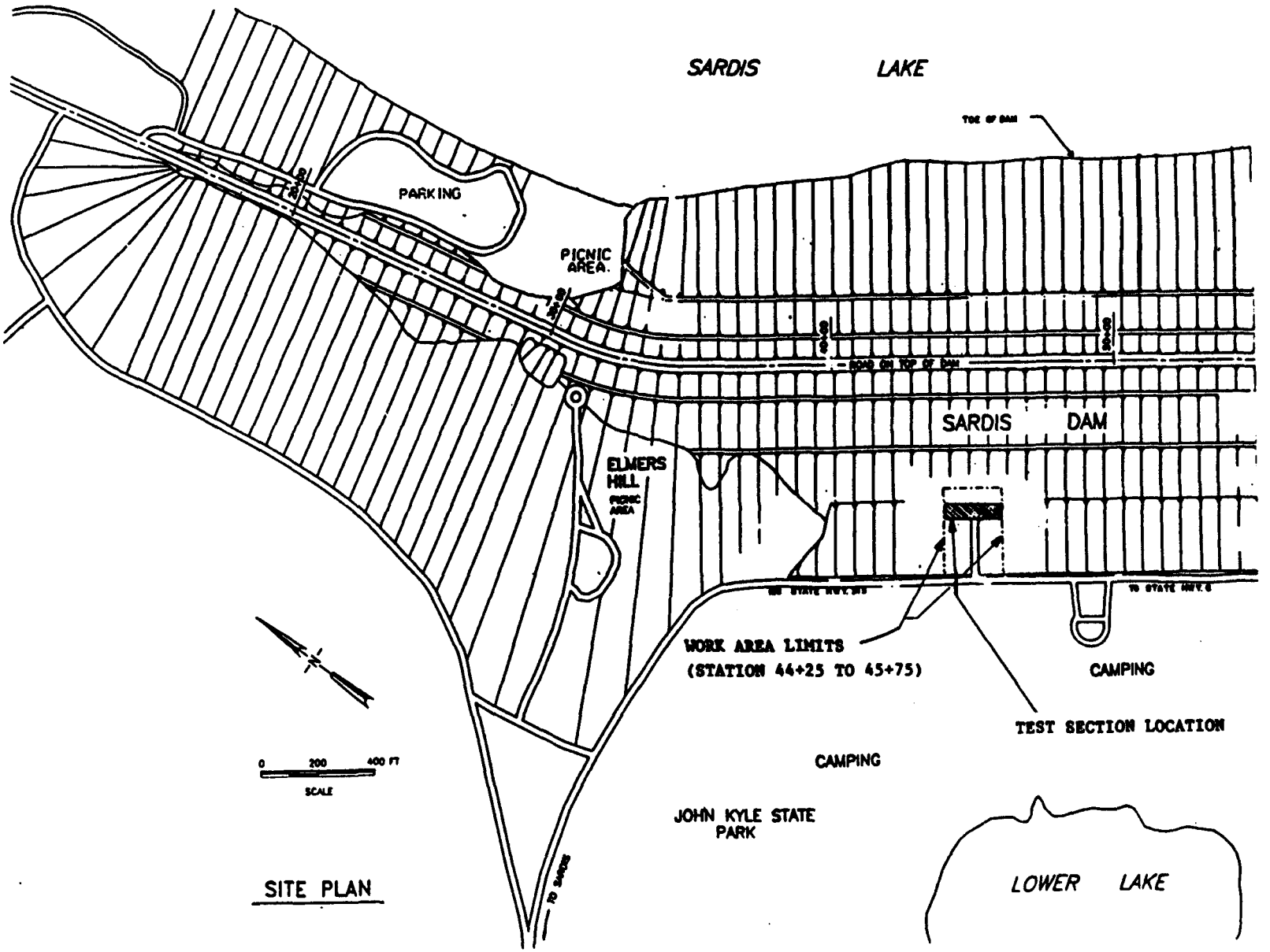

Figure 5. Location of pile test section

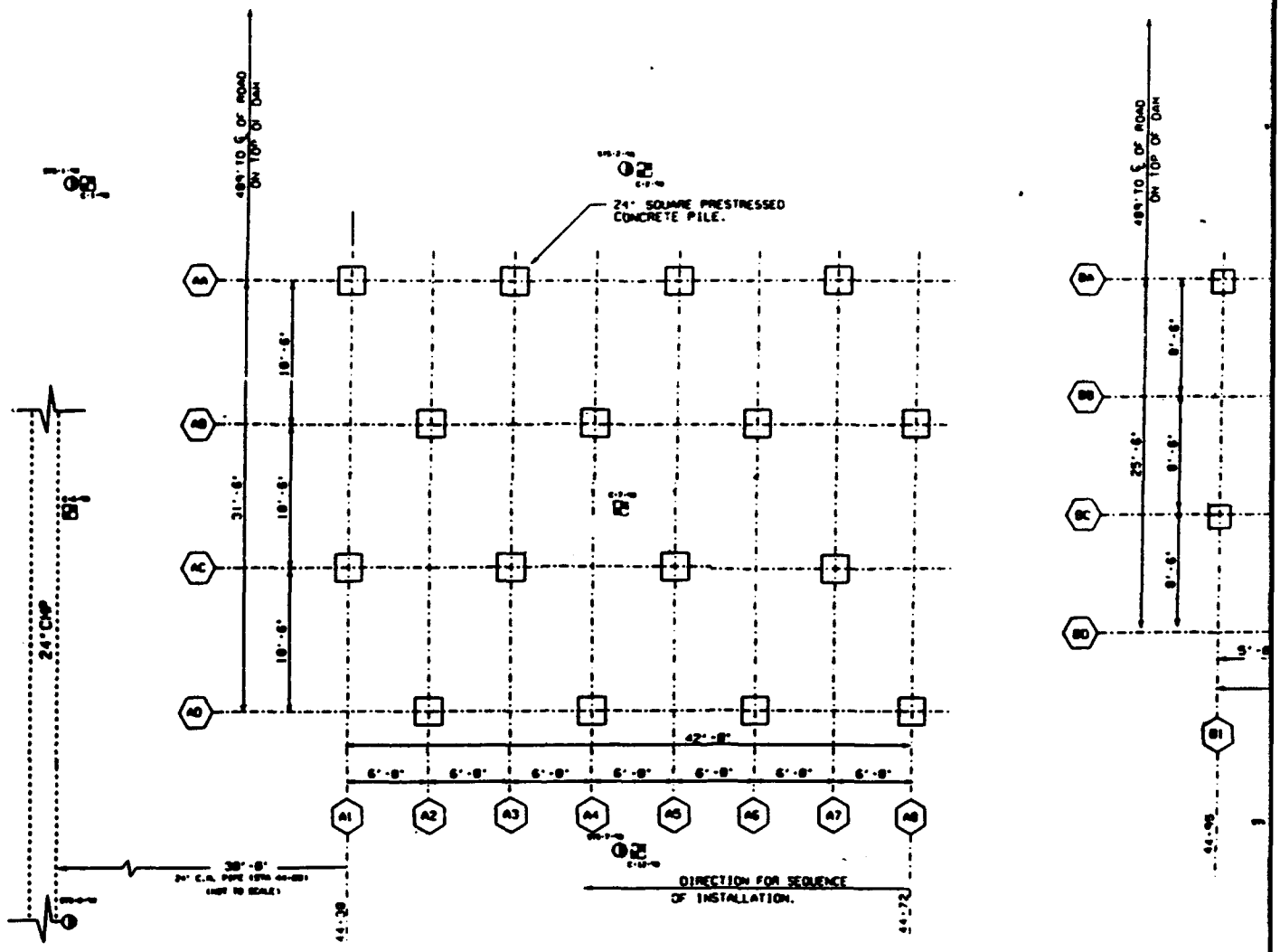

Pile Group A

24-in square prestressed concrete piles

20-in squ

Figure 6. Location and layou

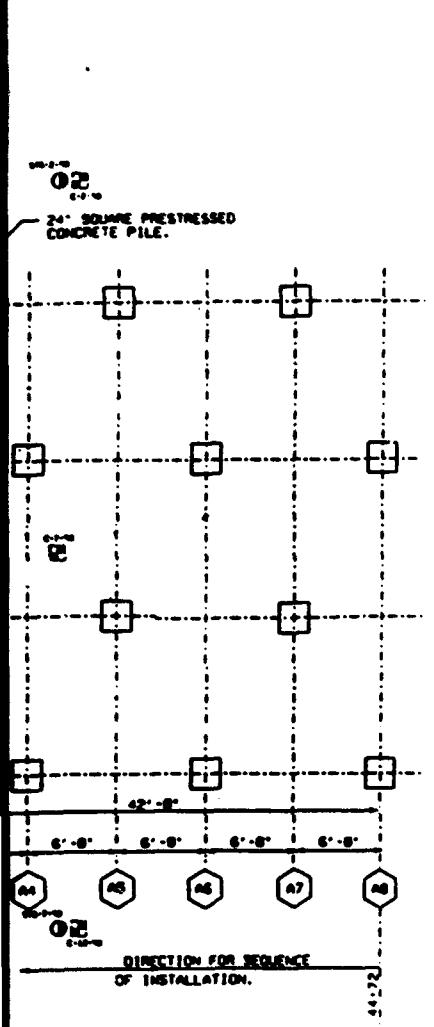

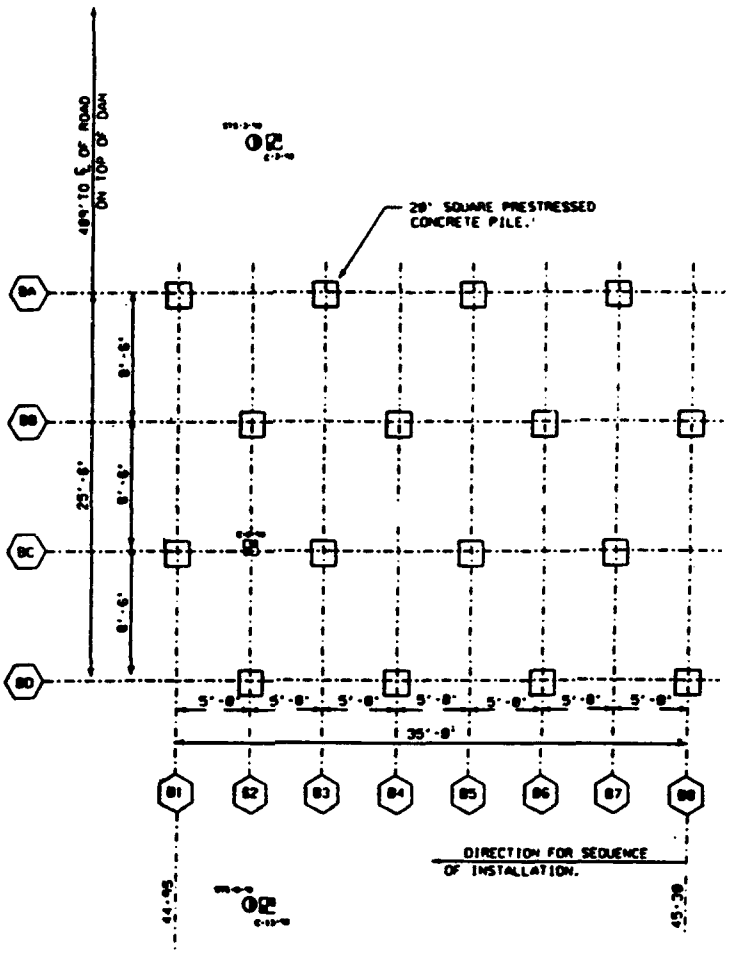

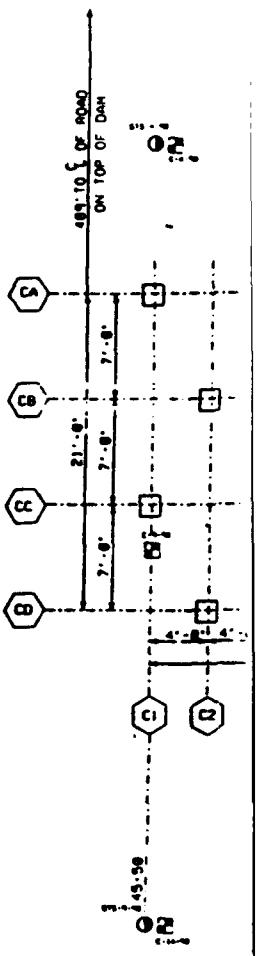

e Group A
stressed concrete piles

Pile Group B
20-in square prestressed concrete piles

Pi
16-in square pr

Figure 6. Location and layout of pile groups A, B, and C

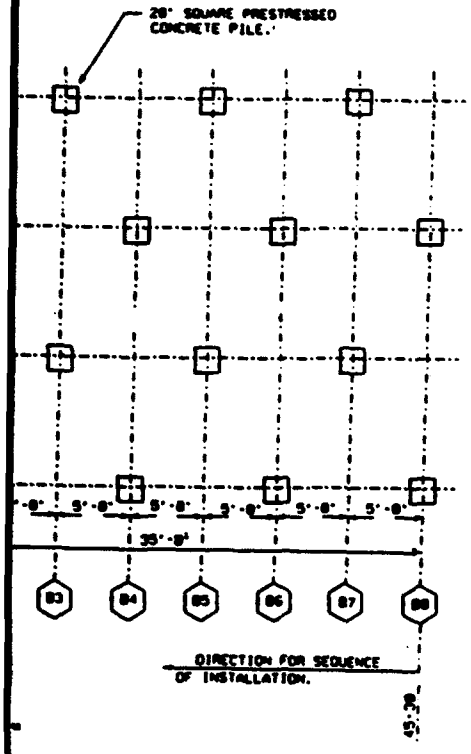

Pile Group B

prestressed concrete piles

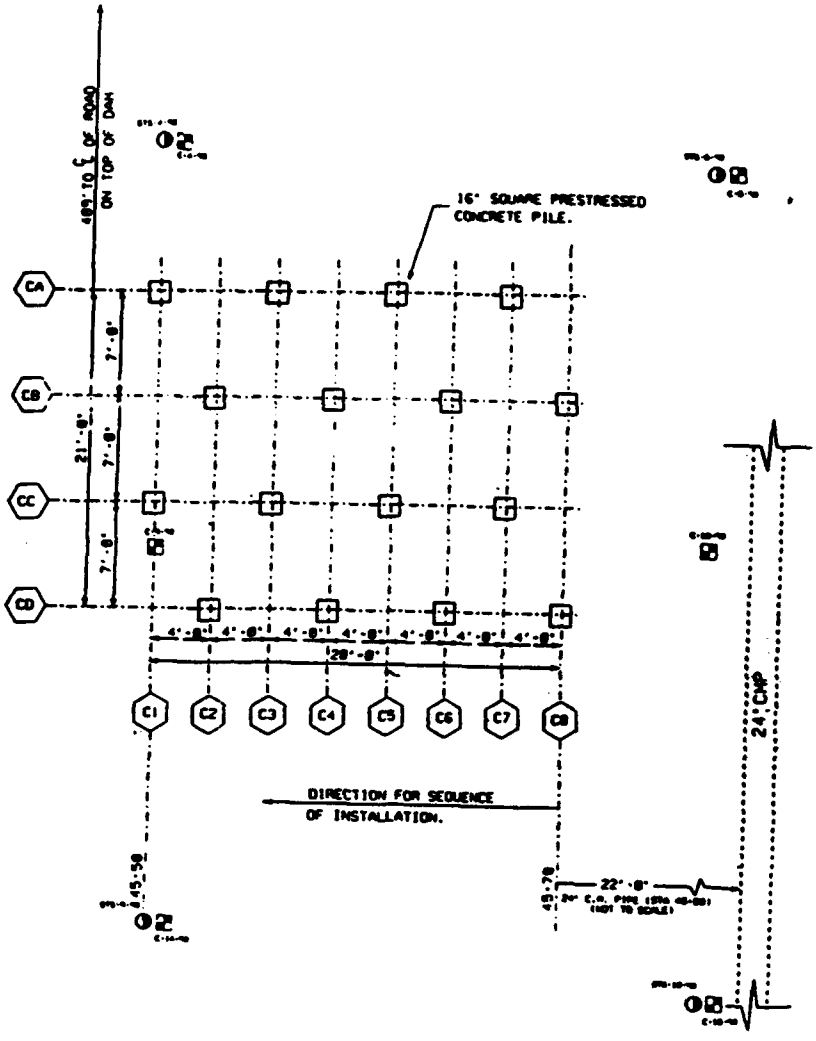

Pile Group C

16-in square prestressed concrete piles

pile groups A, B, and C

(5)

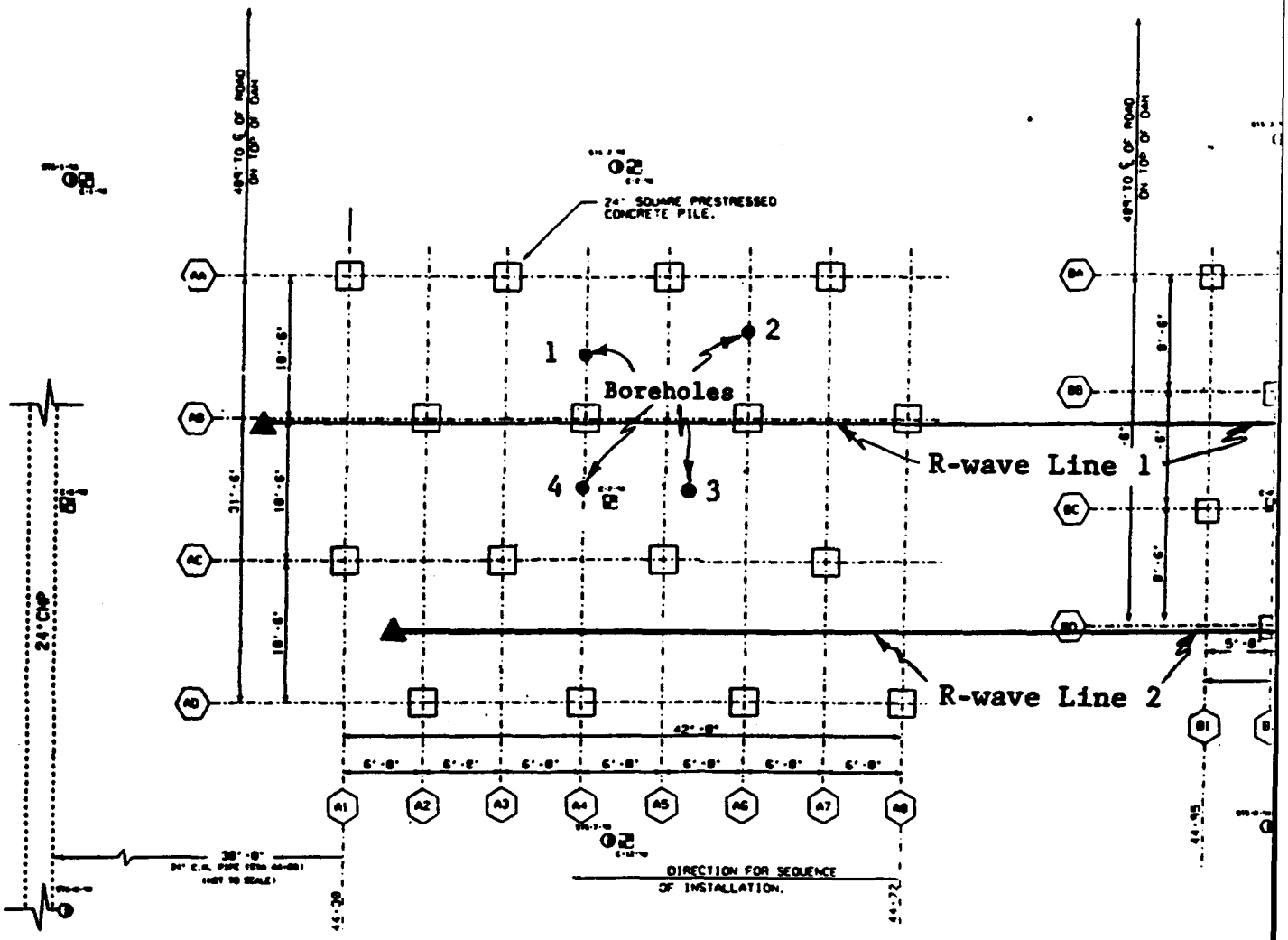

Figure 7. Locatio

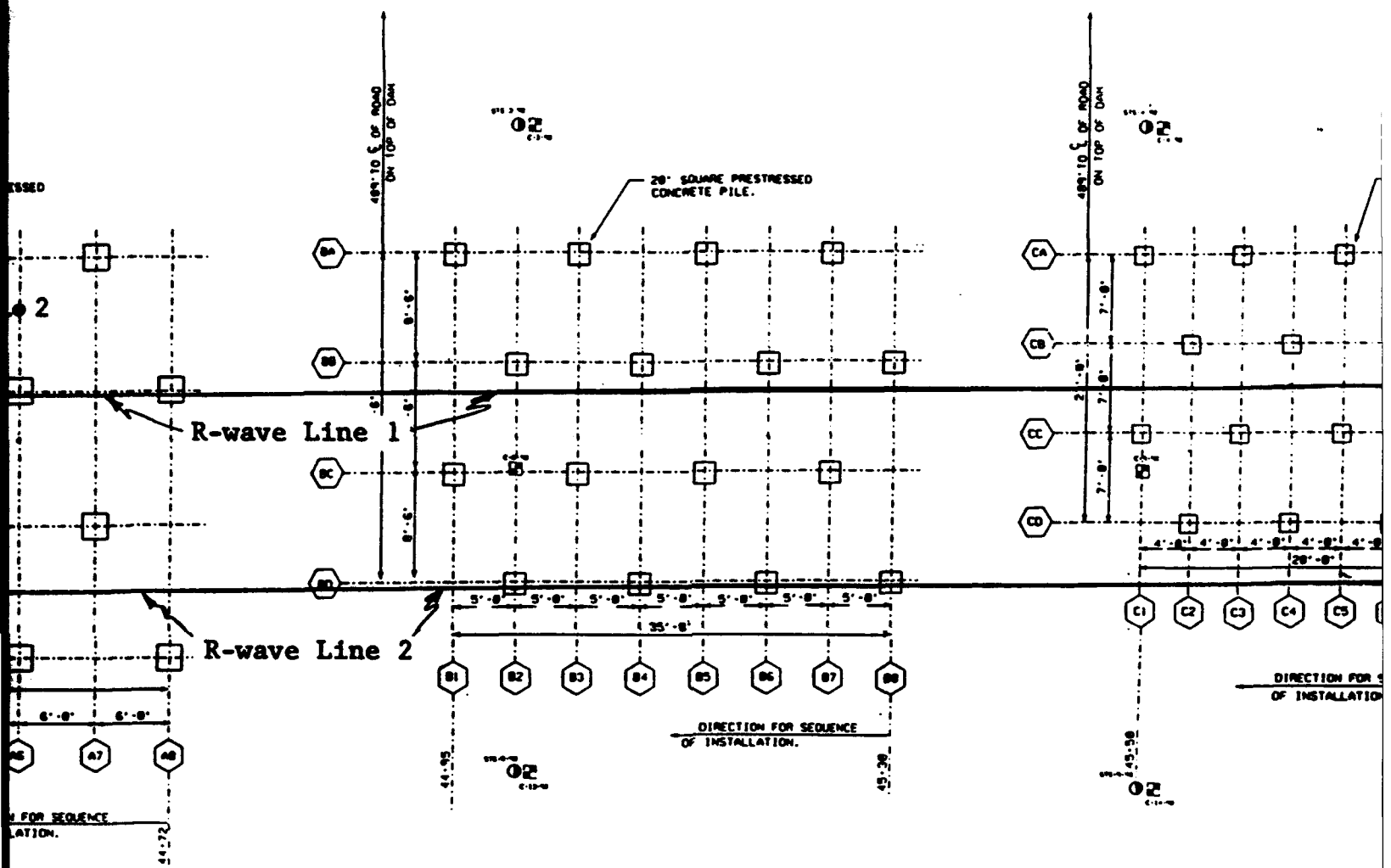

Figure 7. Location and layout of geophysical tests

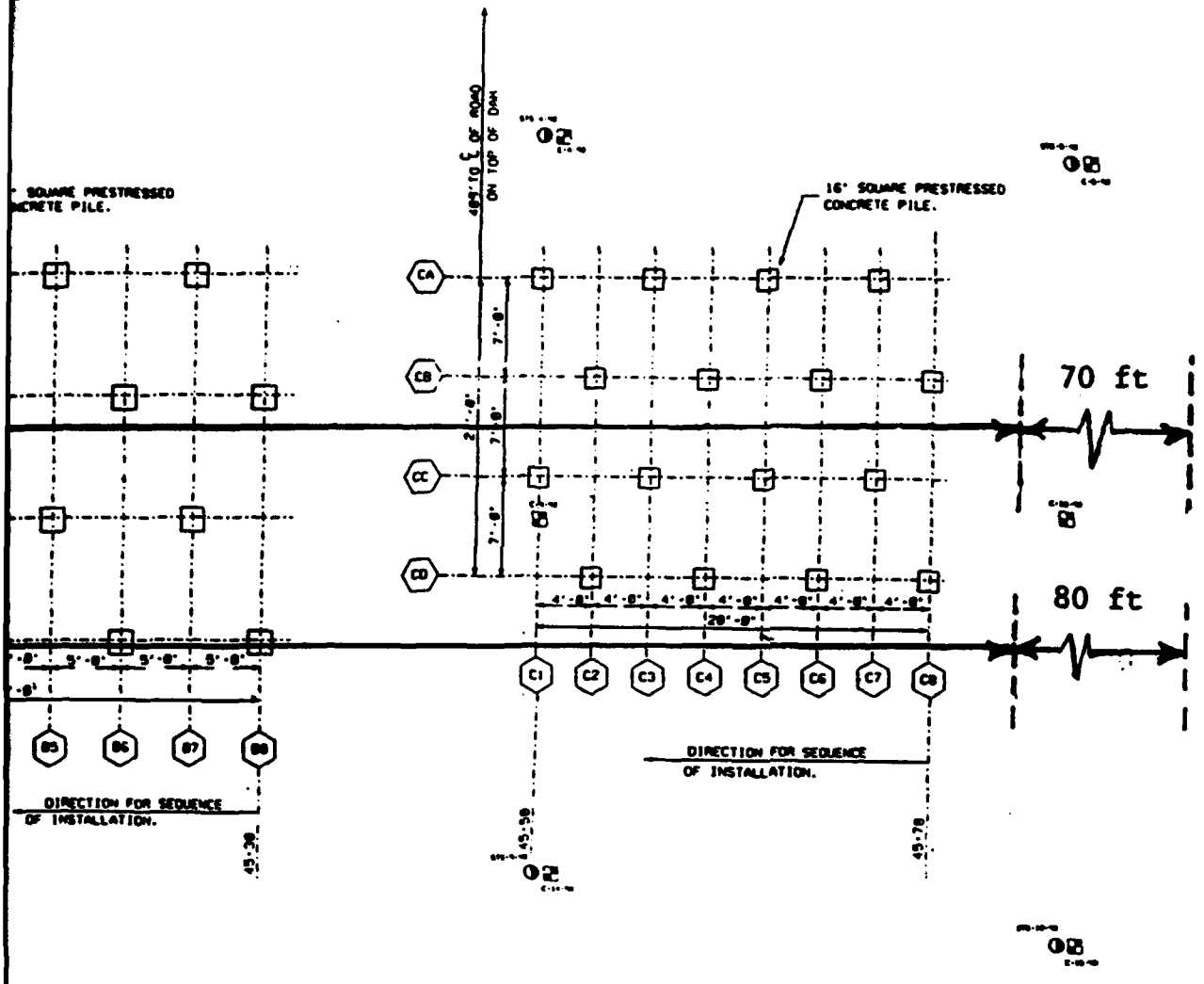

f geophysical tests

a. Deviation probe being lowered into boring

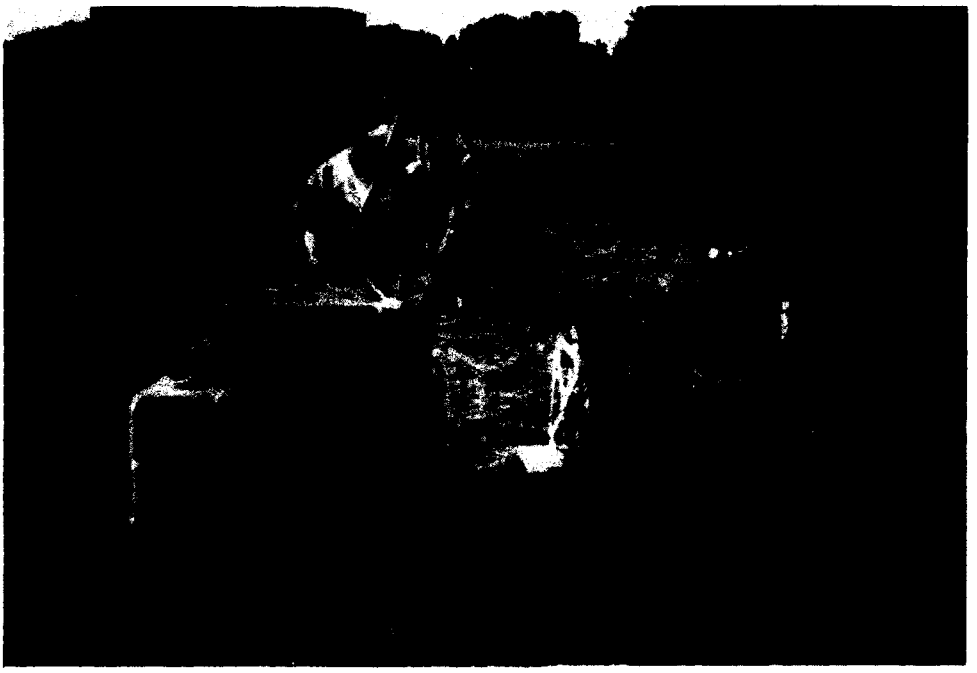

b. Surface control unit and winch

Figure 8. Borehole deviation tool

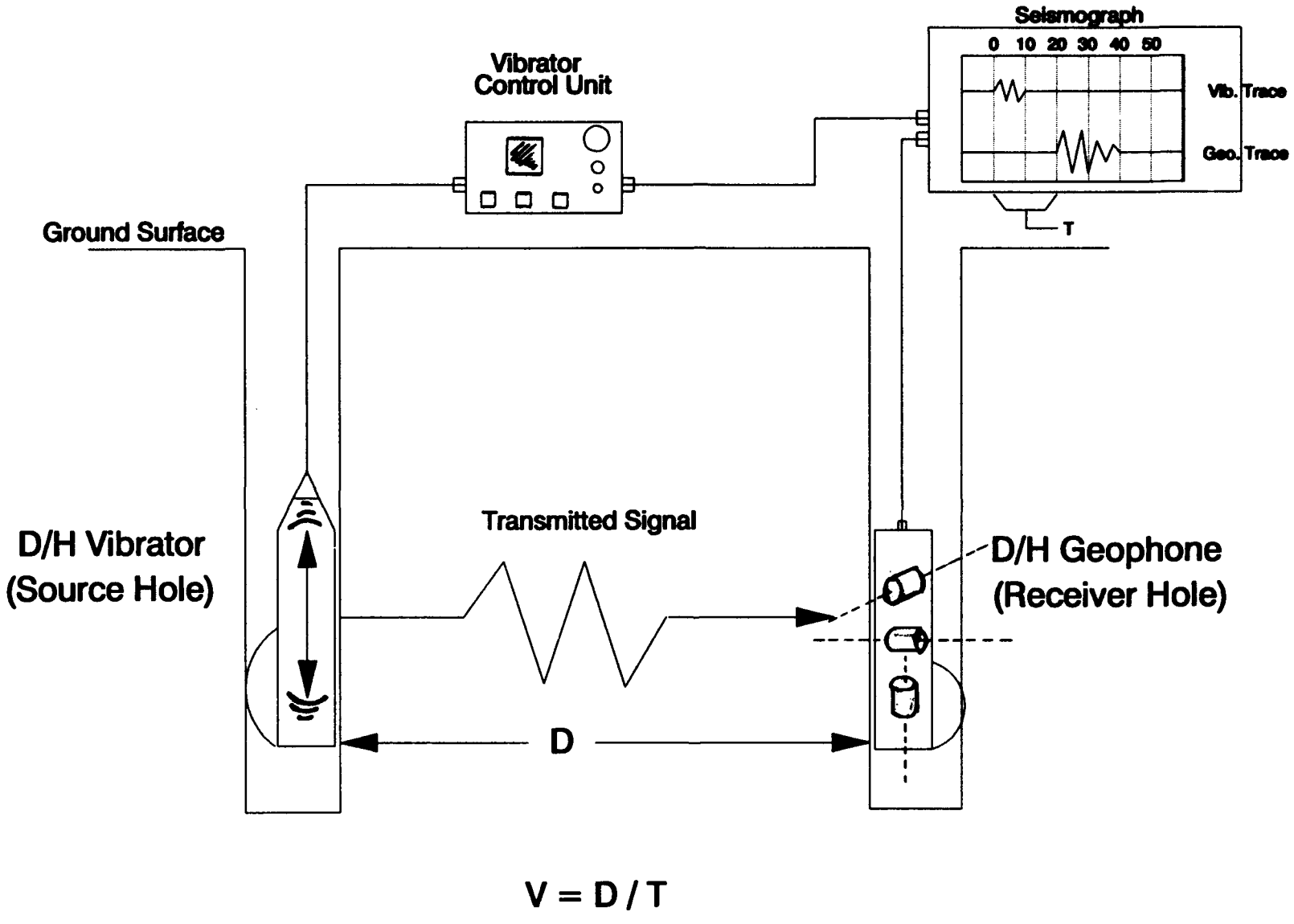

Figure 9. Crosshole S-wave testing setup

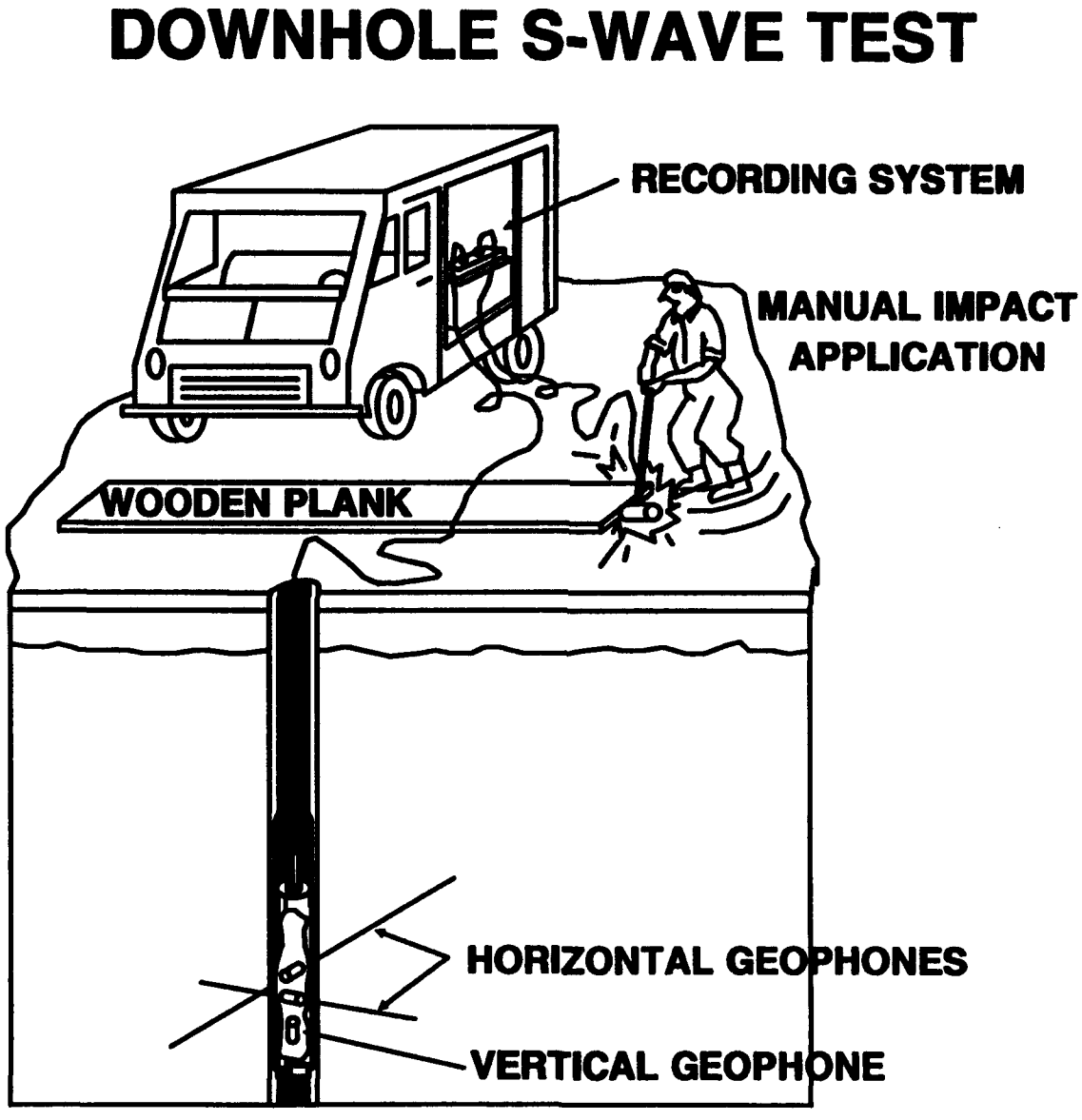

Figure 10. Downhole S-wave testing setup

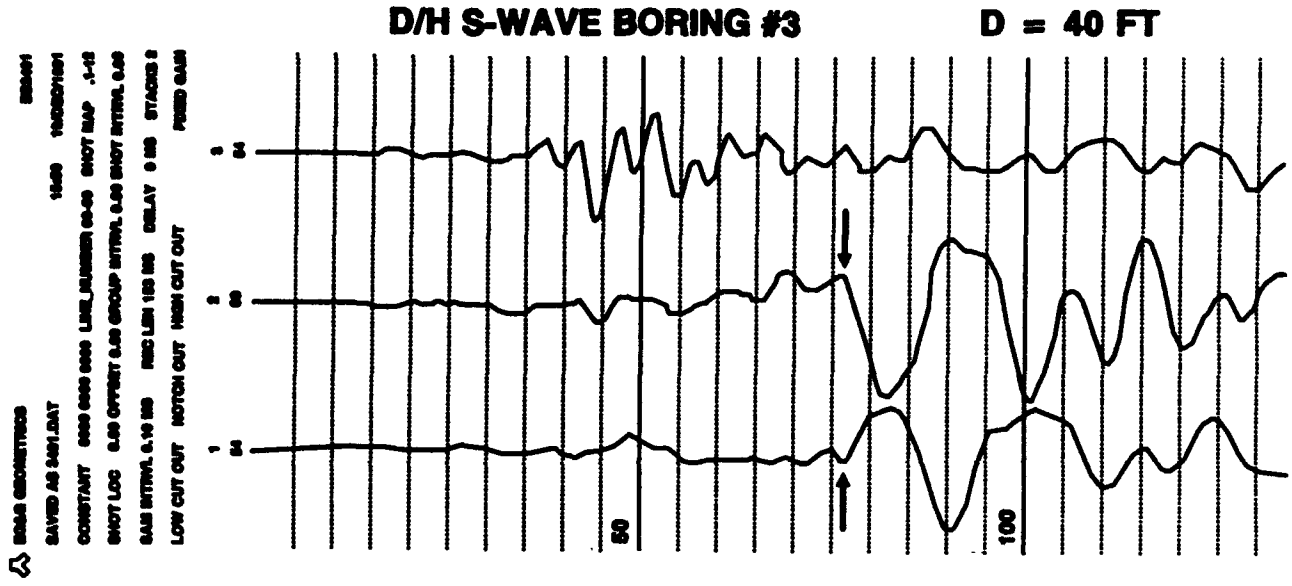

a. Downhole S-wave record obtained from stiking the east end of the board

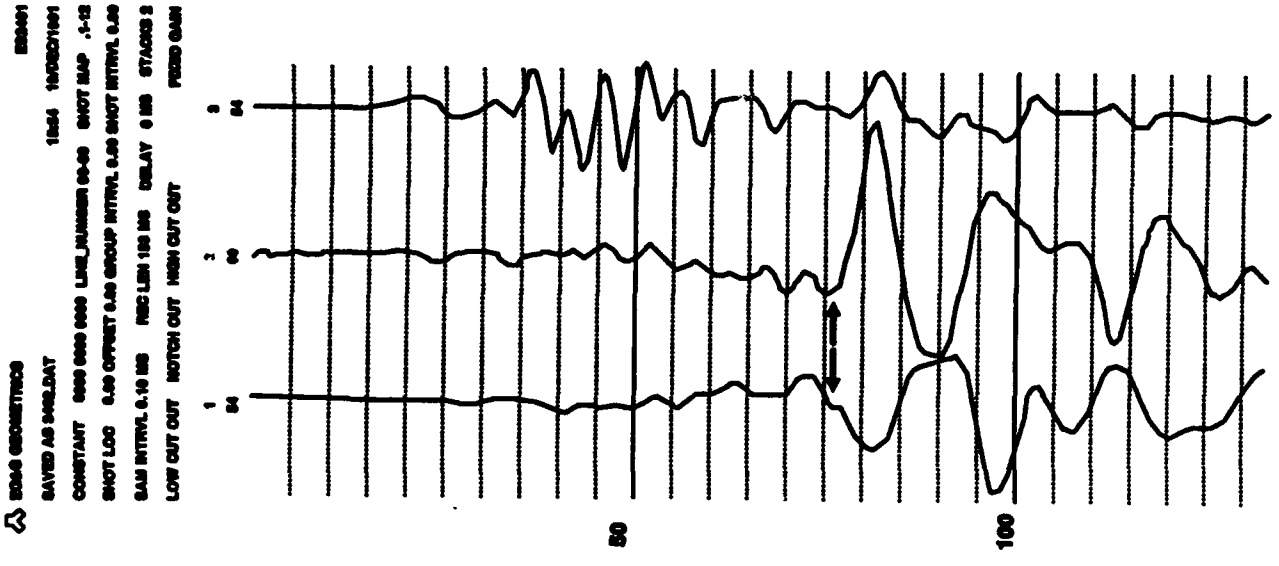

b. Downhole S-wave record obtained from stiking the west end of the board

Figure 11. Example of downhole S-wave trace reversals obtained by striking opposite ends of board

Figure 12. Vibratory truck used to conduct surface vibratory tests

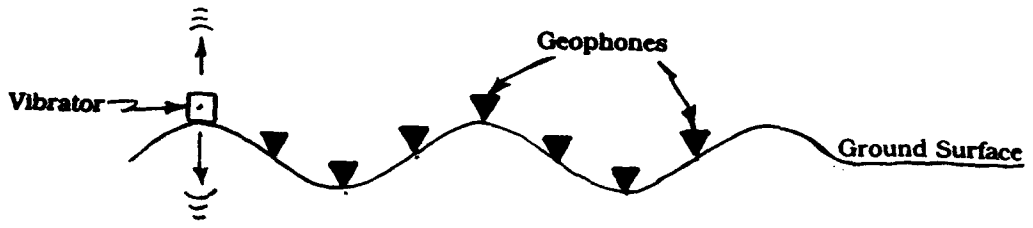

a. Vibrator exciting the ground surface

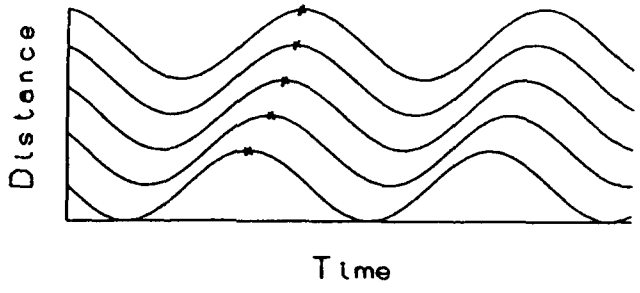

b. Geophone traces

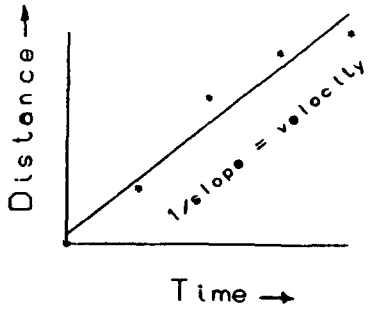

c. T-D plot

$$\lambda = V/f$$

where:

λ = wavelength

V = velocity

f = frequency

$$\text{depth} \approx \lambda/2$$

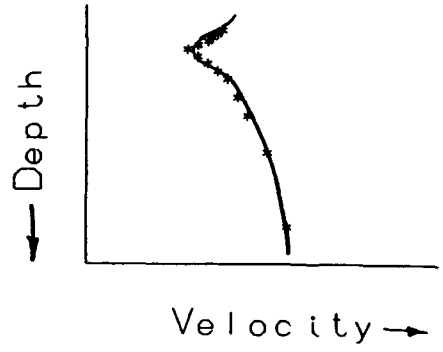

d. Velocity versus depth plot

Figure 13. Surface vibratory data reduction procedure

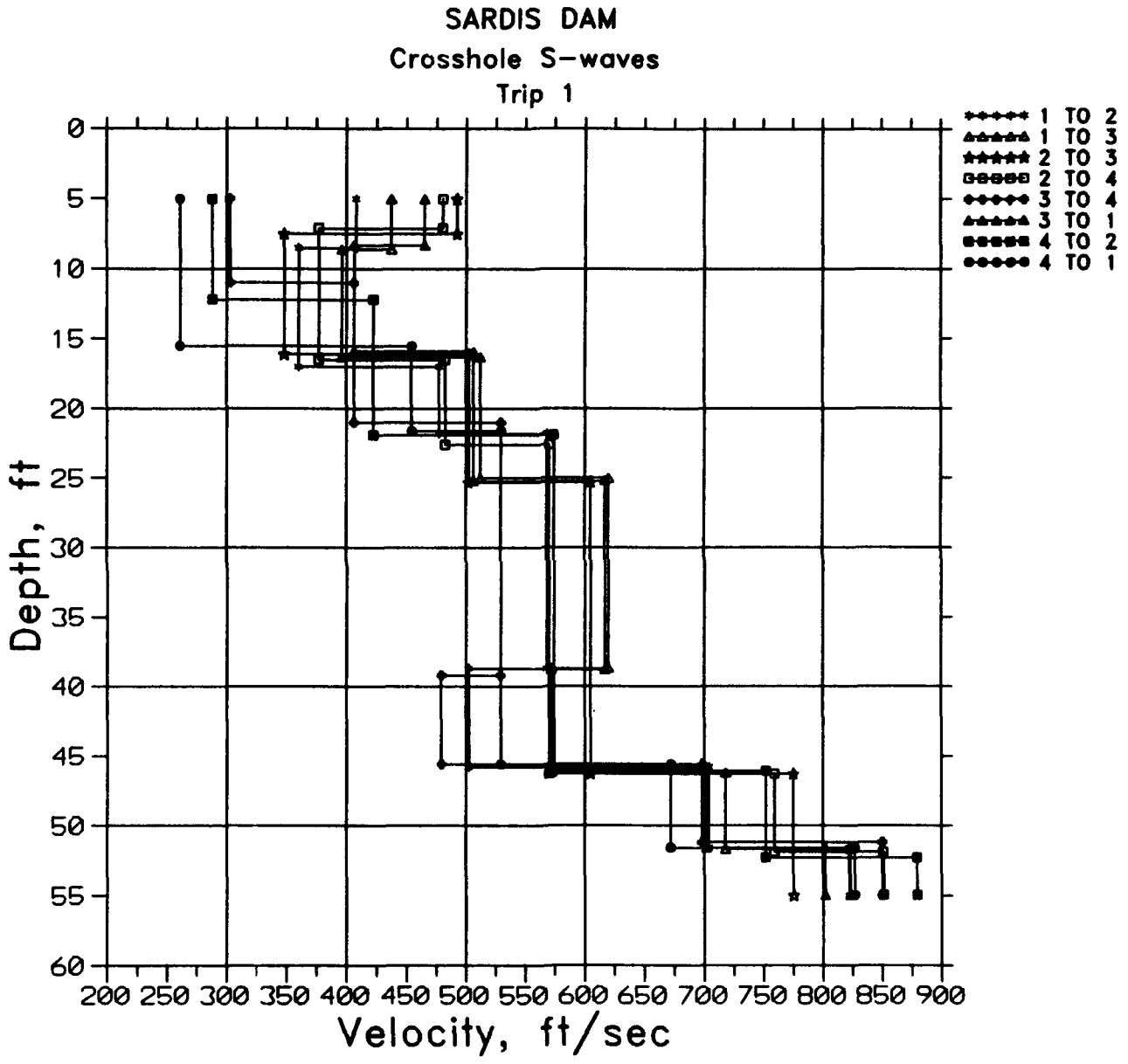

Figure 14. Crosshole S-wave velocity versus depth, Trip 1

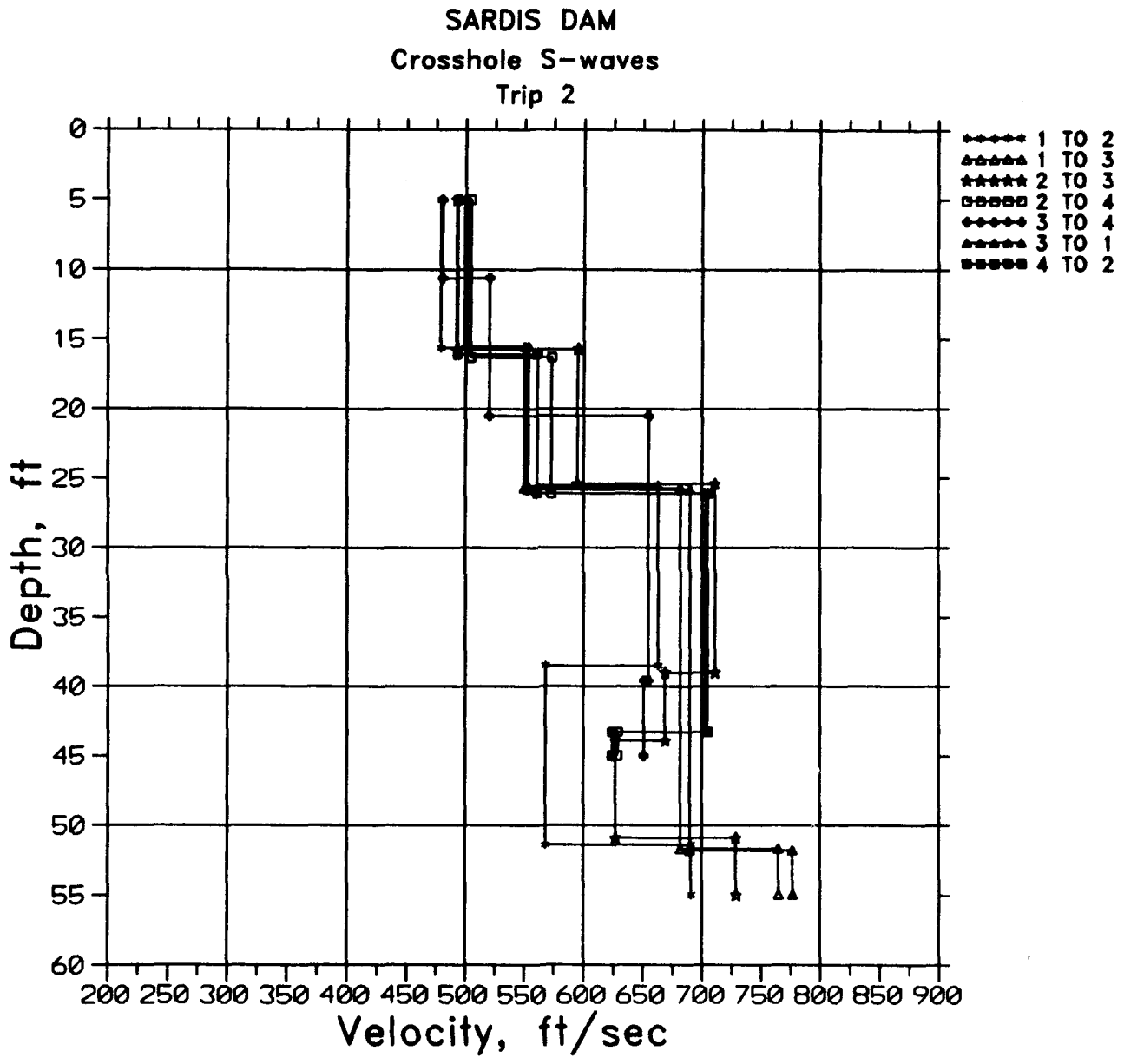

Figure 15. Crosshole S-wave velocity versus depth, Trip 2

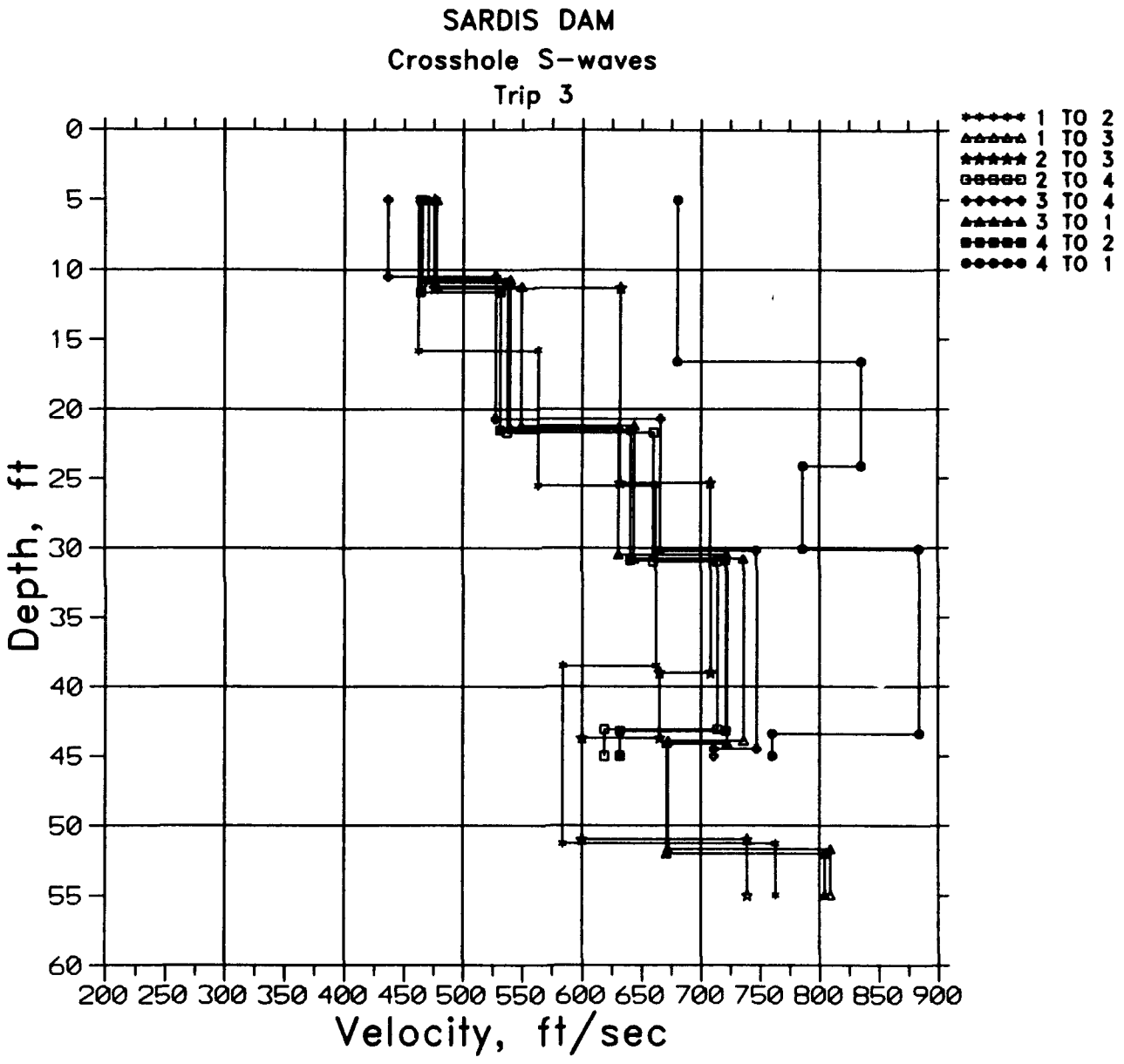

Figure 16. Crosshole S-wave velocity versus depth, Trip 3

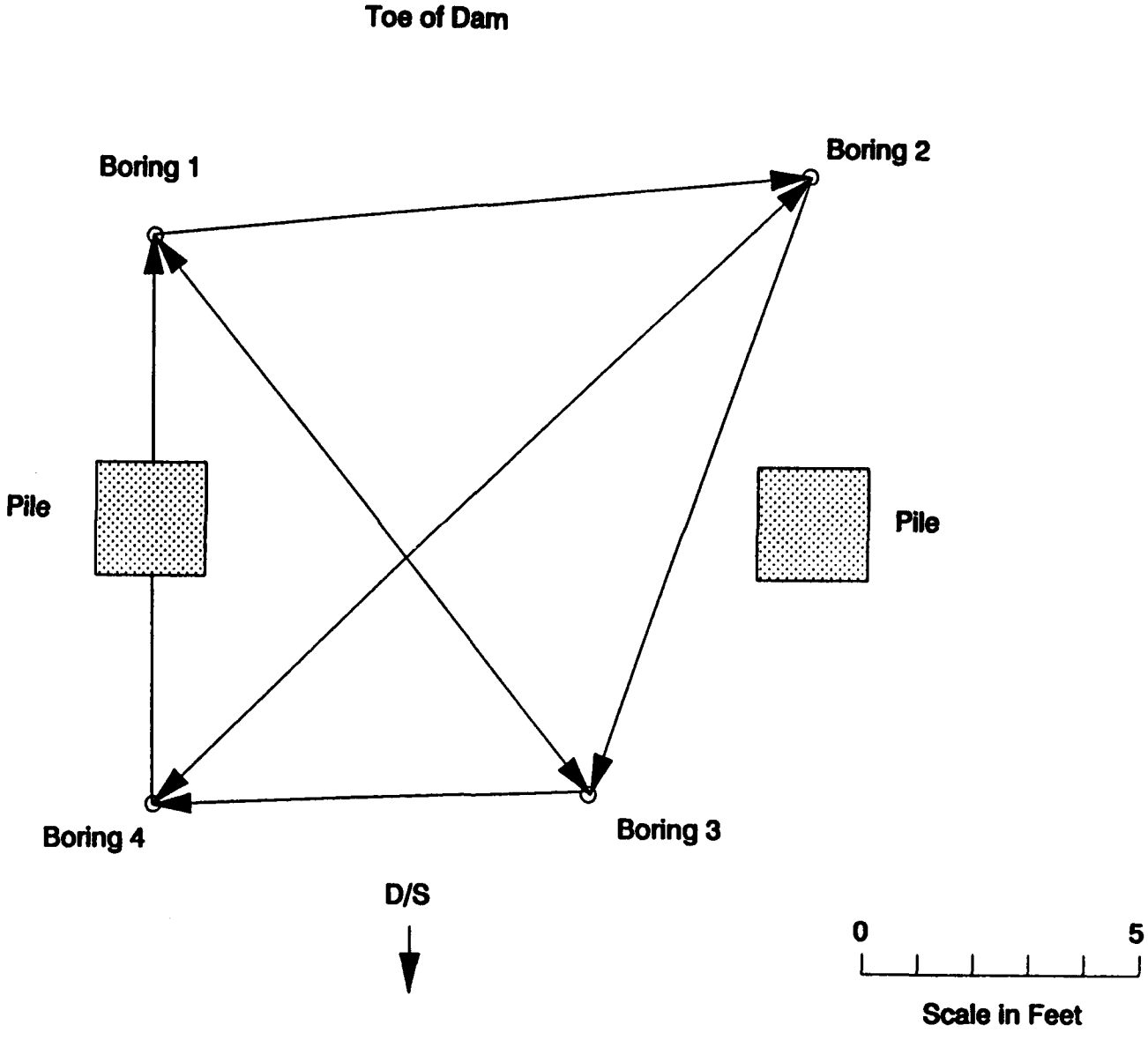

Figure 17. Position of piles relative to the crosshole borings

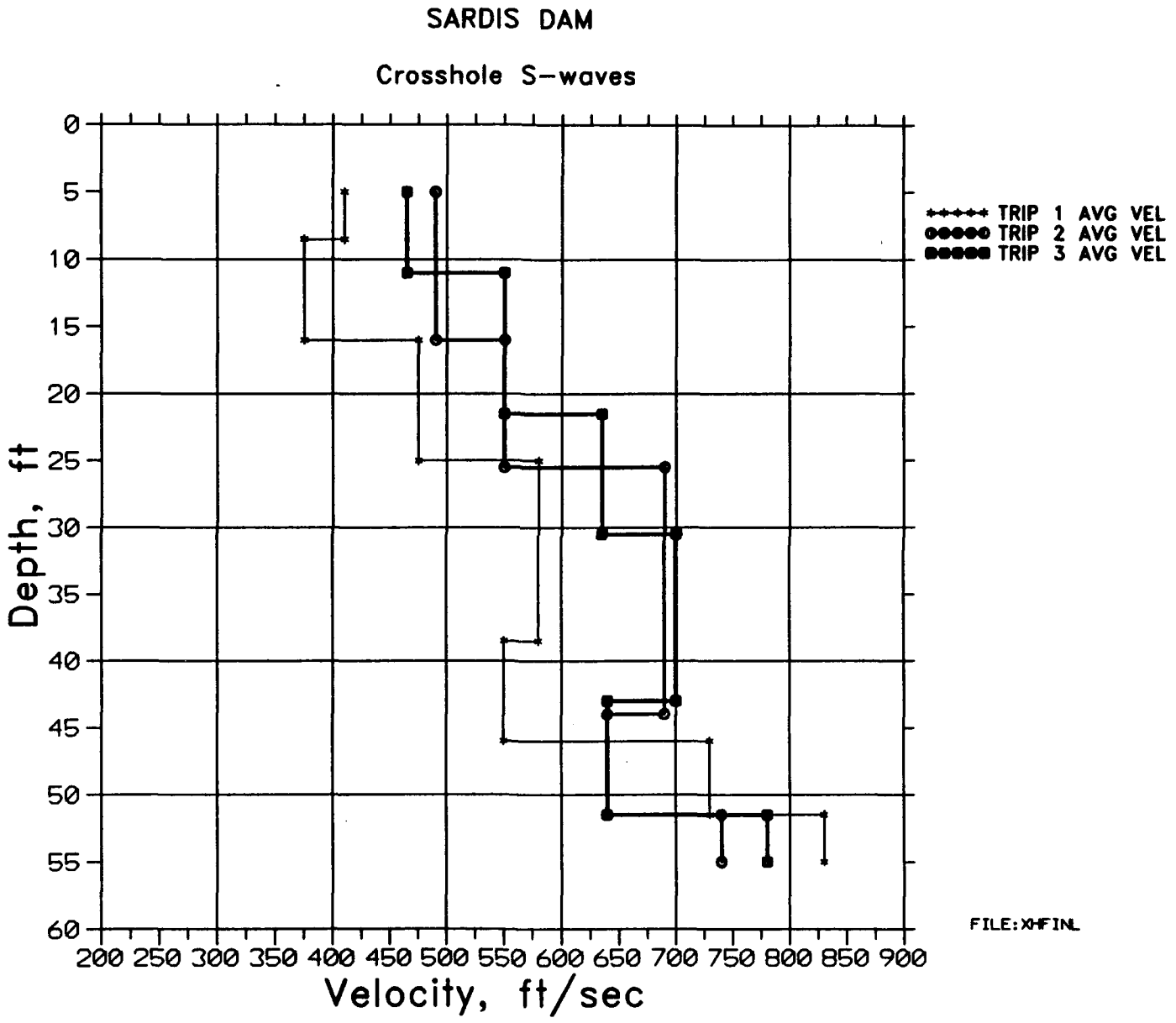

Figure 18. Average crosshole S-wave velocities for Trips 1, 2, and 3

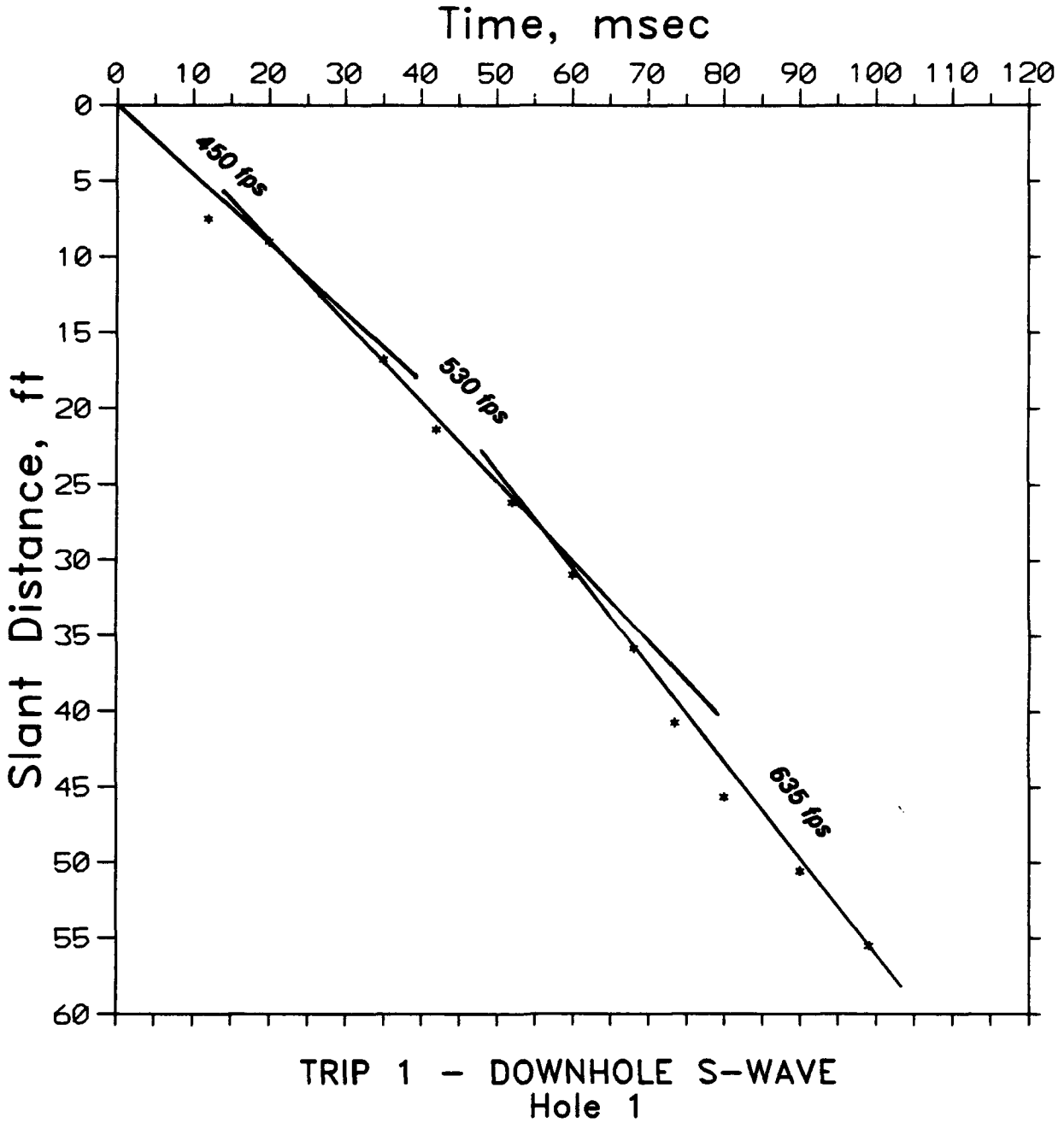

Figure 19. Downhole S-wave velocity versus depth, Trip 1, boring 1

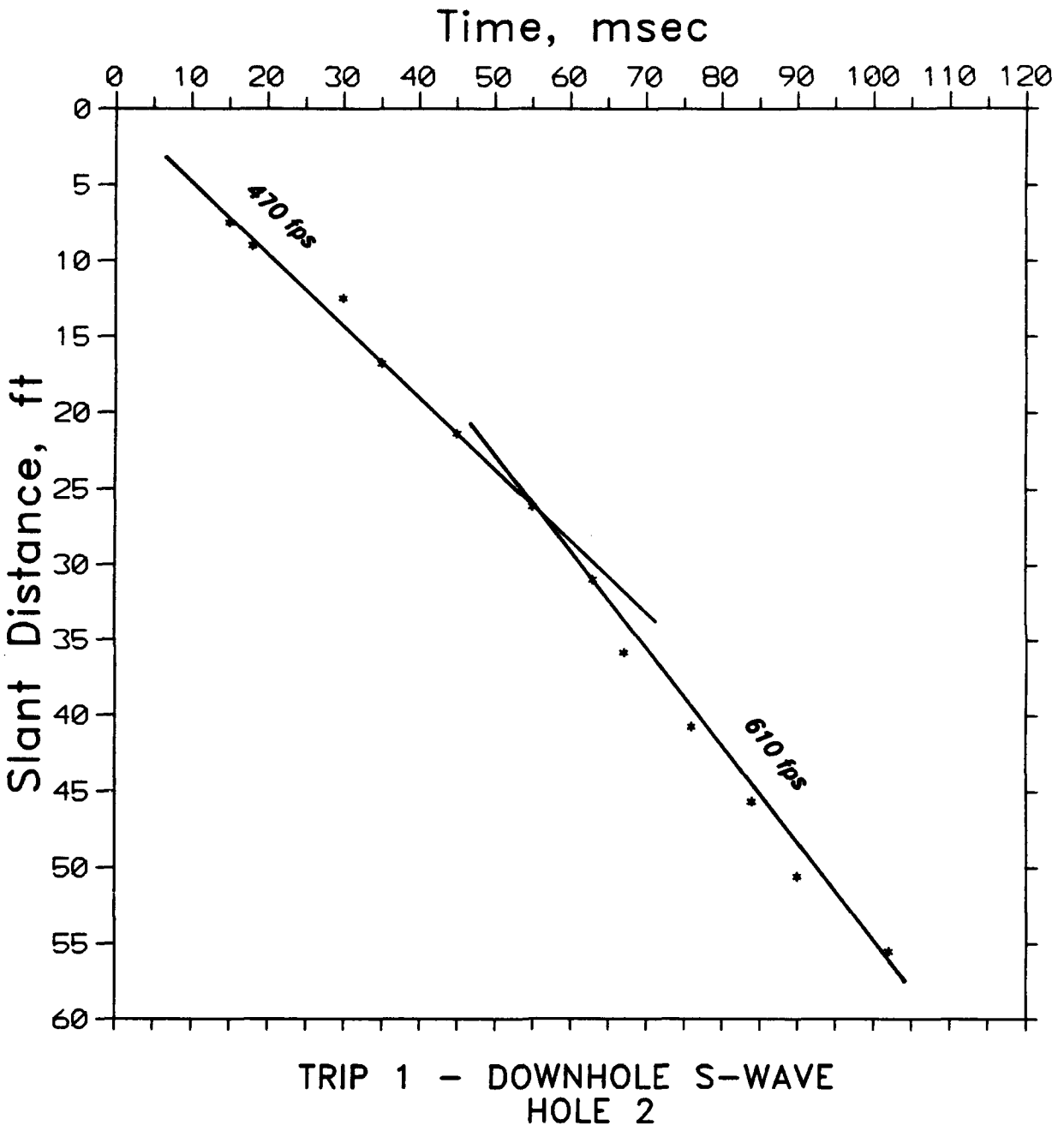

Figure 20. Downhole S-wave velocity versus depth, Trip 1, boring 2

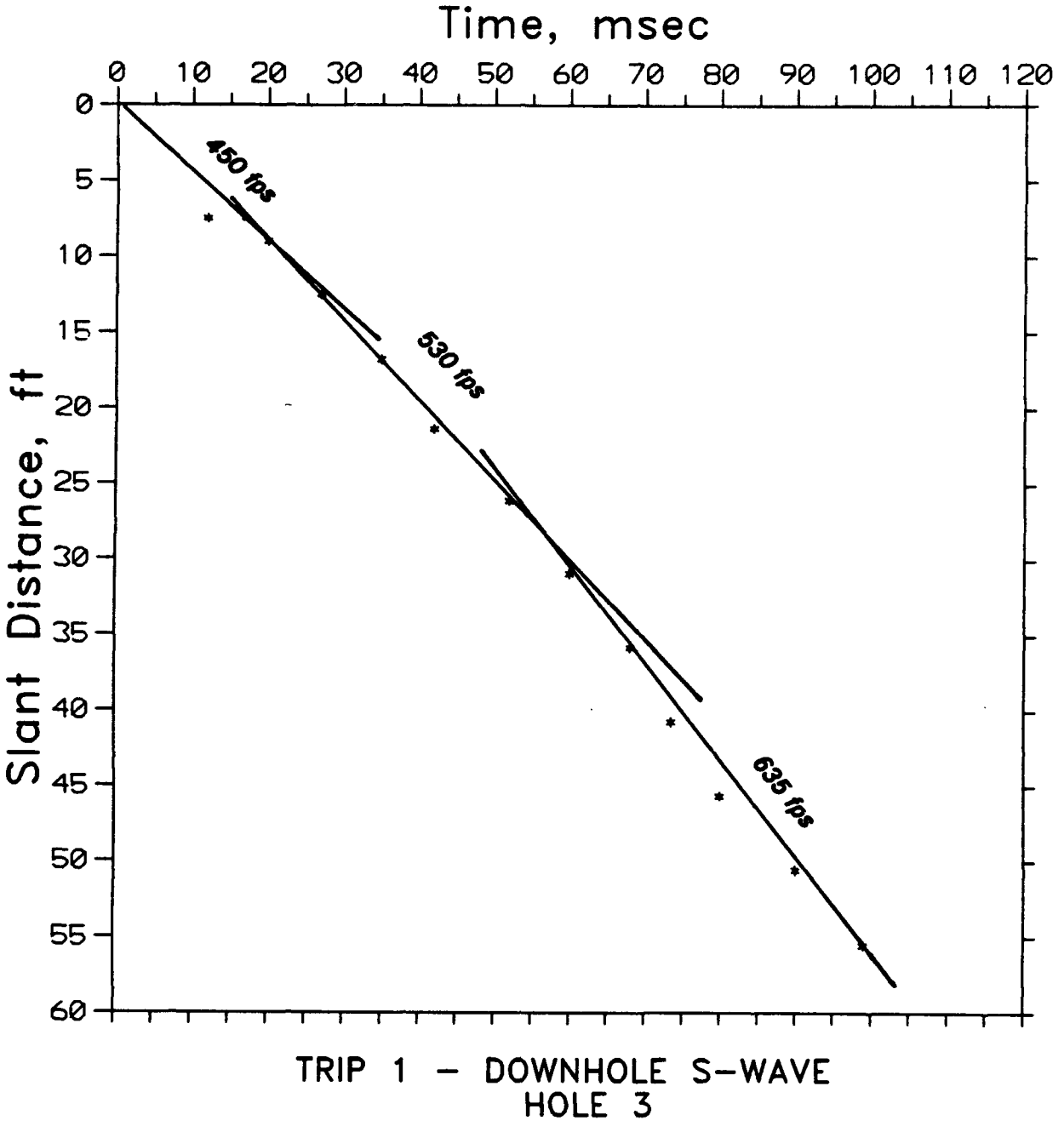

Figure 21. Downhole S-wave velocity versus depth, Trip 1, boring 3

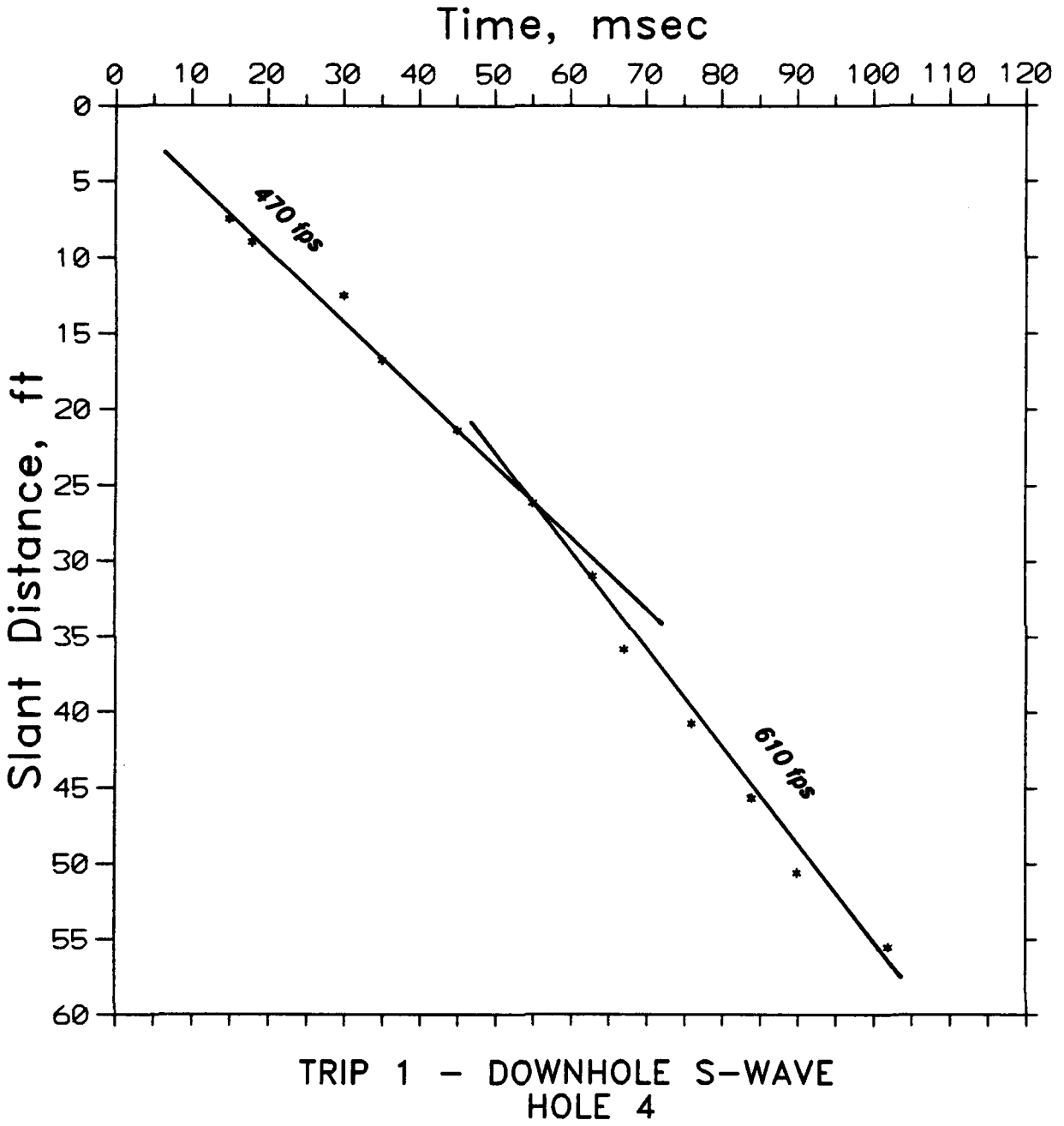

Figure 22. Downhole S-wave velocity versus depth, Trip 1, boring 4

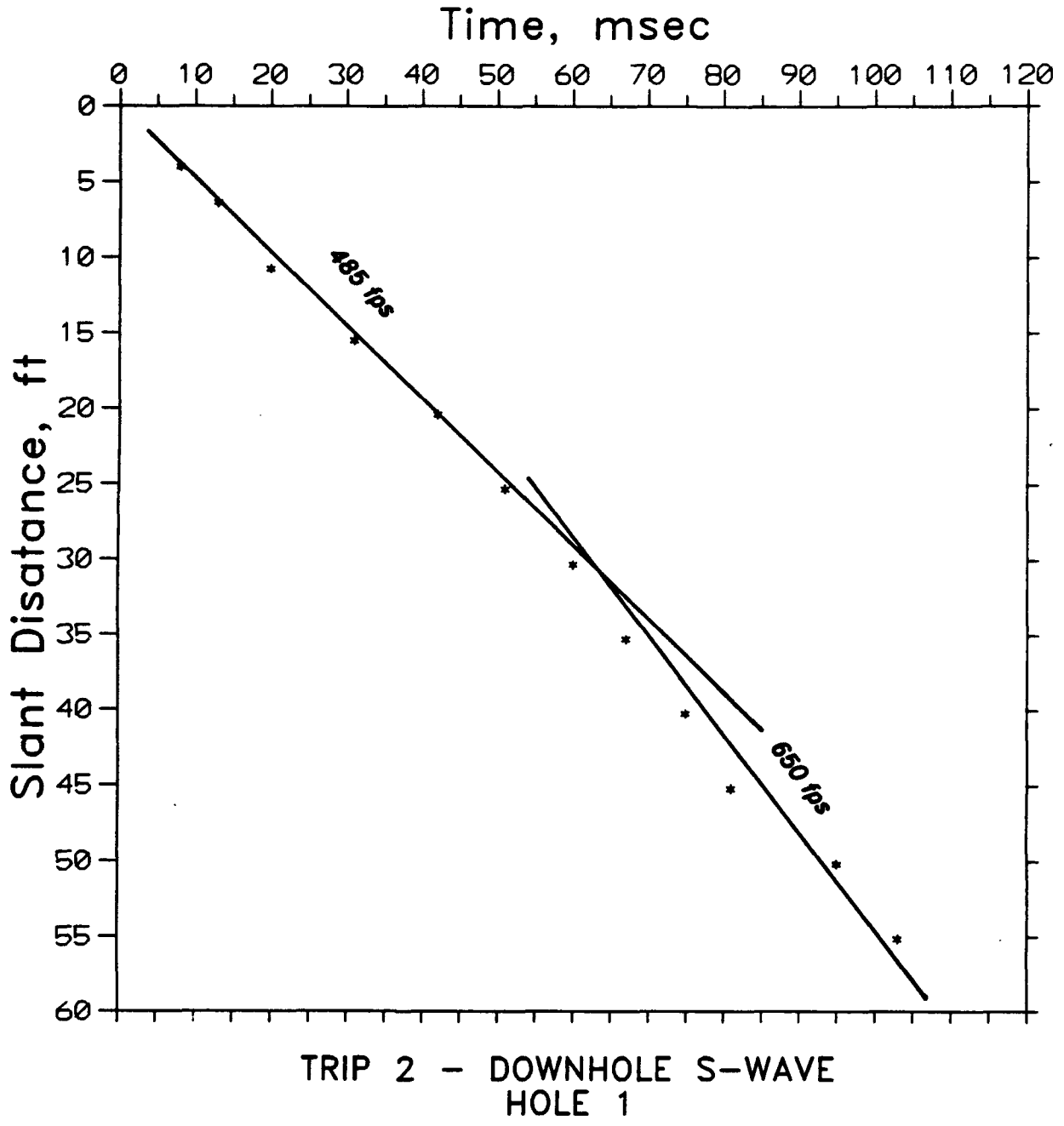

Figure 23. Downhole S-wave velocity versus depth, Trip 2, boring 1

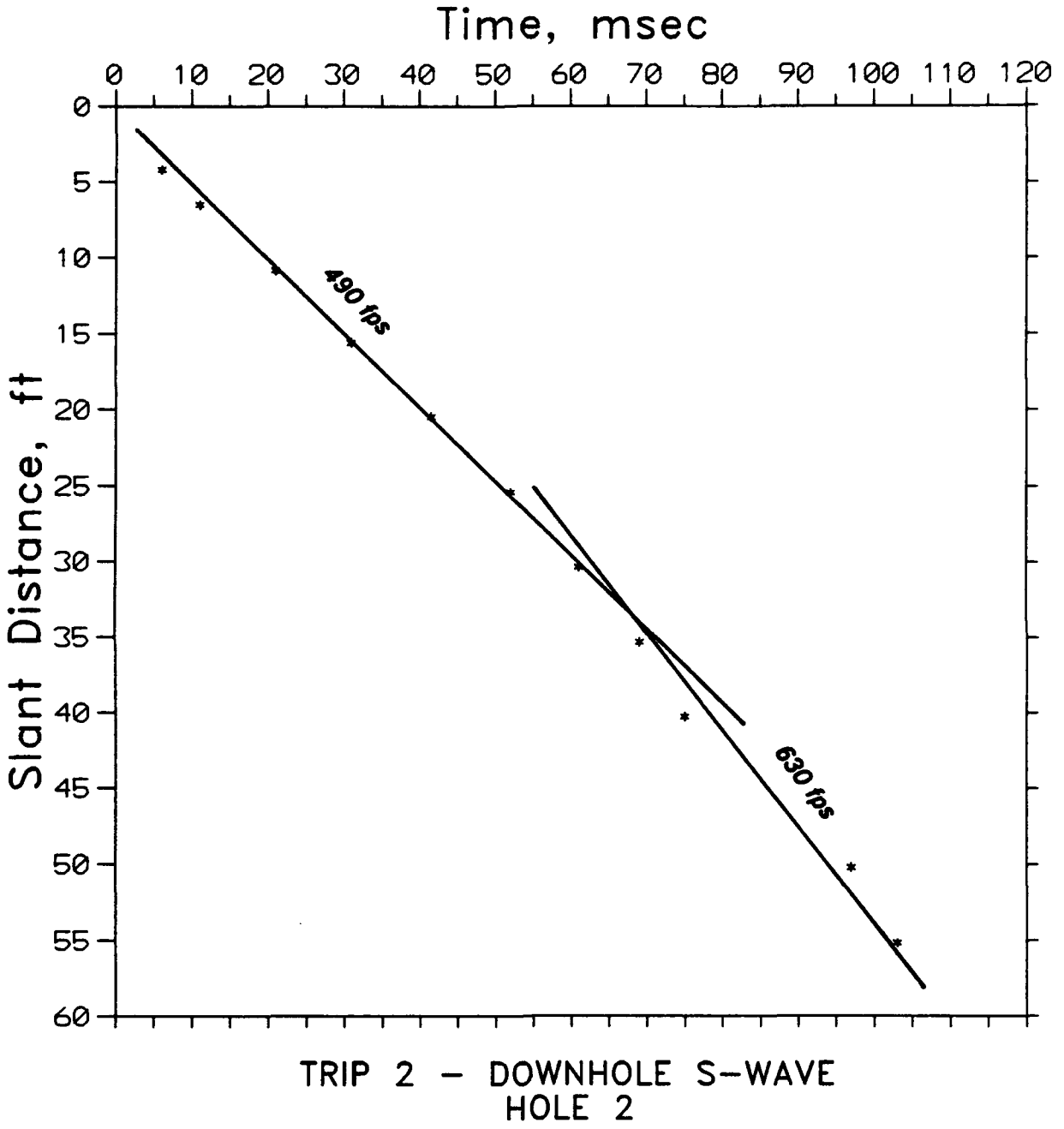

Figure 24. Downhole S-wave velocity versus depth, Trip 2, boring 2

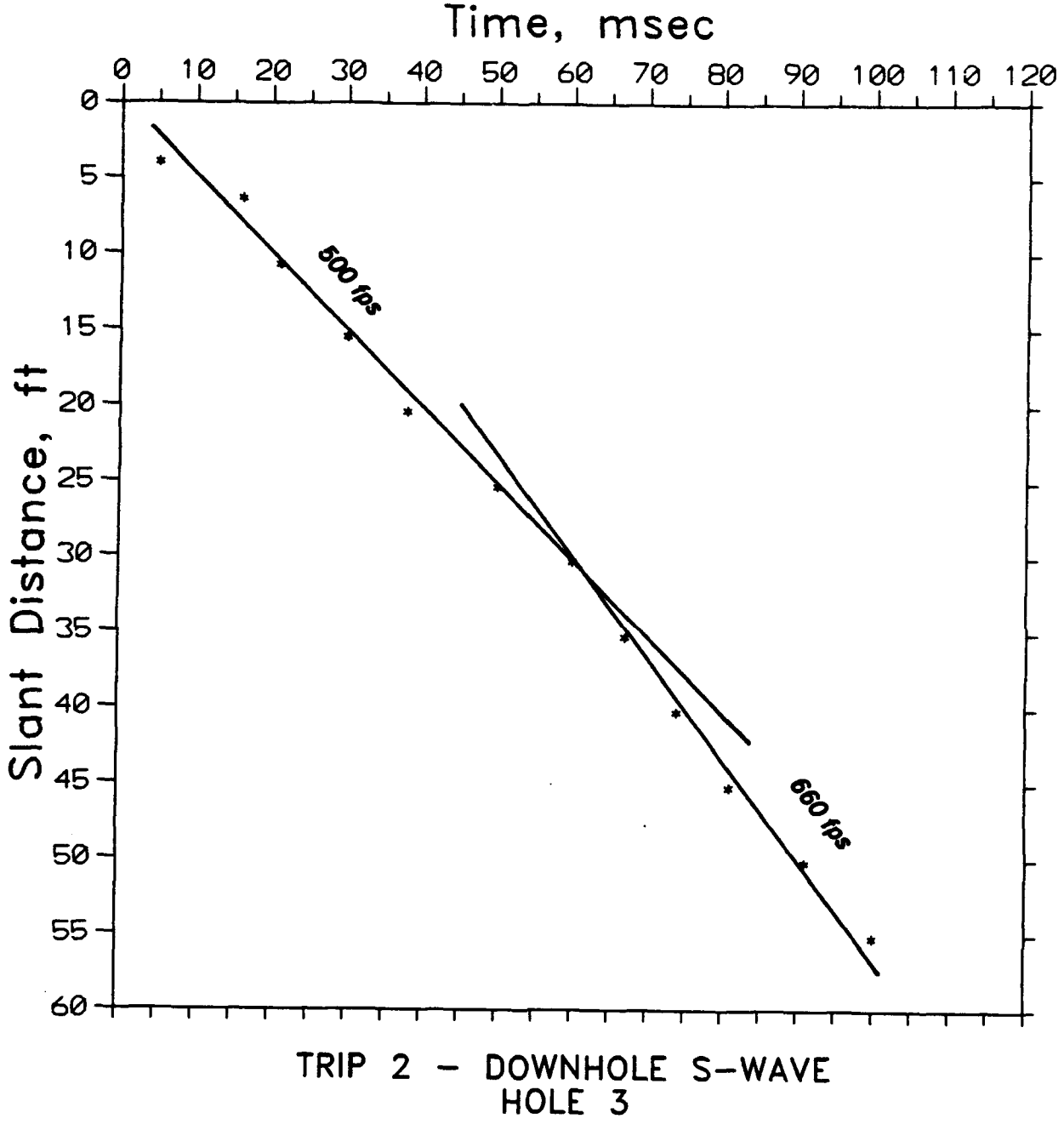

Figure 25. Downhole S-wave velocity versus depth, Trip 2, boring 3

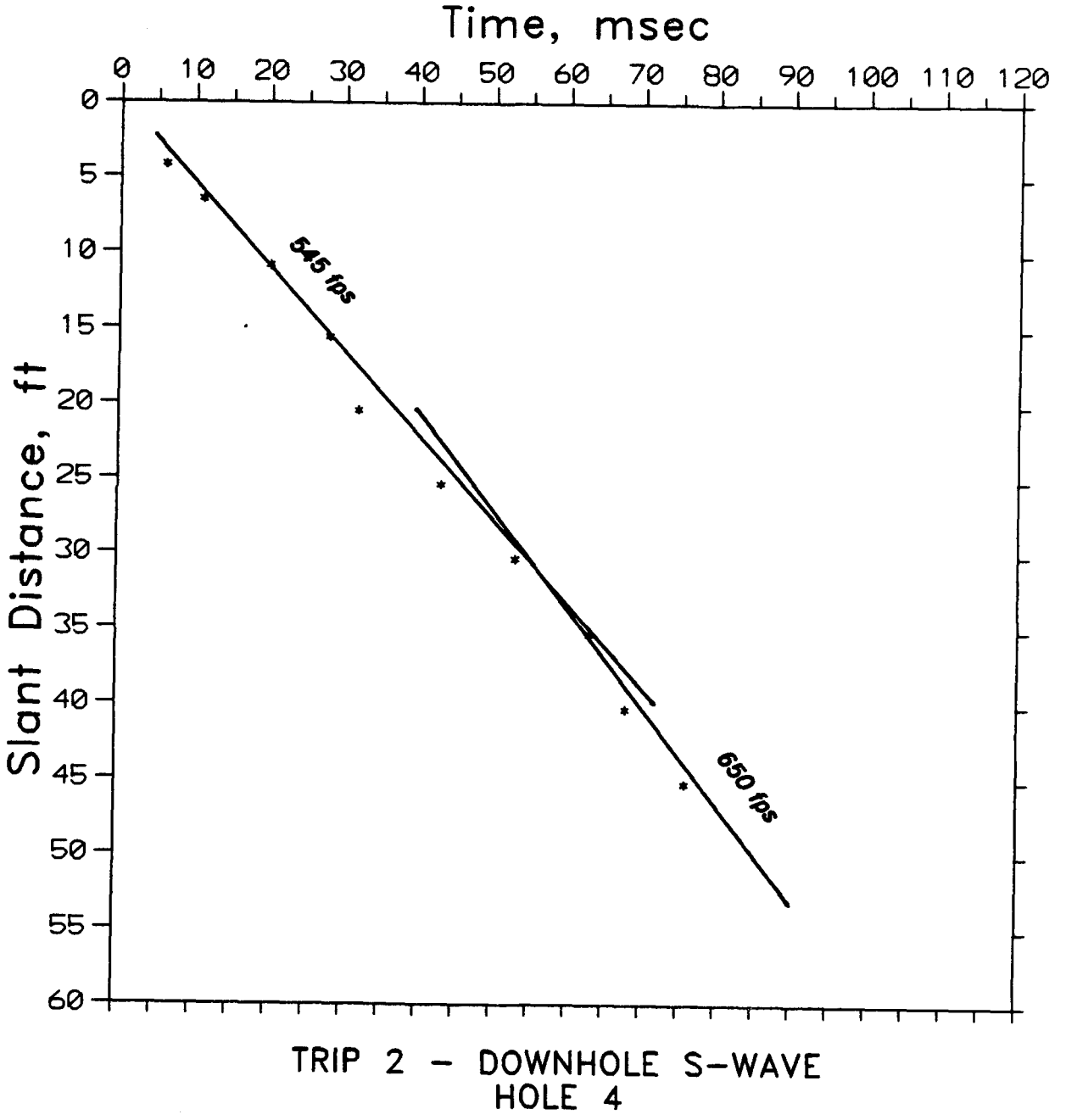

Figure 26. Downhole S-wave velocity versus depth, Trip 2, boring 4

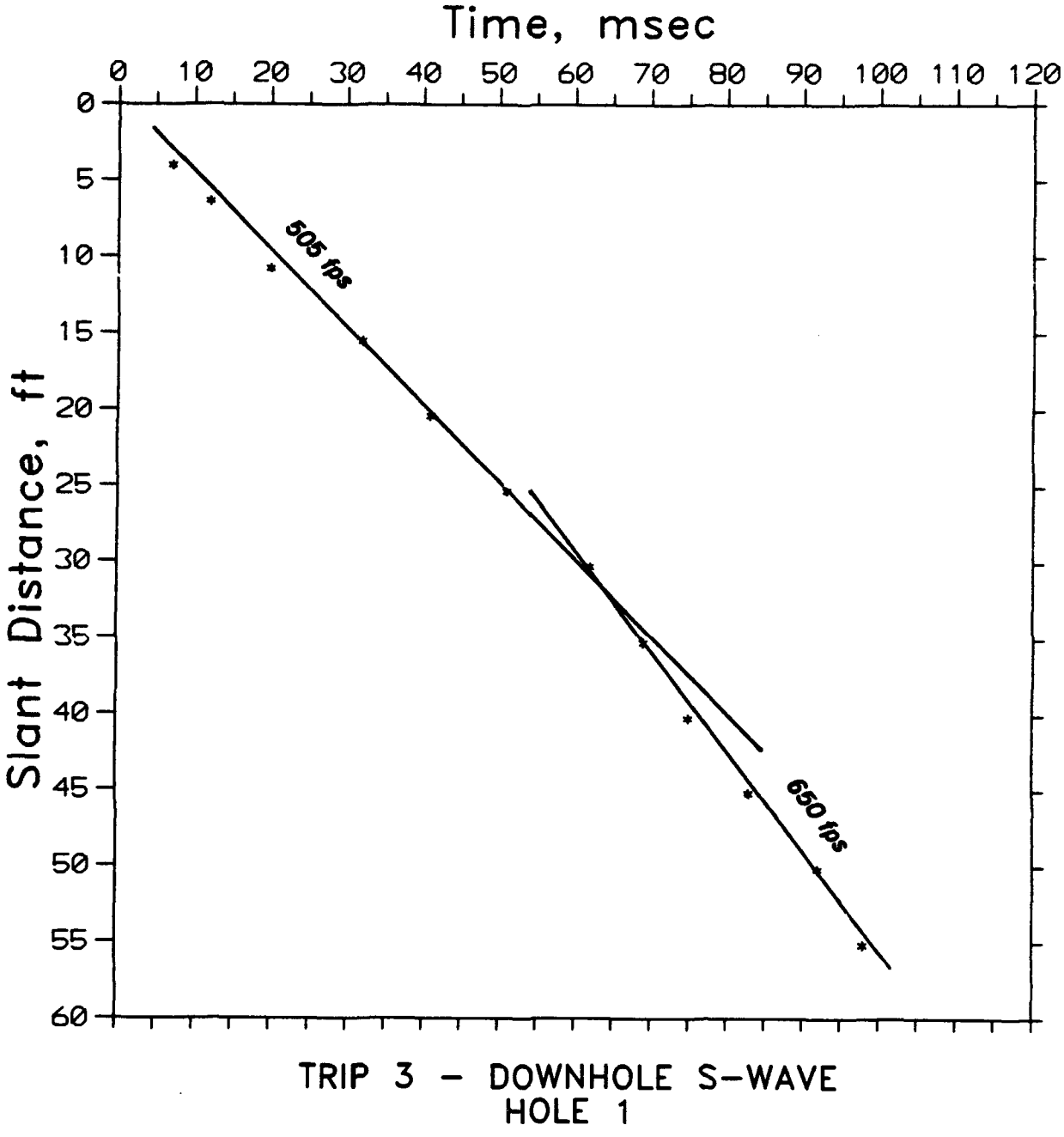

Figure 27. Downhole S-wave velocity versus depth, Trip 3, boring 1

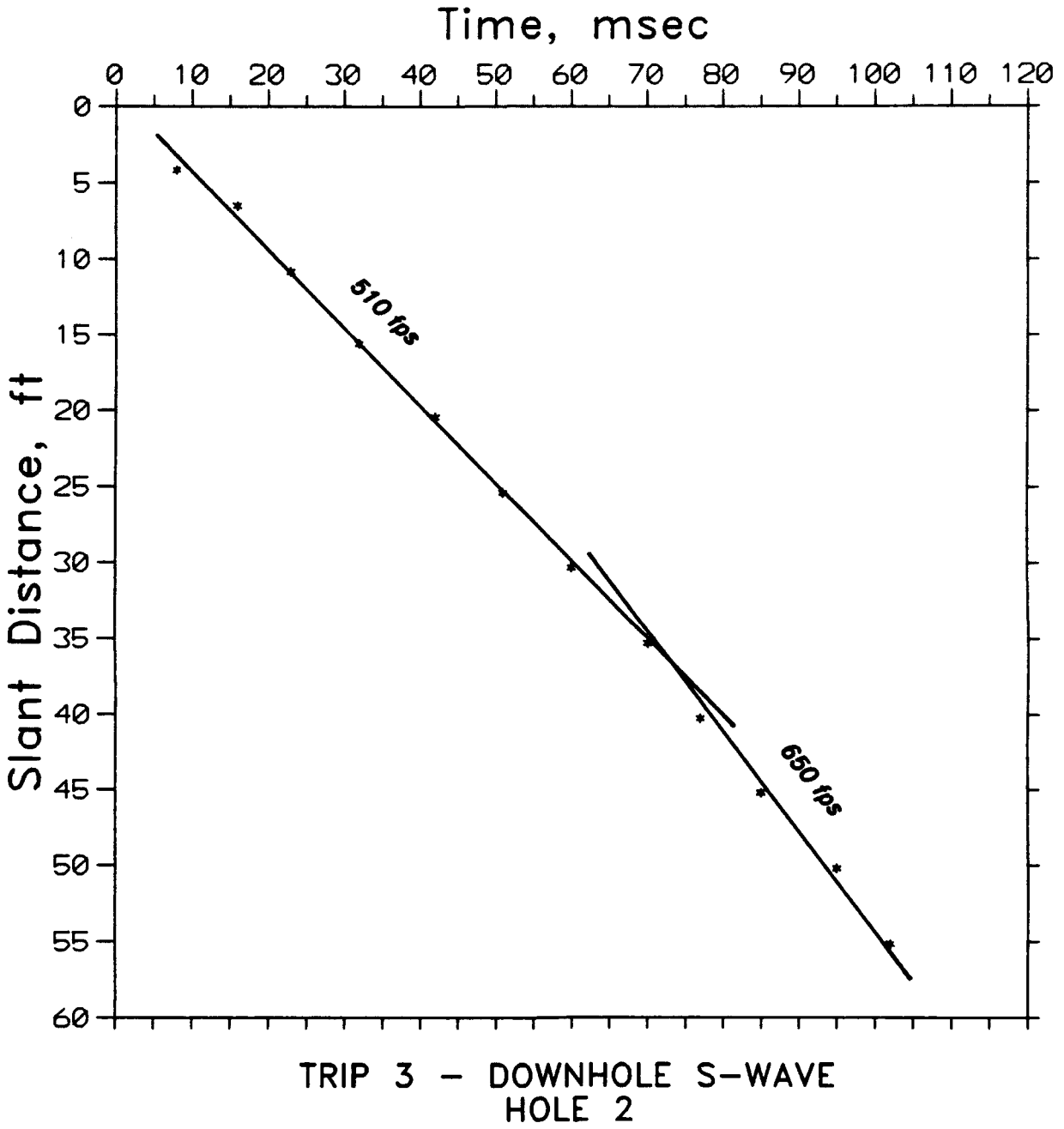

Figure 28. Downhole S-wave velocity versus depth, Trip 3, boring 2

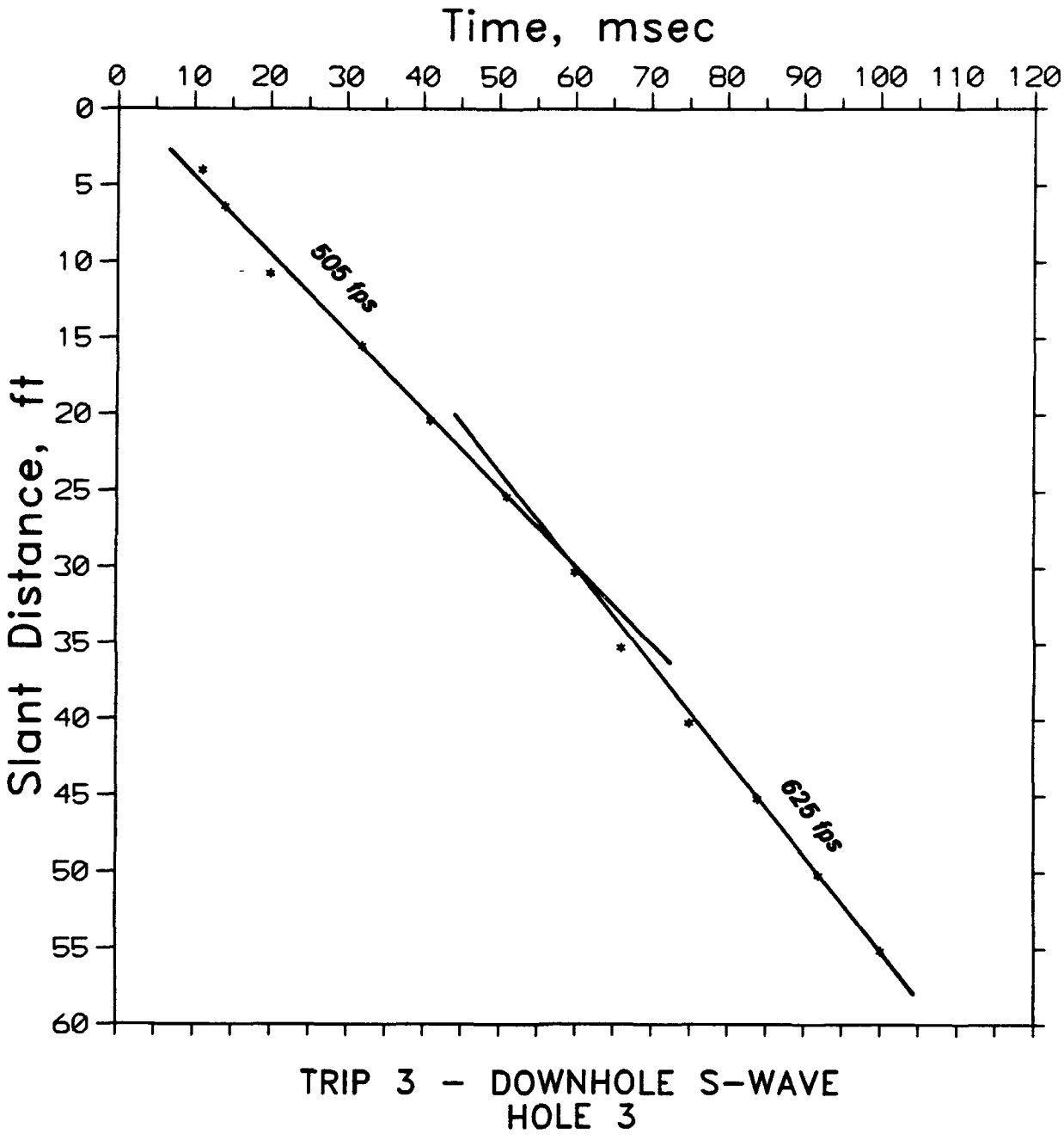

Figure 29. Downhole S-wave velocity versus depth, Trip 3, boring 3

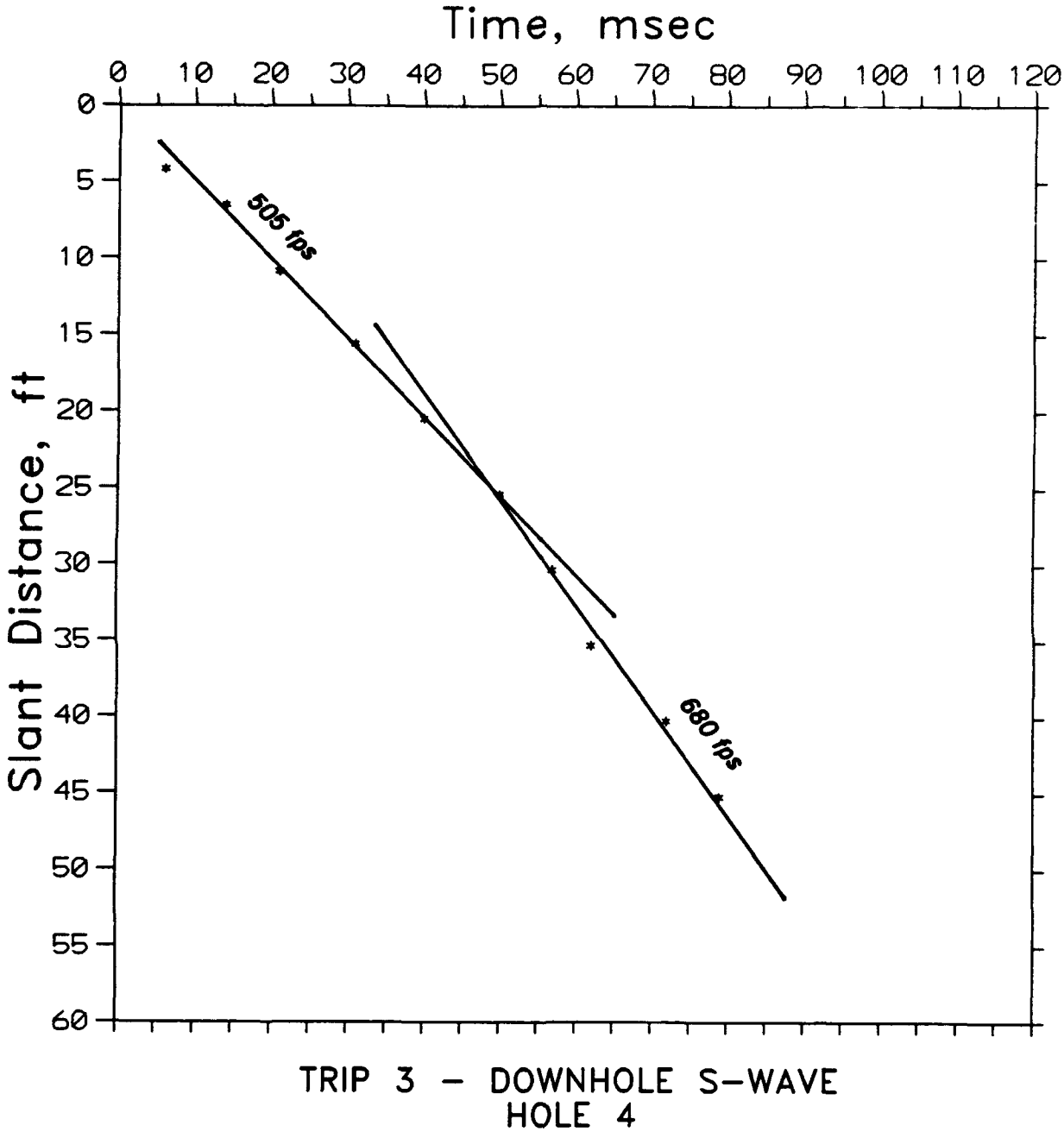

Figure 30. Downhole S-wave velocity versus depth, Trip 3, boring 4

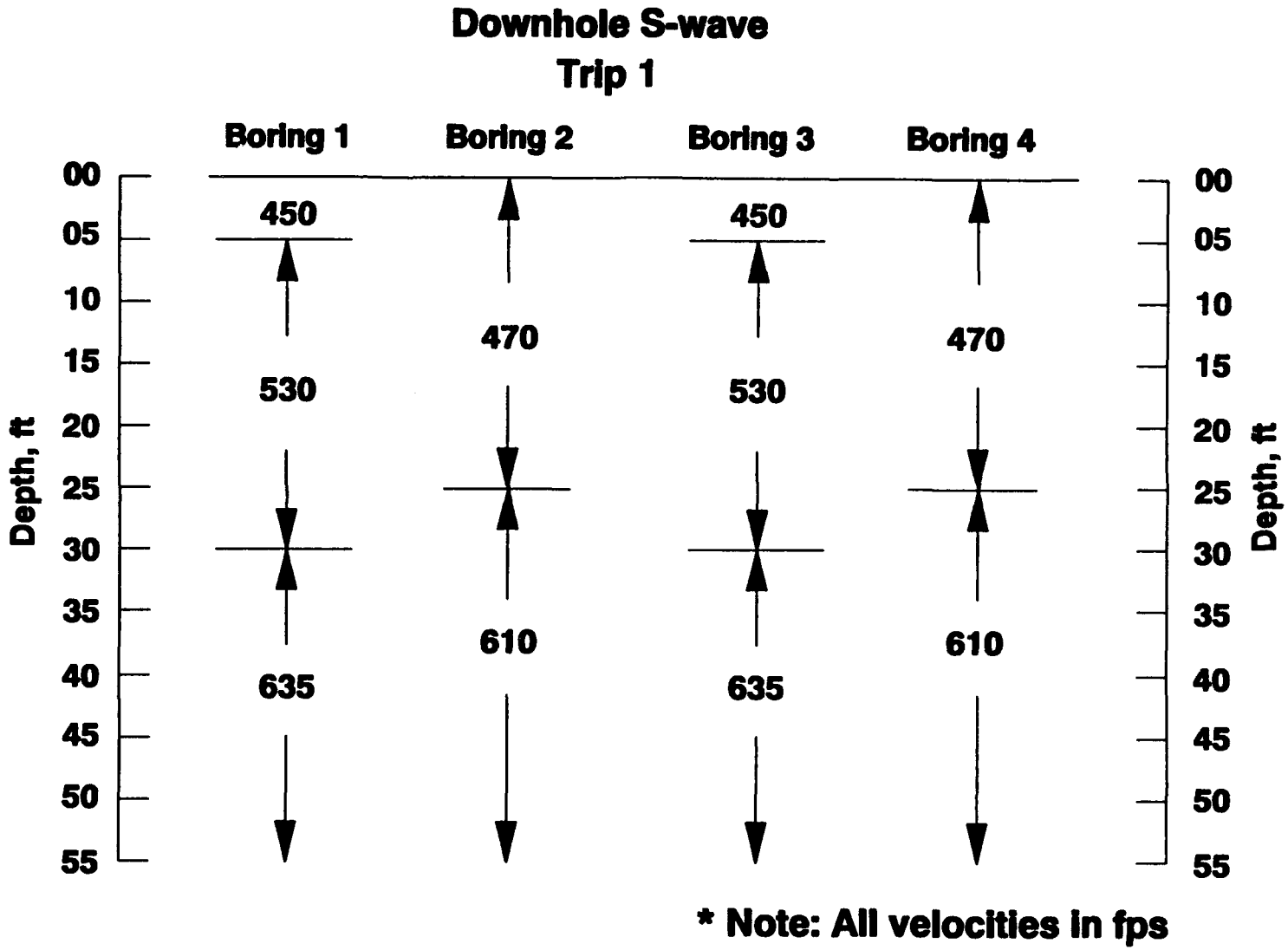

Figure 31. Downhole S-wave composite, Trip 1

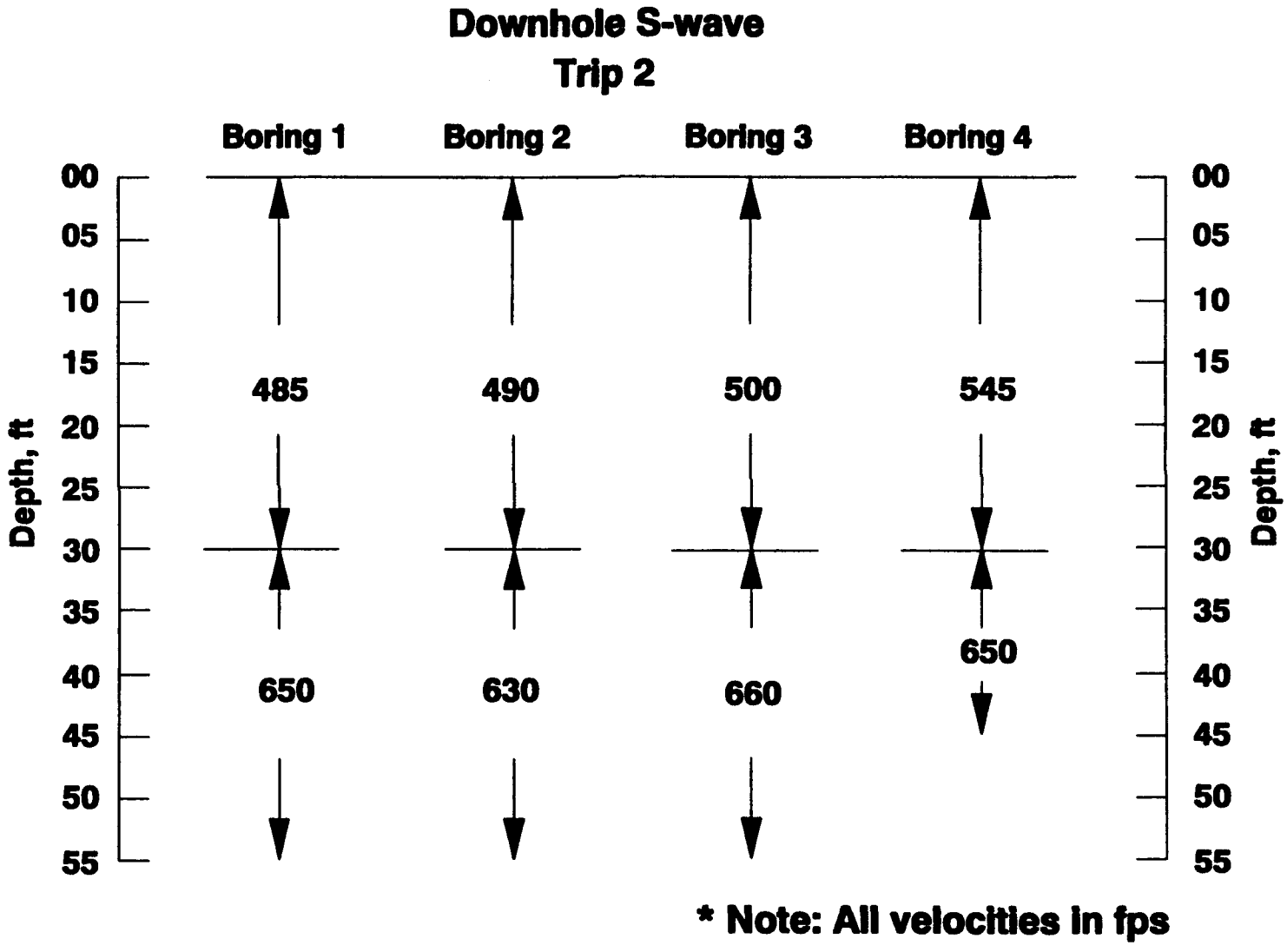

Figure 32. Downhole S-wave composite, Trip 2

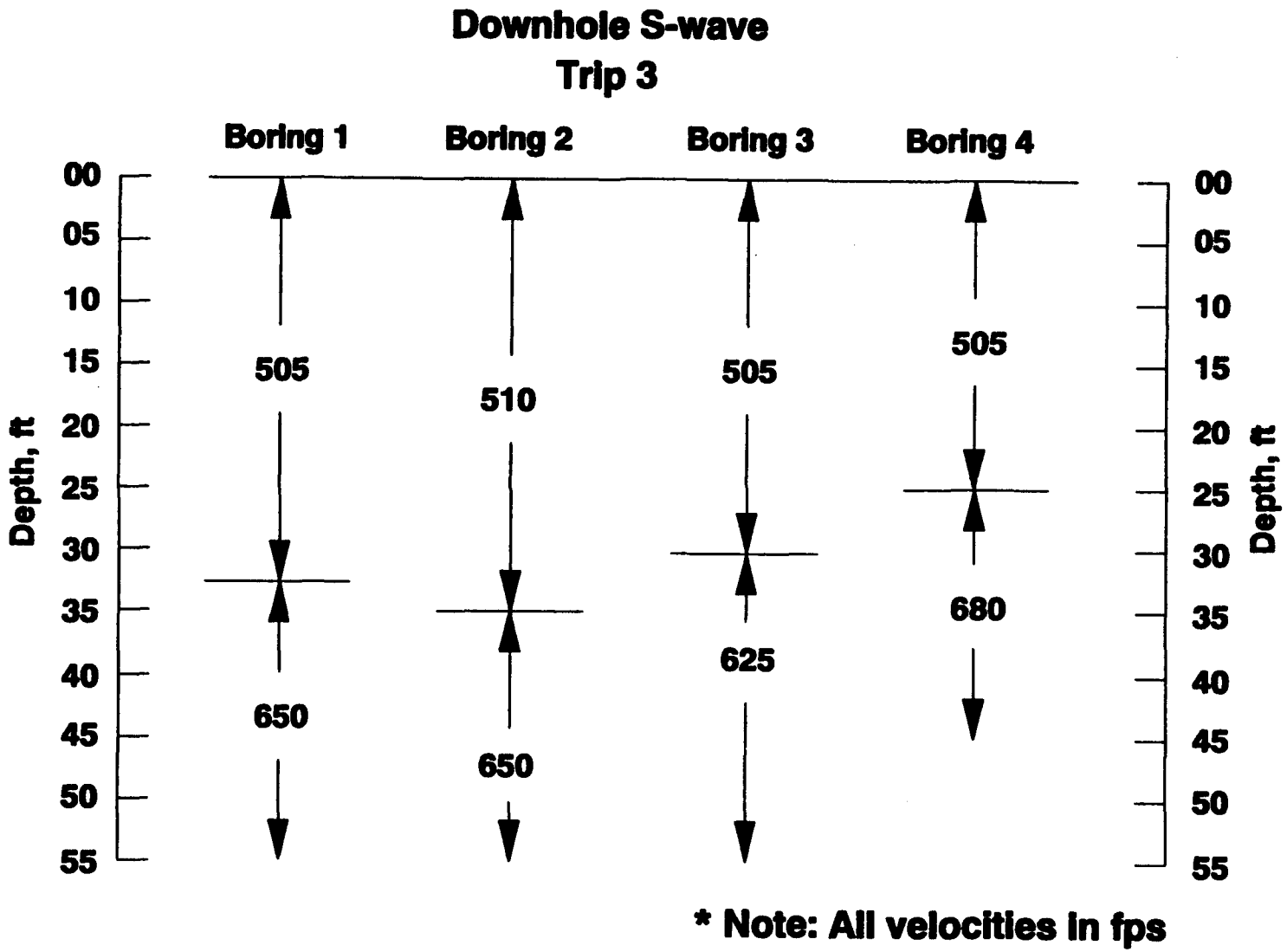

Figure 33. Downhole S-wave composite, Trip 3

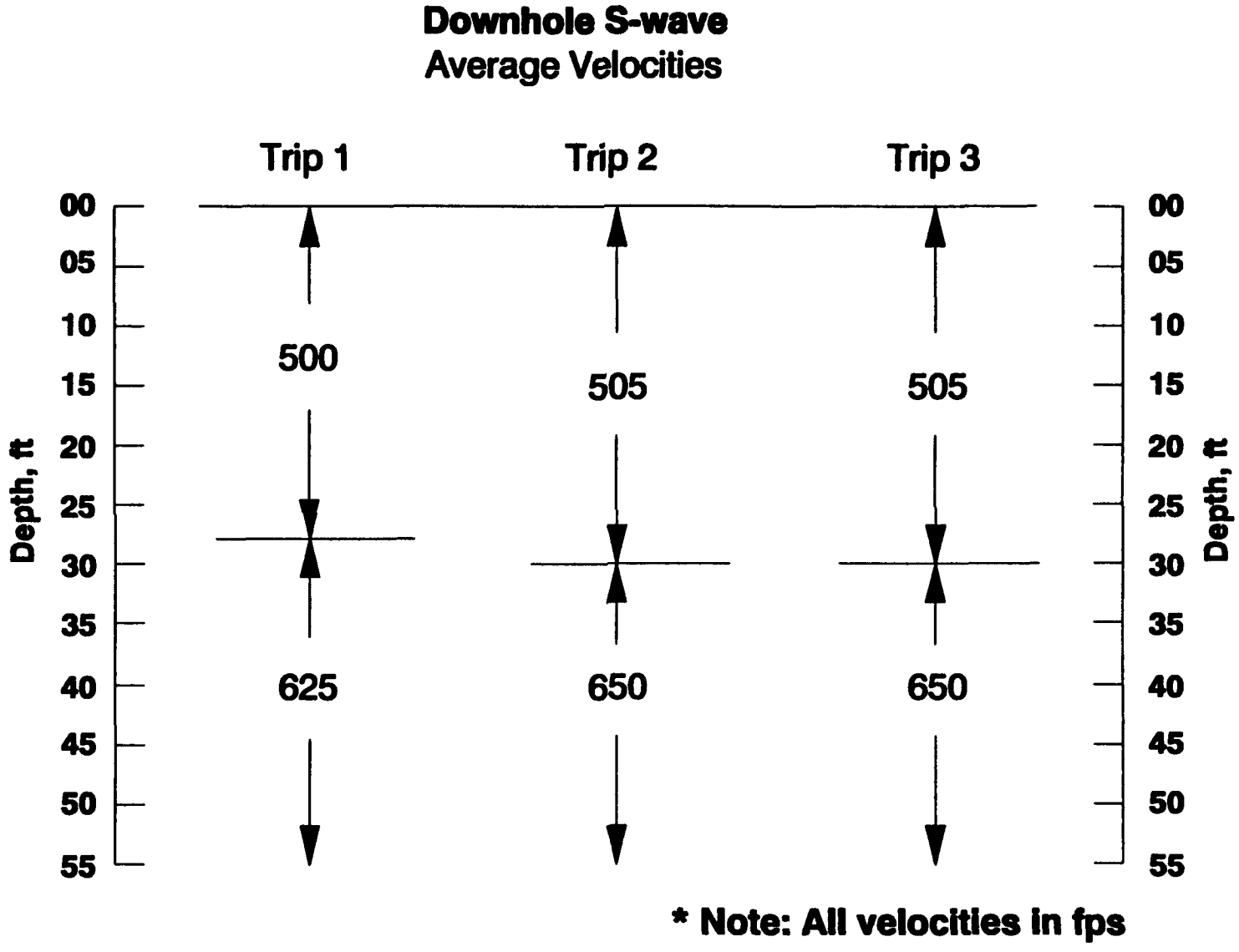

Figure 34. Average downhole S-wave velocities for Trips 1, 2, and 3

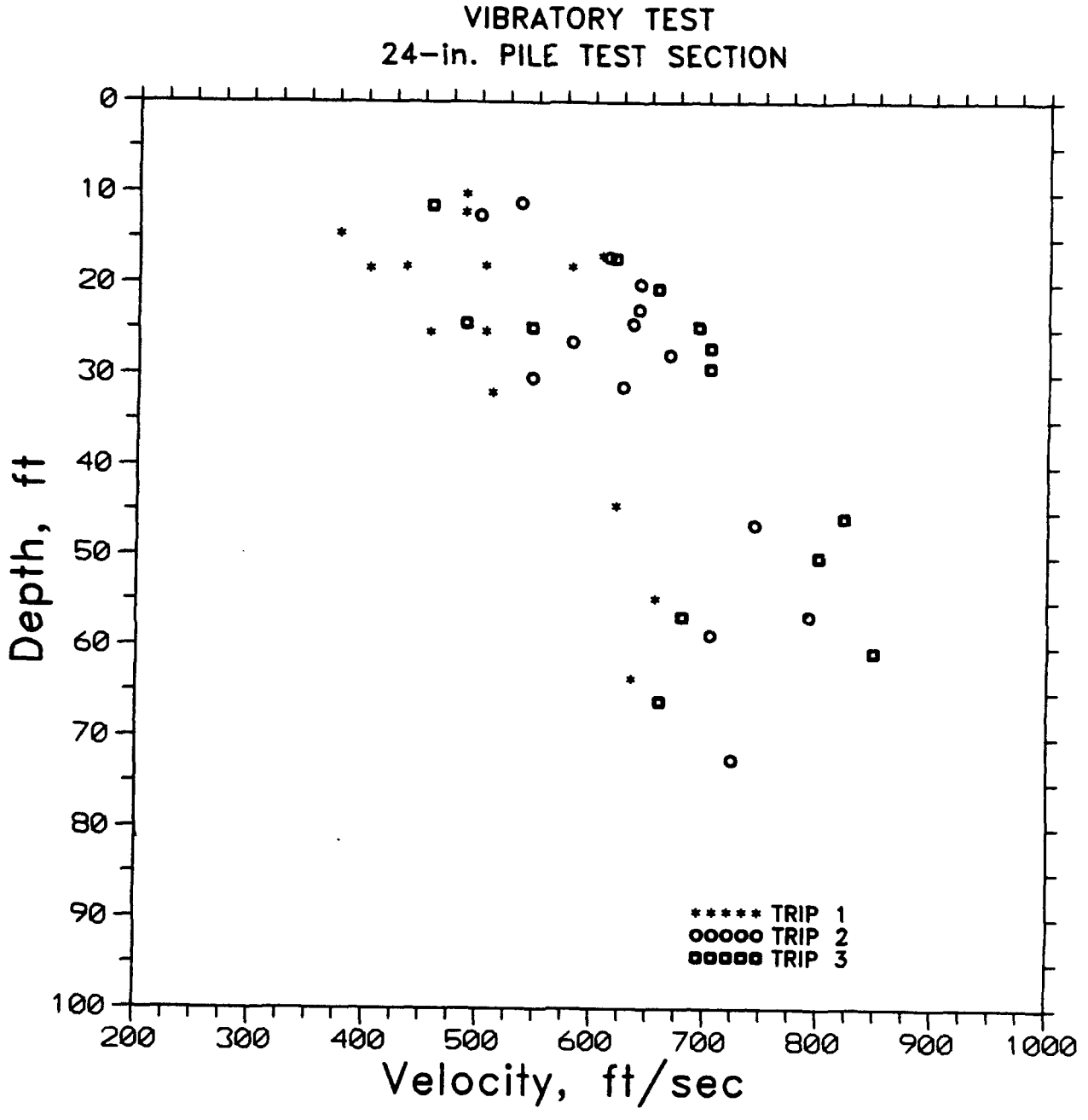

Figure 35. R-wave velocity versus depth, Line 1, 24-in pile test section, Trips 1, 2, and 3

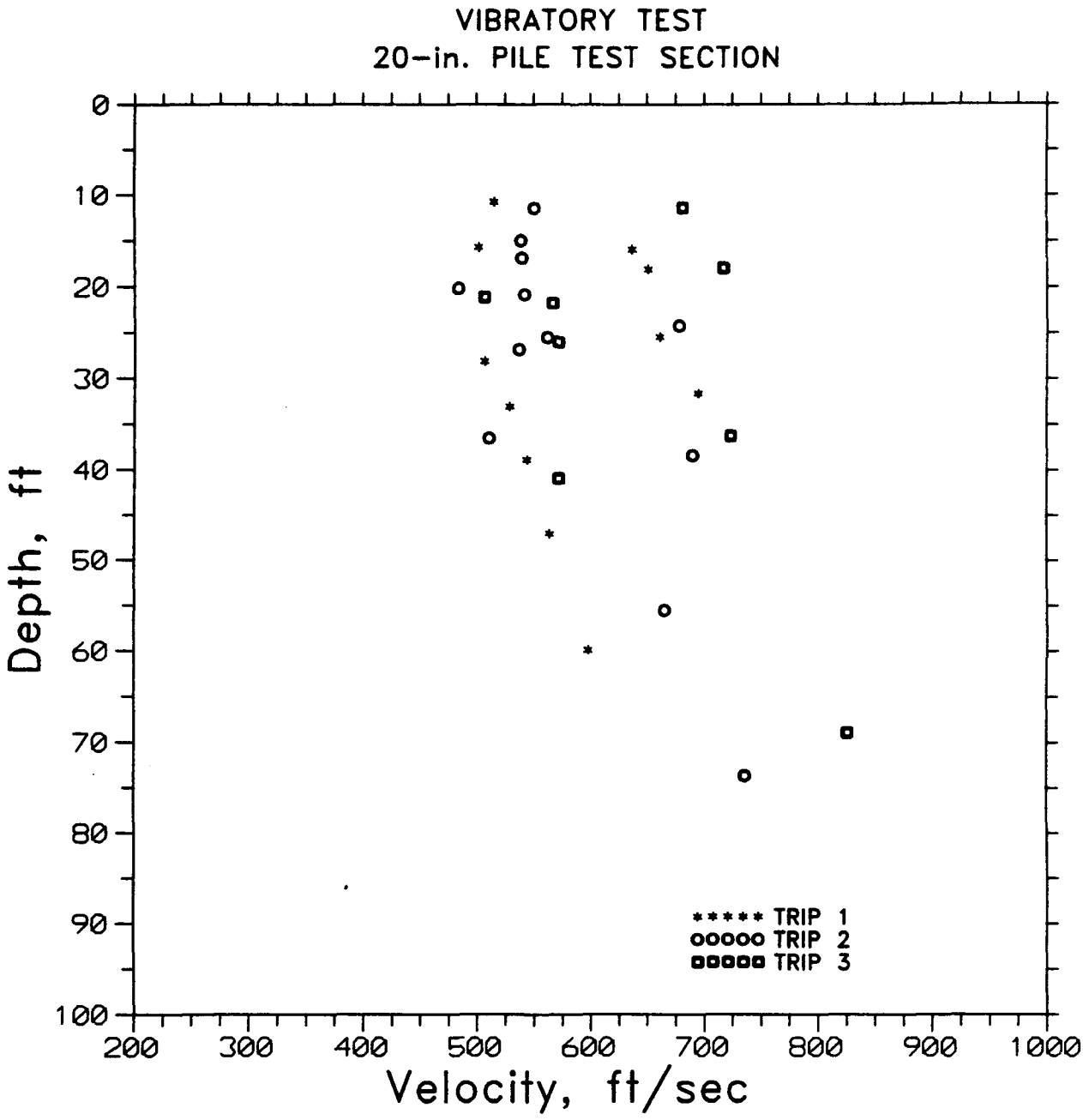

Figure 36. R-wave velocity versus depth, Line 1, 20-in pile test section, Trips 1, 2, and 3

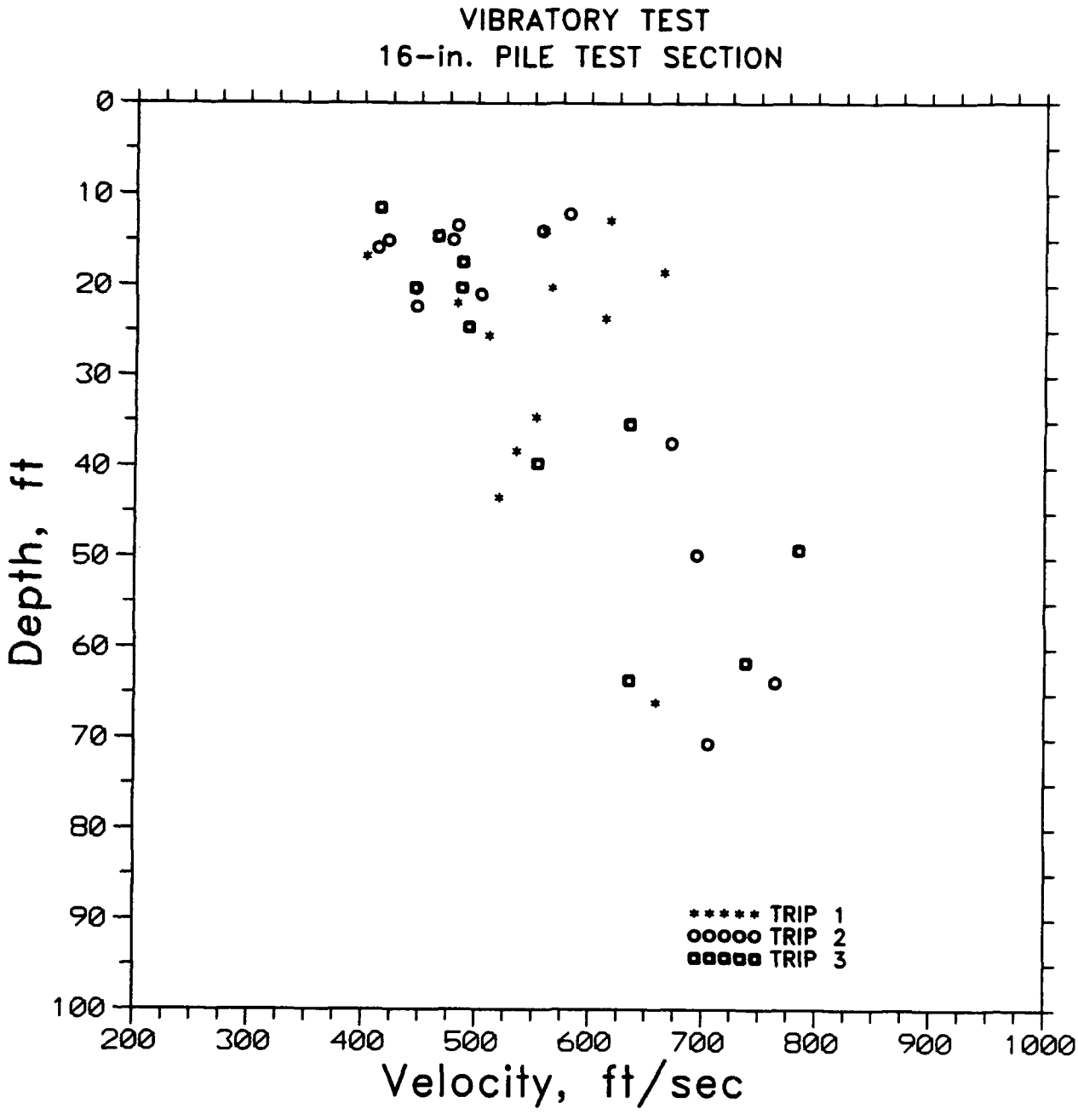

Figure 37. R-wave velocity versus depth, Line 1, 16-in pile test section, Trips 1, 2, and 3

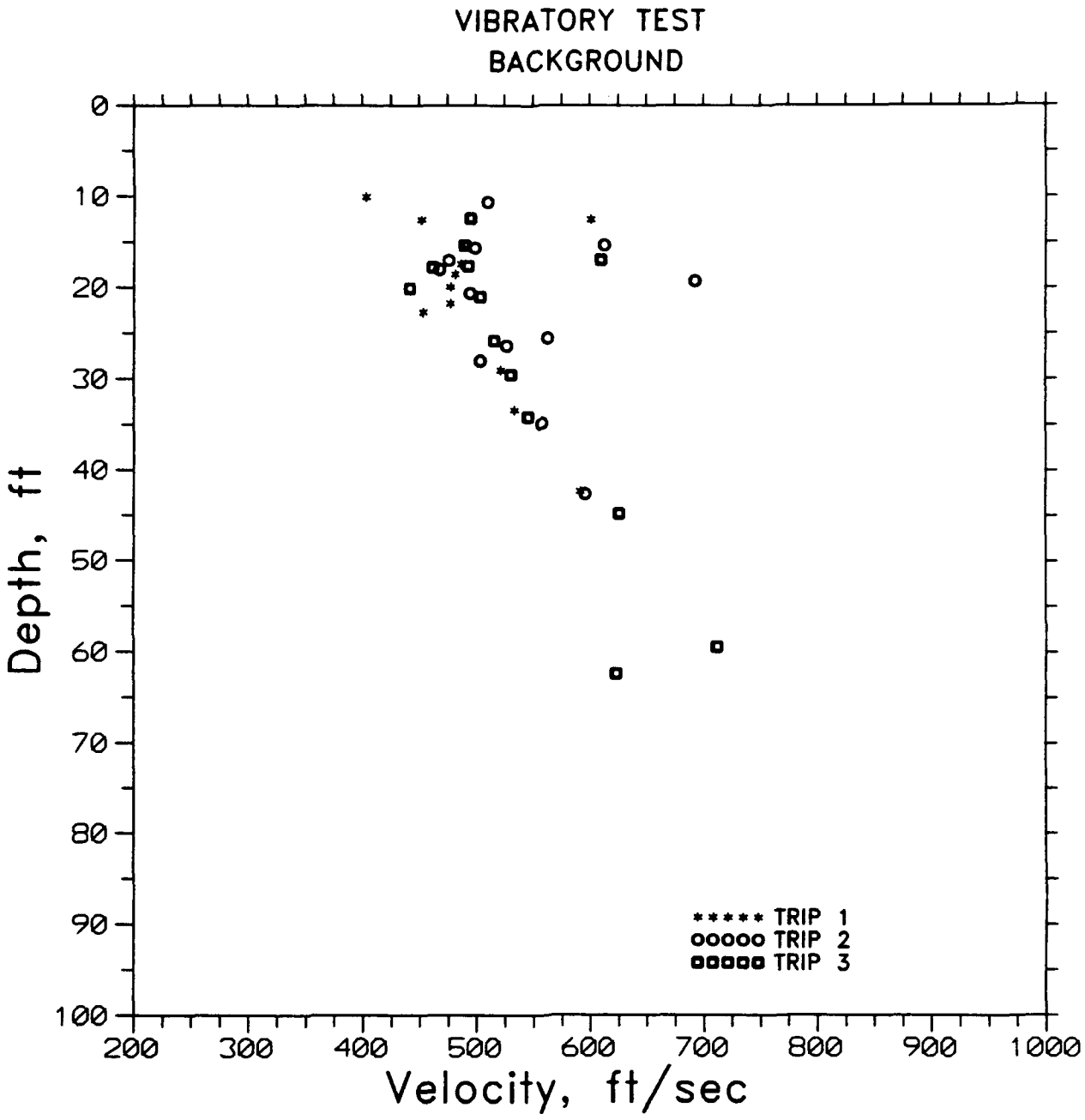

Figure 38. R-wave velocity versus depth, Line 1, background area, Trips 1, 2, and 3

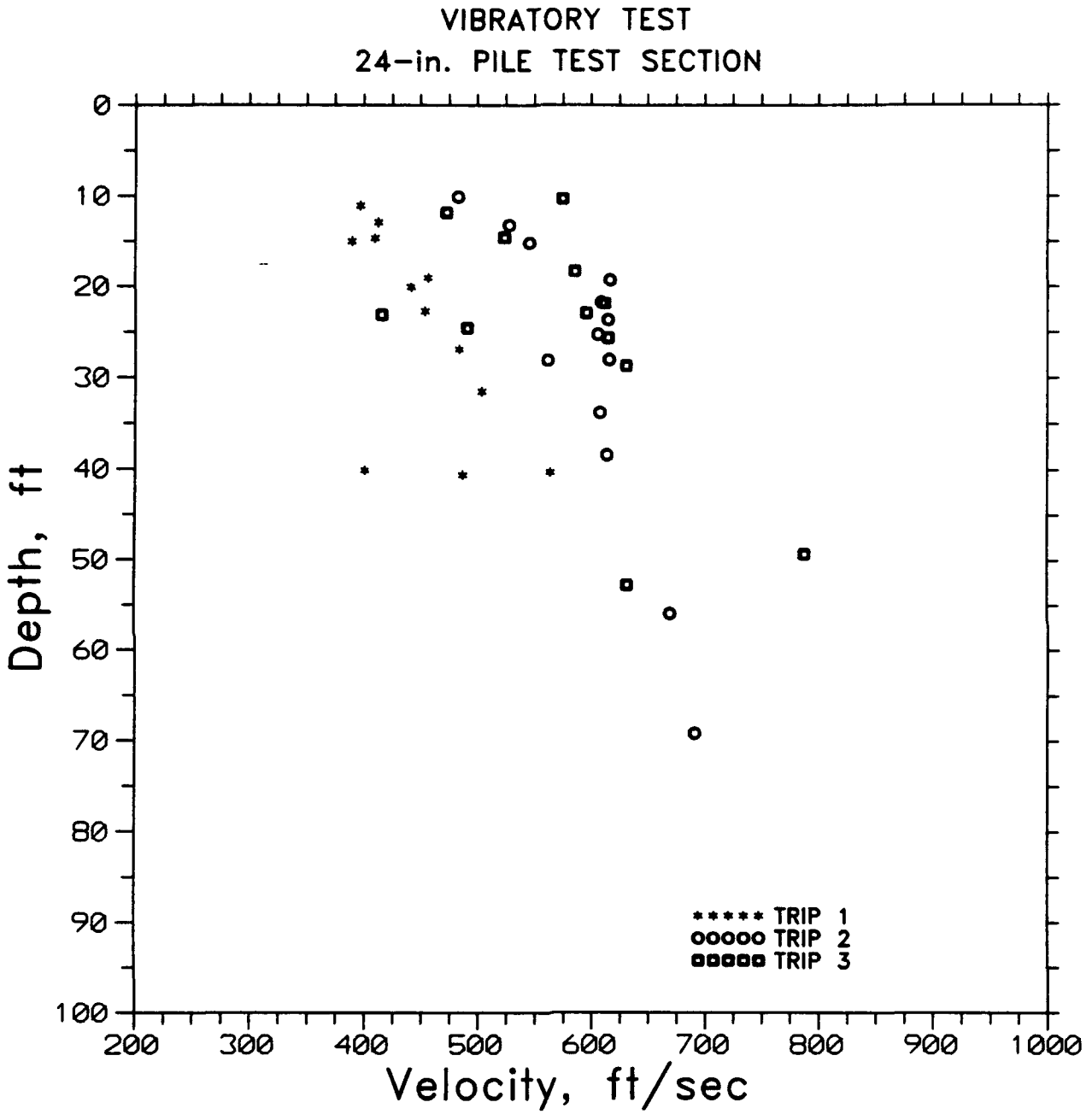

Figure 39. R-wave velocity versus depth, Line 2, 24-in pile test section, Trips 1, 2, and 3

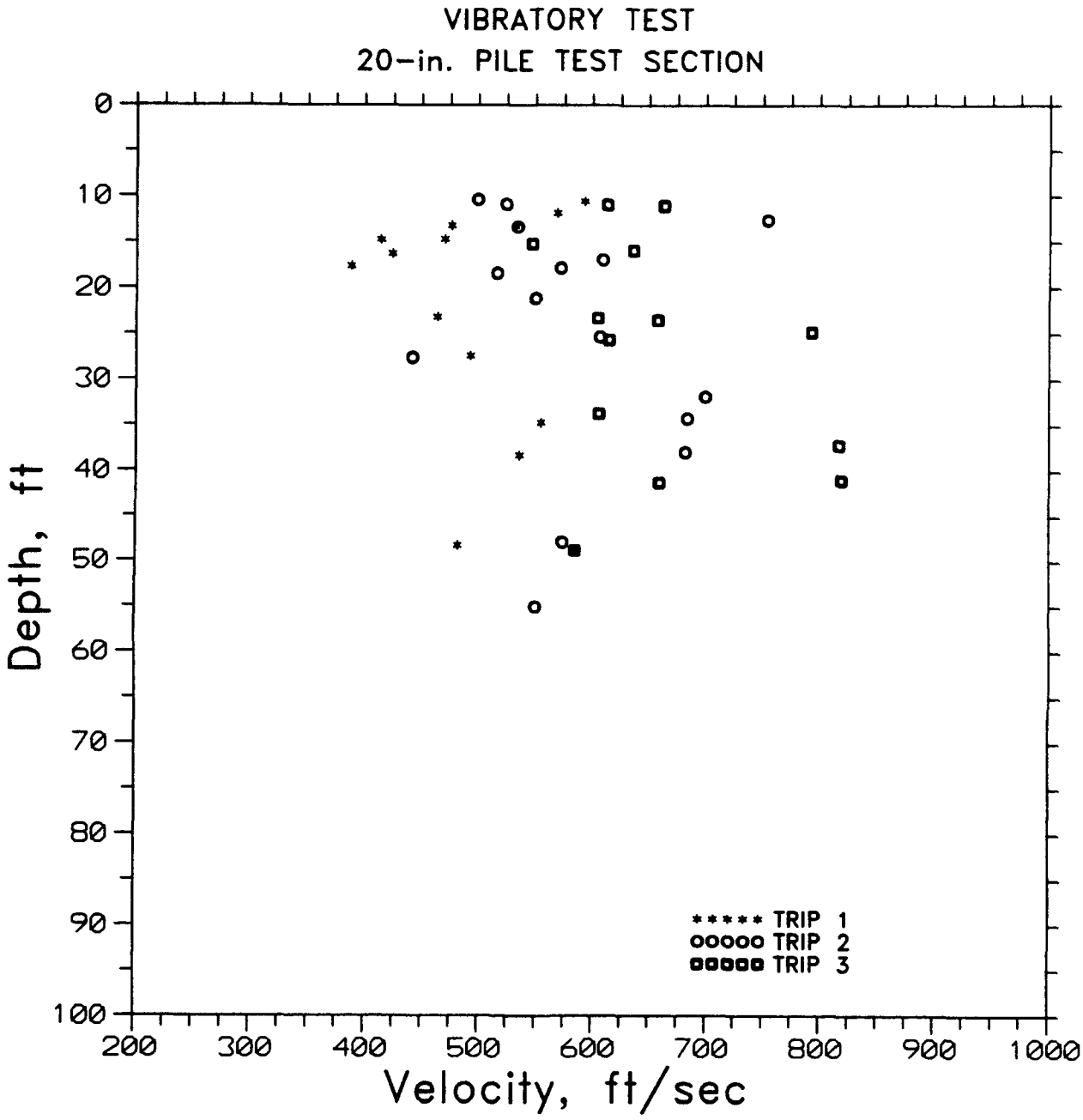

Figure 40. R-wave velocity versus depth, Line 2, 20-in pile test section, Trips 1, 2, and 3

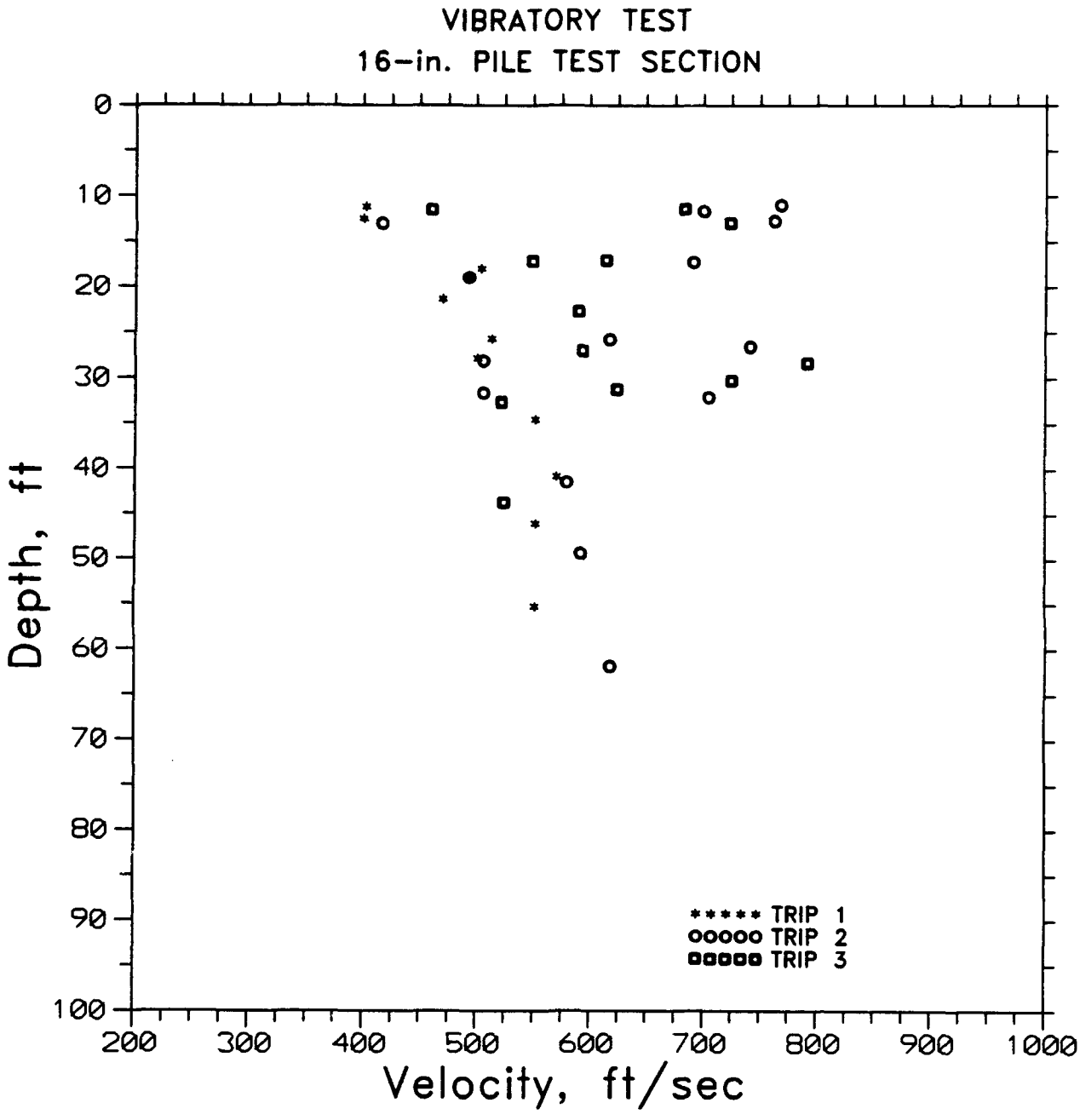

Figure 41. R-wave velocity versus depth, Line 2, 16-in pile test section, Trips 1, 2, and 3

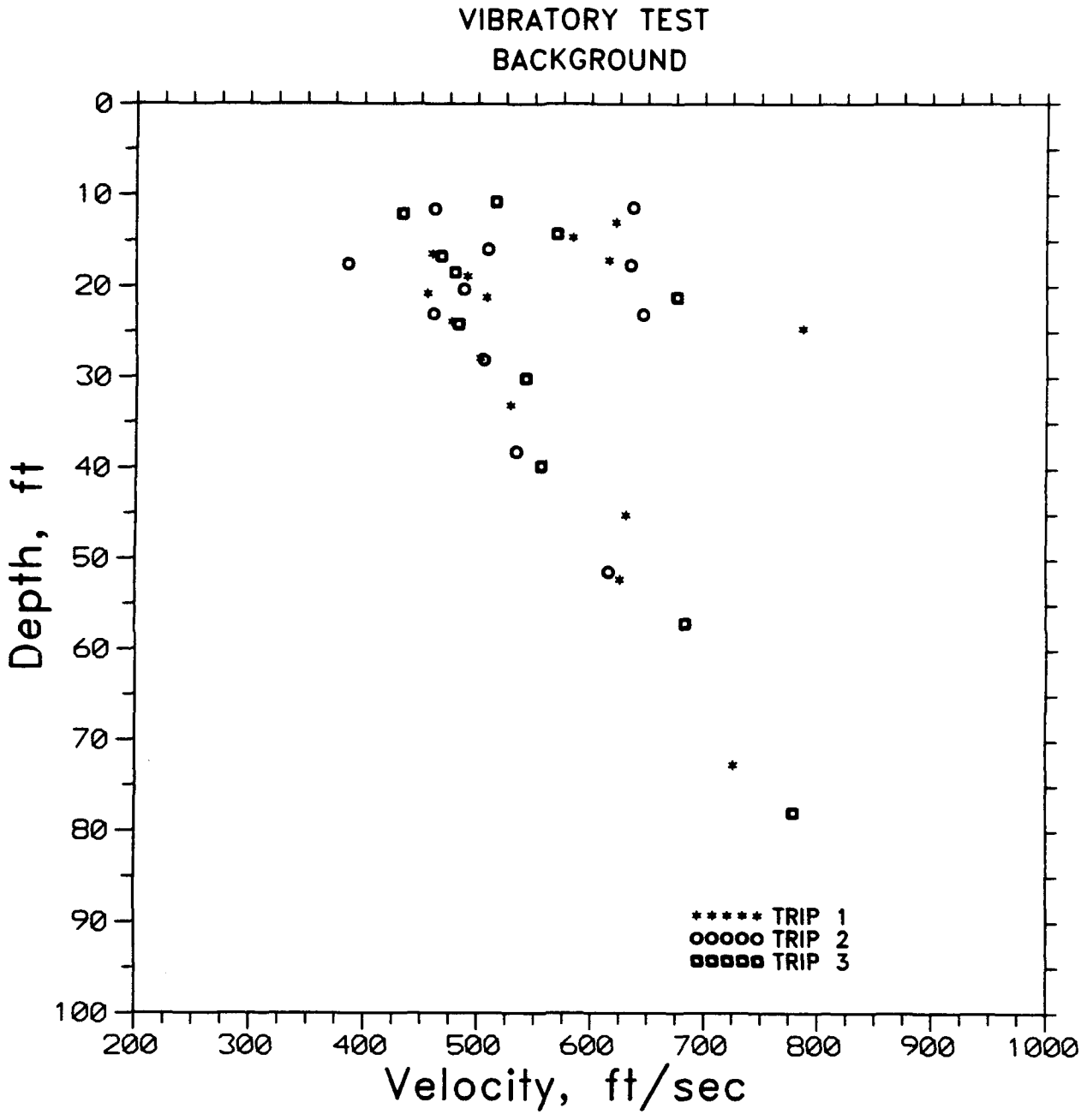

Figure 42. R-wave velocity versus depth, Line 2, background area, Trips 1, 2, and 3

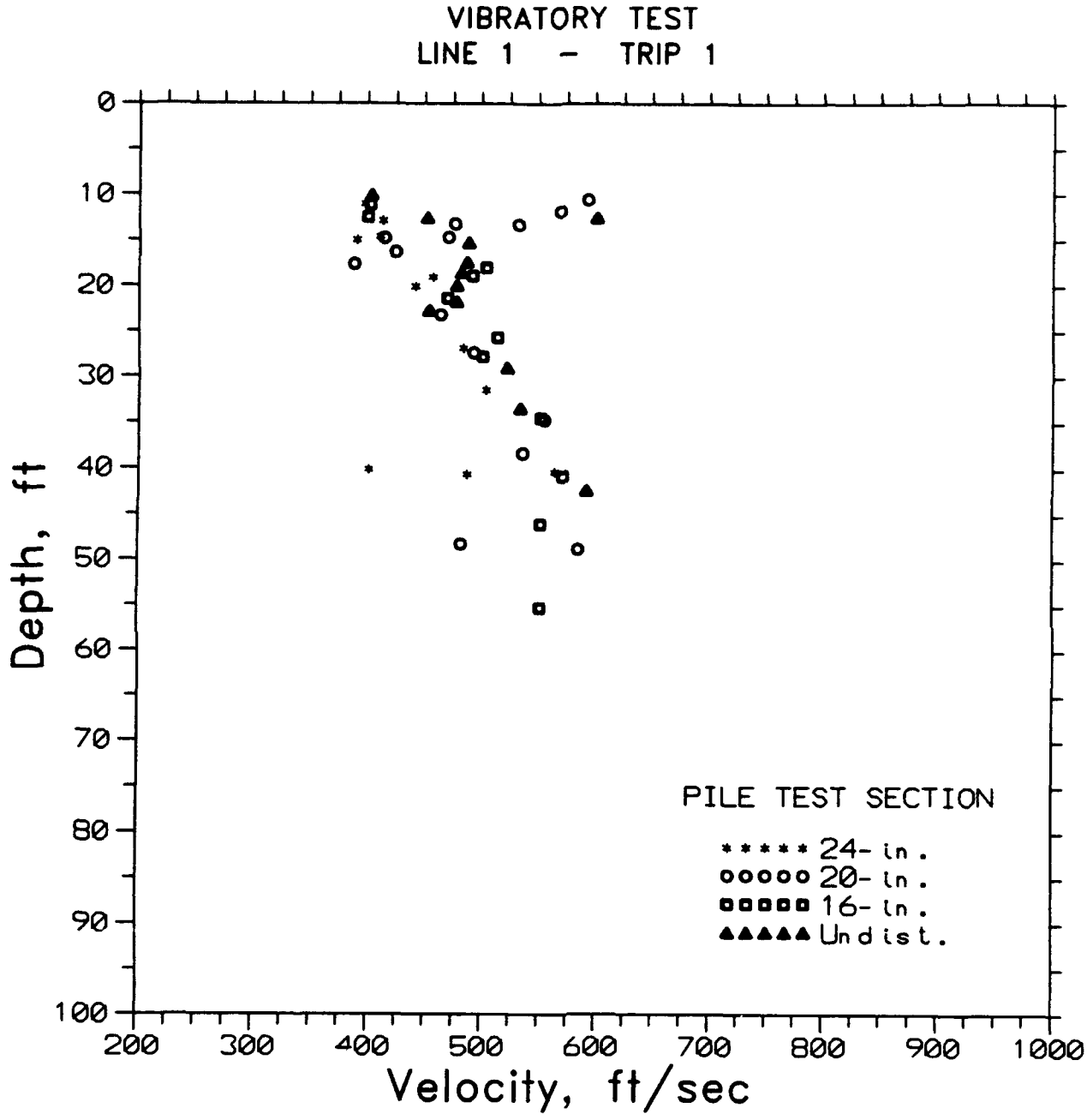

Figure 43. R-wave velocity versus depth, Line 1, Trip 1, pile test sections A, B, C, and background

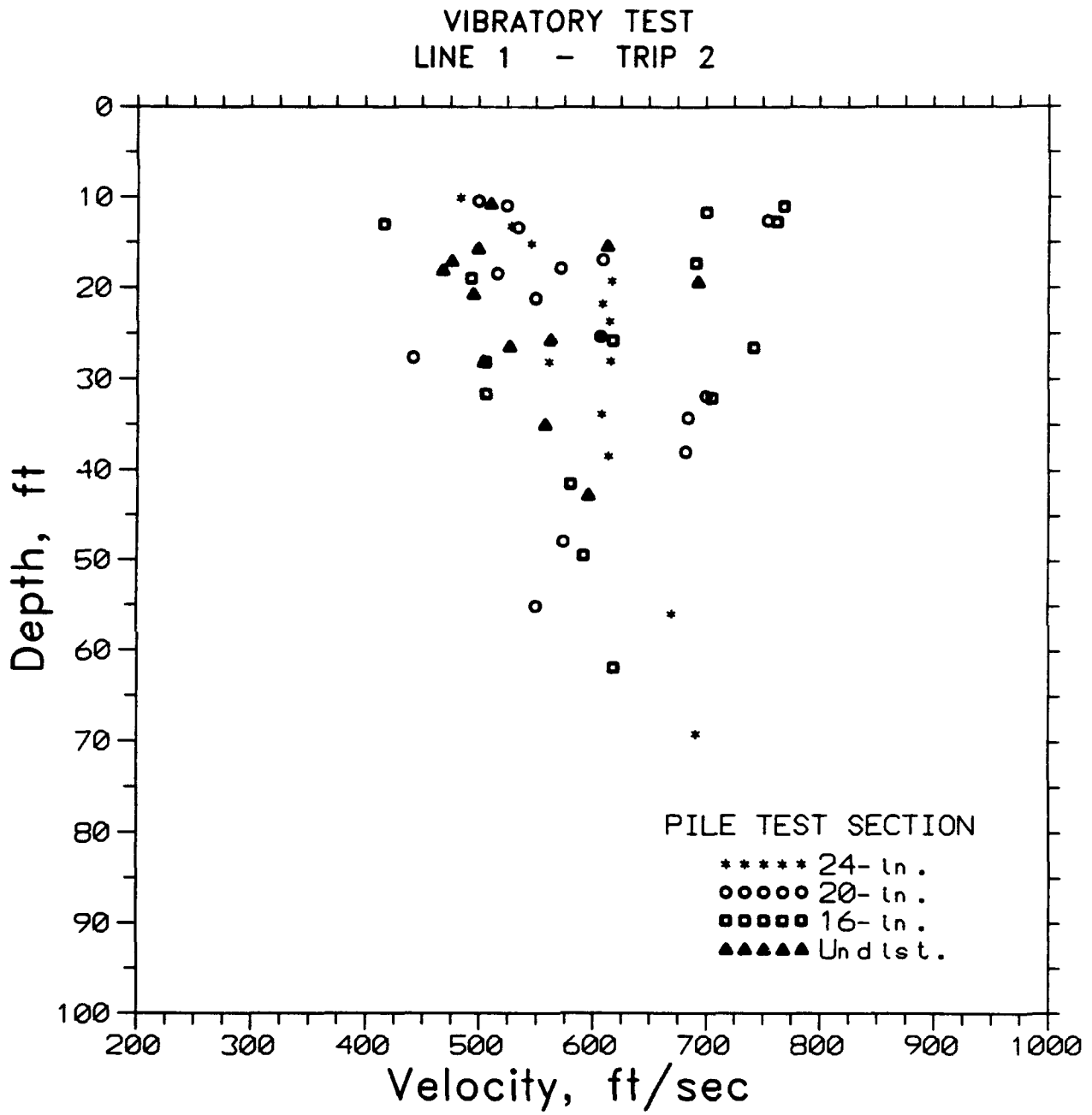

Figure 44. R-wave velocity versus depth, Line 1, Trip 2, pile test sections A, B, C, and background

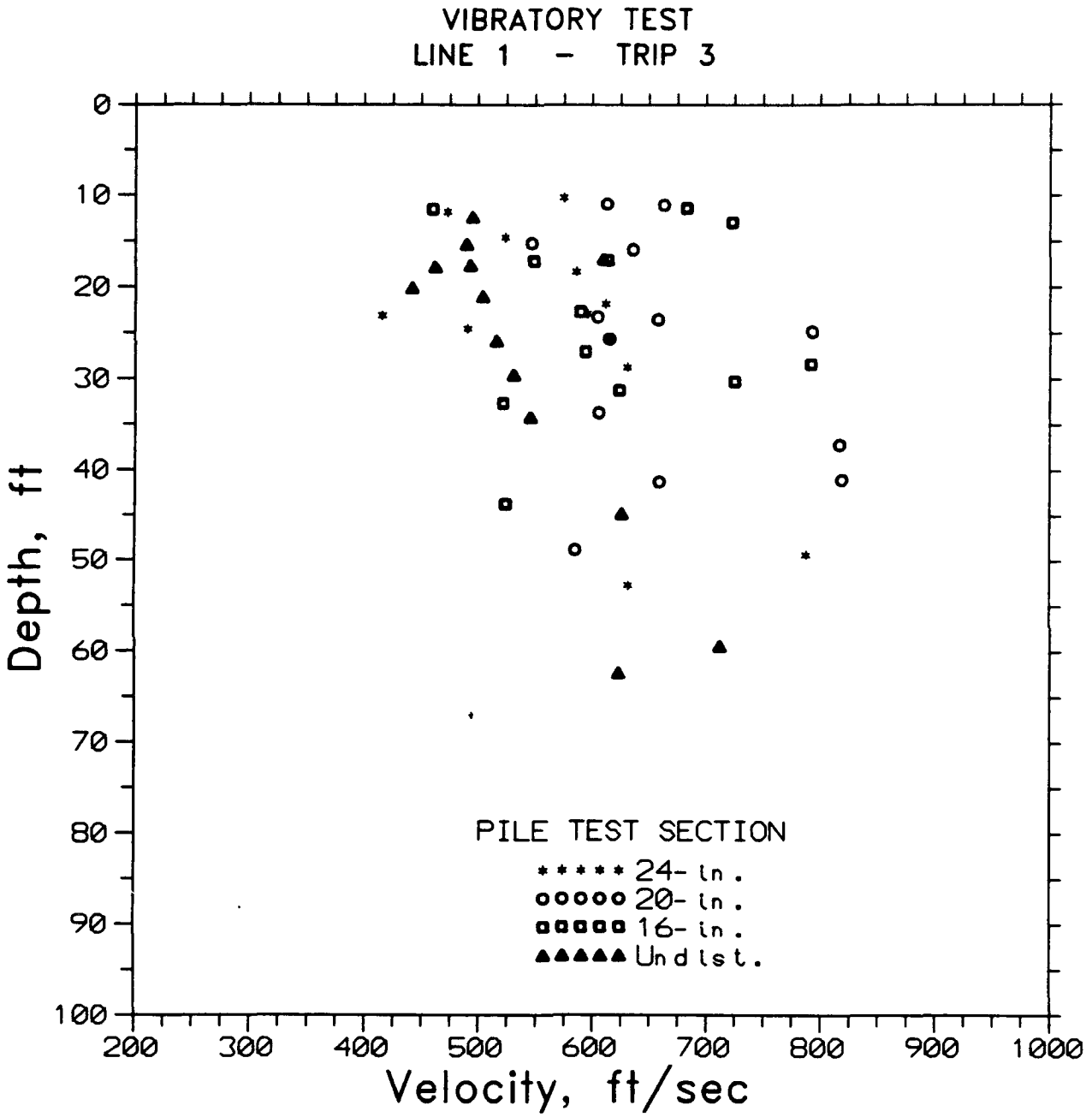

Figure 45. R-wave velocity versus depth, Line 1, Trip 3, pile test sections A, B, C, and background

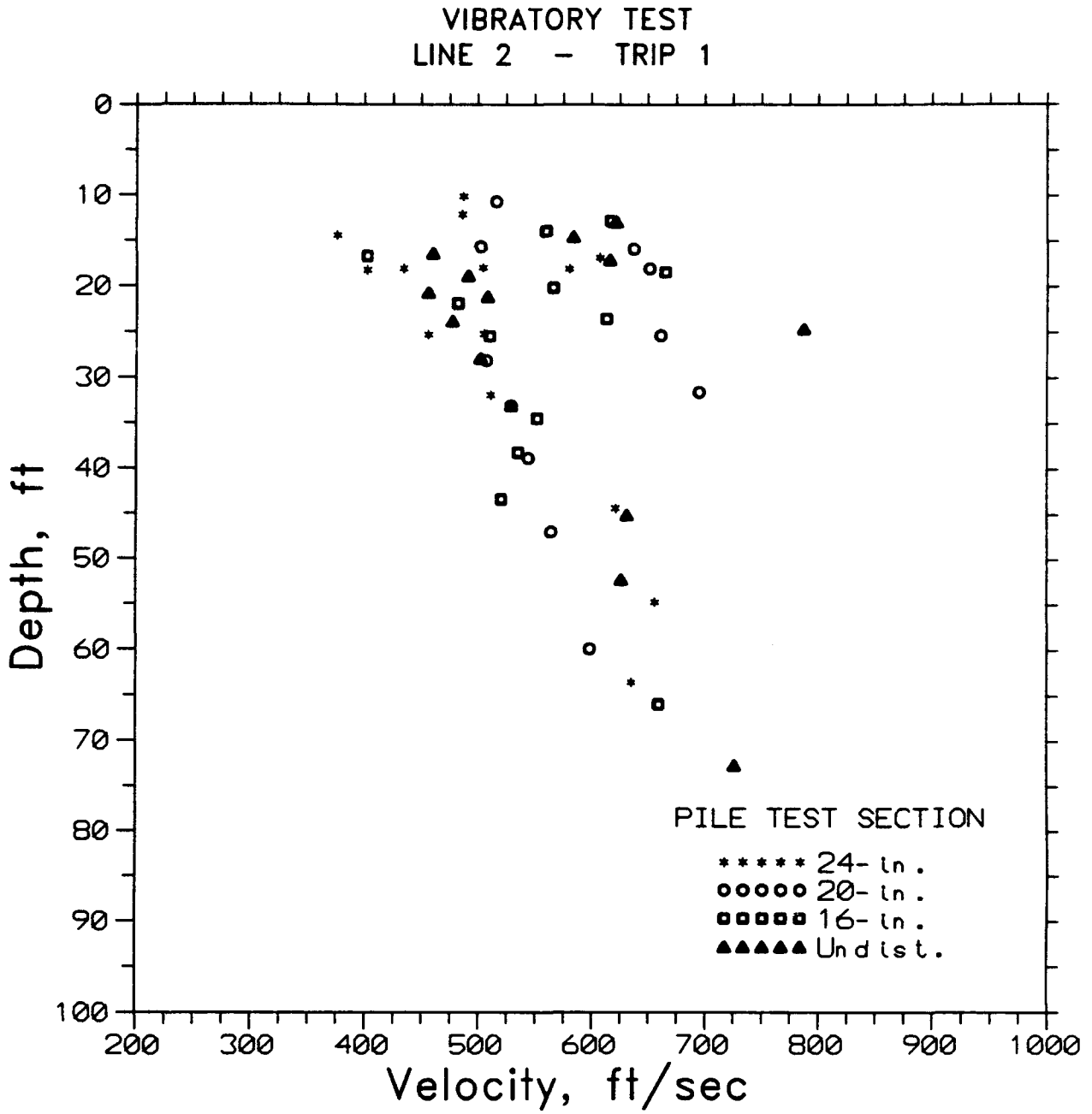

Figure 46. R-wave velocity versus depth, Line 2, Trip 1, pile test sections A, B, C, and background

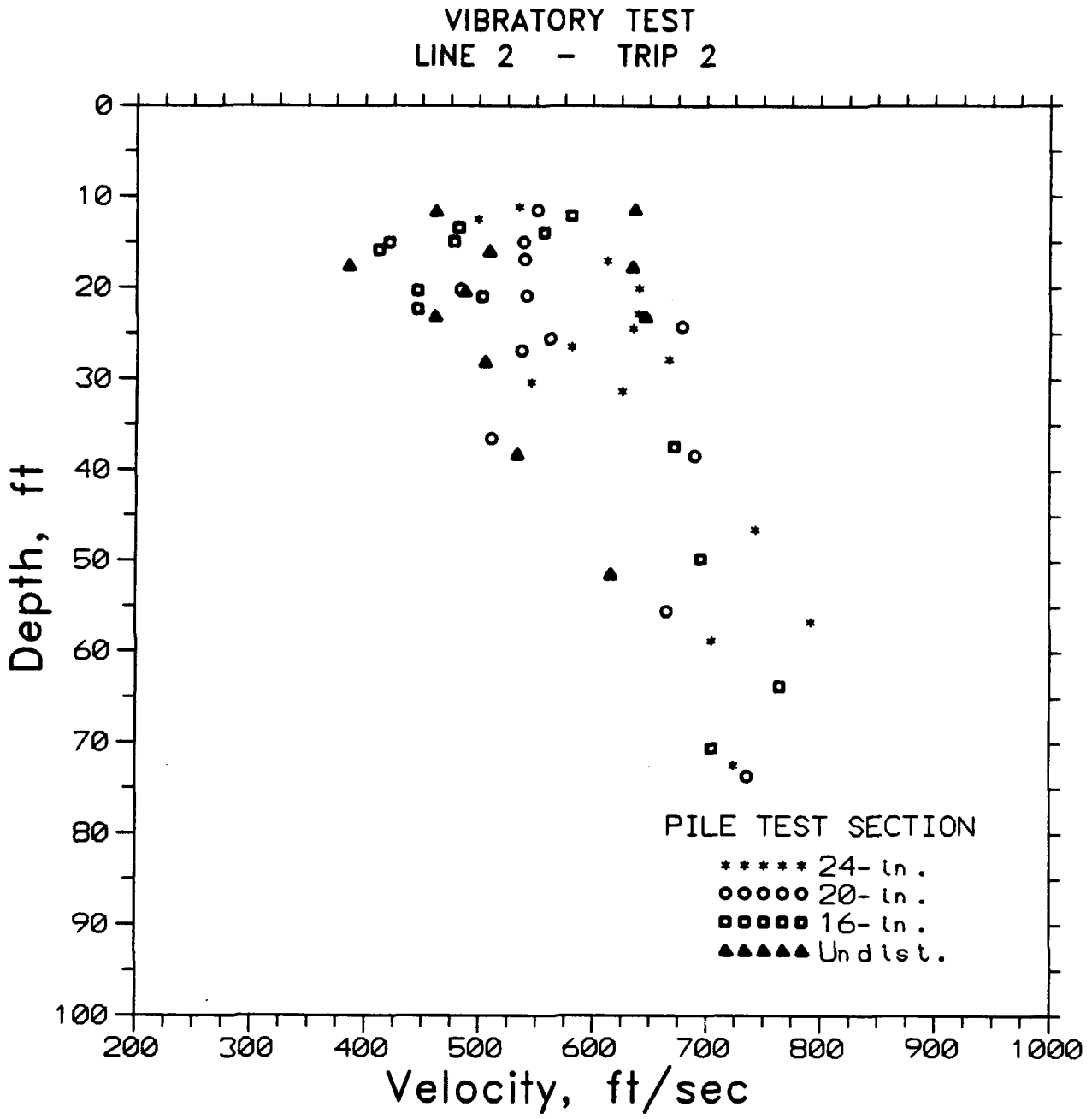

Figure 47. R-wave velocity versus depth, Line 2, Trip 2, pile test sections A, B, C, and background

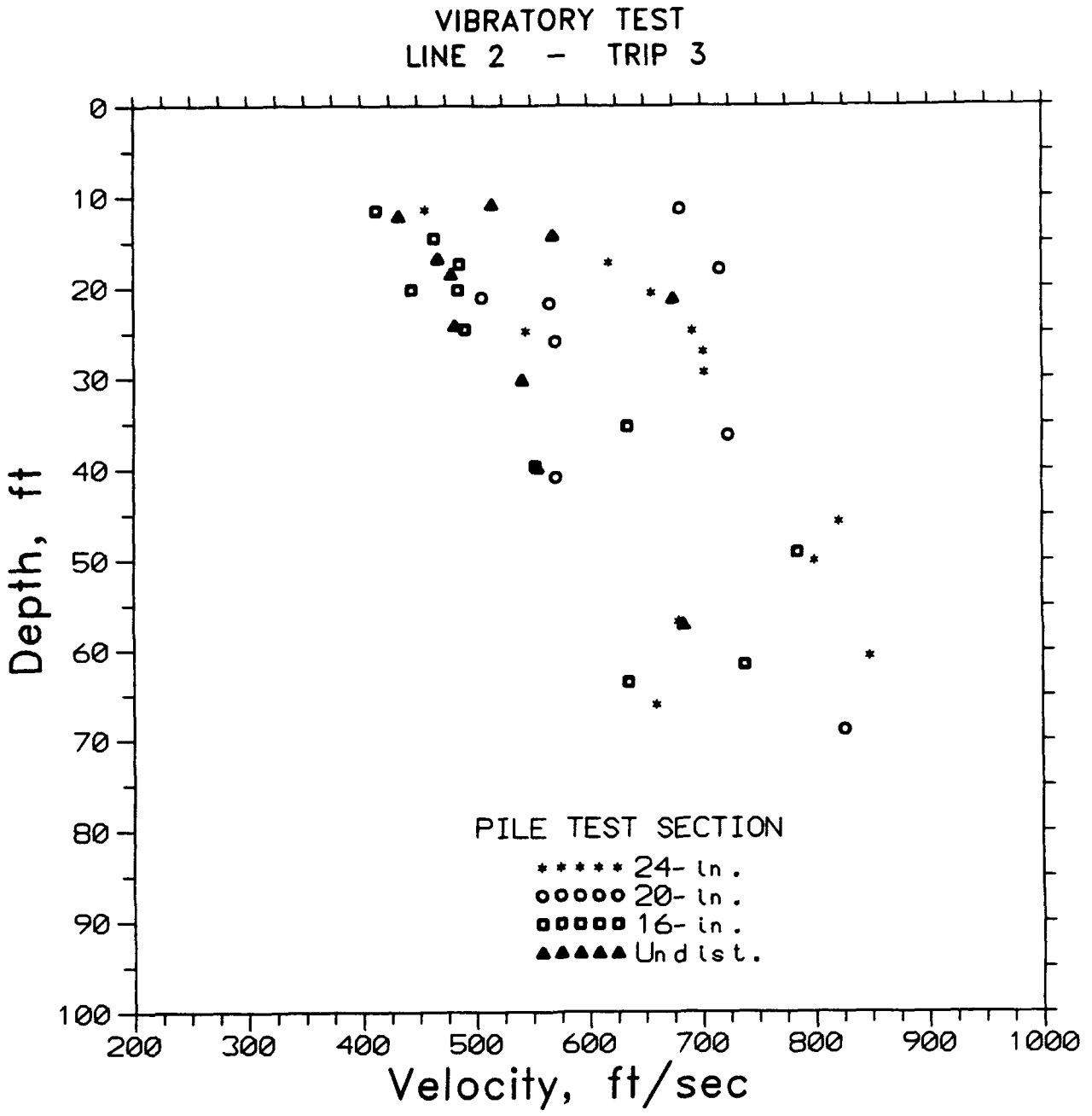

Figure 48. R-wave velocity versus depth, Line 2, Trip 3, pile test sections A, B, C, and background

REPORT DOCUMENTATION PAGE

Form Approved
OMB No. 0704-0188

1. AGENCY USE ONLY (Leave blank)	2. REPORT DATE	3. REPORT TYPE AND DATES COVERED
	January 1994	Final Report

4. TITLE AND SUBTITLE
In Situ Geophysical Investigation of the Pile Test Section, Sardis Dam, Mississippi

5. FUNDING NUMBERS
MIPR No. 5119
REMR CDGRL

6. AUTHOR(S)
José L. Llopis

7. PERFORMING ORGANIZATION NAME(S) AND ADDRESS(ES)
U.S. Army Engineer Waterways Experiment Station
3909 Halls Ferry Rd
Vicksburg, MS 39180-6199

8. PERFORMING ORGANIZATION REPORT NUMBER
Technical Report
GL-94-1

9. SPONSORING/MONITORING AGENCY NAME(S) AND ADDRESS(ES)
U. S. Army Engineer District, Vicksburg
Vicksburg, MS 39180-6190
Office Chief of Engineers
Washington, D.C.

10. SPONSORING/MONITORING AGENCY REPORT NUMBER

11. SUPPLEMENTARY NOTES
This report is available from the National Technical Information Service, 5285 Port Royal Road, Springfield, VA 22164

12a. DISTRIBUTION/AVAILABILITY STATEMENT
Approved for public release; distribution is unlimited

12b. DISTRIBUTION CODE

13. ABSTRACT (Maximum 200 words)

An in situ geophysical investigation consisting of crosshole and downhole shear wave (S-wave) and surface vibratory tests was performed at Sardis Dam, located on the Tallahatchie River in northwest Mississippi. The tests were conducted in a pile test section at the downstream toe of the dam. The purpose of the investigation was to determine changes in S-wave velocities, which are related to soil strength, in the test section due to pile driving activities.

The tests were conducted prior to driving the piles, immediately after and 3 months after the piles had been driven. The S-wave crosshole and surface vibratory tests indicated a significant velocity increase due to the driving of the piles in the test section. The downhole S-wave test did not detect any significant velocity increases.

14. SUBJECT TERMS
Crosshole, Geophysics, Sardis Dam, Elastic waves, Rayleigh waves, Shear waves

15. NUMBER OF PAGES
68

16. PRICE CODE

17. SECURITY CLASSIFICATION OF REPORT	18. SECURITY CLASSIFICATION OF THIS PAGE	19. SECURITY CLASSIFICATION OF ABSTRACT	20. LIMITATION OF ABSTRACT
Unclassified	Unclasified		